QATAR UNIVERSITY

COLLEGE OF ARTS AND SCIENCES

# EFFECT OF PHENOL AS A CONTAMINANT ON THE WILD PEARL OYSTER PINCTADA IMBRICATA RADIATA IN QATAR: ECOTOXICOLOGICAL APPROACH AND USE OF OYSTER SHELL STRUCTURE AS A POTENTIAL MITIGATION TOOL FOR PHENOLS REMOVAL FROM WATER

BY

FARAHNAZ GHOLAMREZA BARAH

A Thesis Submitted to

the College of Arts and Sciences

in Partial Fulfillment of the Requirements for the Degree of

Masters of Science in Environmental Sciences

June 2022

# COMMITTEE PAGE

The members of the Committee approve the Thesis of
Farahnaz Gholamreza Barah defended on [Defense Date][Defense Date].

Prof. Mohamed Najib Daly Yahia
Thesis/Dissertation Supervisor

Prof. Mohammad Al-Ghouti
Co-supervisor

Prof. Nabil Zouari
Committee Member

Dr. Lama Soubra
Committee Member

Approved:

Prof. Ahmed Elzatahry, Dean, college of Arts and Sciences

ABSTRACT

BARAH, FARAHNAZ, G., Masters : June : 2022, Environmental Sciences

Title: Effect of Phenol as a Contaminant on the Wild Pearl Oyster Pinctada Imbricata Radiata in Qatar: Ecotoxicological Approach and Use of Oyster Shell Structure as a Potential Mitigation Tool for Phenols Removal From Water.

Supervisor of Thesis: Prof. Mohamed Najib Daly Yahia and Prof. Mohammad Al-Ghouti.

Phenol removal is a vital environmental concern due to its toxicity and hazard effects. The current study investigates the removal of phenol by Pearl oyster *Pinctada imbricata radiata* for the first time in this region.

The first objective of this study was to investigate the ecotoxicity of Pearl oyster *Pinctada imbricata radiata* for different concentrations of phenol by measuring the activity of some biomarkers of oxidative stress such as Catalase (CAT) and Superoxide Dismutase (SOD) activities. The biometric analysis of the maitained *Pinctada imbricata radiata* showed that the dominated size class was (4.5 cm -5.5 cm) in length representing 70% of the population. Furthermore, the biometric relations (length, width, and height versus weight) between size classes of *Pinctada imbricata radiata* showed negative allometric growth. The total proteins values decreased over time during the 96h acute toxicity experiment with no significant differences ($p > 0.001$). CAT and SOD enzymatic activities for both gills and digestive glands showed an increase in values compared to the control organisms with significant differences ($p < 0.001$). These results indicated that Pearl oyster *Pinctada imbricata radiata* is an excellent bioindicator of phenol pollution and should be used for other pollutants indicator and in marine environmental pollution monitoring programs.

The second objective was to use silver-impregnated oyster shell nanoparticles

(OSNP-S) as a novel technique for the detoxification of phenol from water. Pearl oyster shell nanoparticles (OSNP) were prepared by a simple ball-milling process and impregnated with silver. A batch adsorption study was conducted at different pH values, temperatures, and initial phenol concentrations. The physical and chemical characterization of both OSNP and OSNP-S were determined with Scanning Electron Microscopy (SEM) and Fourier transform infrared spectrophotometer (FTIR). The surface area, pore radius, and pore volume were measured with Brunauer, Emmett, & Teller (BET) and Transmission electron microscope (TEM). Batch adsorption isotherms (Langmuir isotherm, Freundlich isotherm, Temkin isotherm, and Dubinin-Radushkevich isotherm models) were used. The results indicated that BET surface area, Langmuir surface area and pore volume of the OSNP were the highest comparing to OSNP-S. However, OSNP-S had the highest average pore volume (145.4 A°). The results of the batch analysis that was conducted at pH 6 were in favor of OSNP in terms of adsorbing the highest amount of phenol removal (36.98%). Whereas, at pH 10, the removal result was in favor of OSNP-S (25.89%). The highest phenol removal occurred at room temperature (25° C) at both pH conditions. The highest phenol removal of real olive wastewater was at pH 10 and room temperature by OSNP-S (56.78%). Based on the adsorption isotherm model, the adsorption capacity decreased by temperature and the coefficient of determination $R^2$ of the Freundlich adsorption isotherm model showed the best equilibrium data for phenol adsorption with the physical interaction adsorption process. $R^2$ at both pH 6 and pH 10 ranged from (0.9318- 0.9954). The Gibbs free energy $\Delta G^o$ was in negative sign, indicating that the adsorption process was thermodynamically feasible, spontaneous, and chemically controlled at all temperatures and both pH 6 and pH 10. The thermodynamic parameters of OSNP-S, positive $\Delta H^o$, and negative $\Delta S^o$ at pH 6 showed that the adsorption process was endothermic with the

decrease in the process randomness and the reduced confusion at solid-solution interface. Nevertheless, this was in reverse at pH 10. The phenol desorption was 97.44% and 98.64% by reacting 0.1 M NaOH and 0.1 M HCl respectively.

# DEDICATION

*This thesis is dedicated to my beloved family, my friends and to those who inspired, encouraged and supported me to catch up the world-building process.*

*May Allah bless them all.*

# ACKNOWLEDGMENTS

" Prays and thanks to Allah almighty who enabled me to accomplish this work. My special thanks to my supervisor Prof. Mohamed Najib Daly Yahia for his supervision, guidance, and encouragement through my thesis work. I also deeply thank my co-supervisor Prof. Mohammad Al-Ghouti for his continuous support, guidance and encouragement all through this work. Many thanks also to my committee members Prof. Nabil Zouari and Dr. Lama Soubra for their continuous help and advice. I would like to thank the members of the Environmental Science Program Mr. Abdulali Moghadasi, Ms. Mariam Khan, and Ms. Dana Adel for their help which, continued until the end of this work. I also specially thank Prof. Siham Al-Qaradawi and Dr. Mohamed Youssry in the Department of Chemistry and Earth Sciences for their full support and help. Special thanks to my colleagues and friends Ms. Siham Hersi and Ms. Maetha Al-Sulaiti for their support and advice."

# TABLE OF CONTENTS

# LIST OF TABLES

# LIST OF FIGURES

# CHAPTER 1: INTRODUCTION

## 1.1.Introduction

Recently the scarcity and purity issues of water increased due to the huge and rapid population and economic growth. Water covers more than 71% of the world, however, only 1% of water is drinkable. The rest suffer from different types of contaminations caused by anthropogenic activities (human activities and industrialization). The main contaminations are heavy and toxic metals, organic compounds, and microorganisms, which even in trace amounts cause many environmental and health problems (Singh et al., 2018).

Phenol is a simple aromatic compound that is considered one of the primary organic pollutants found in industrial wastewater. Phenol is found in the discharged wastewater and sewage sludge of several industries such as petroleum refining, coal gasification, steel and perfume production, agriculture by-products, and pharmaceutical manufacture. Many chemical spills introduce different organic pollutants such as phenol in the ocean and aquatic environment resulting in severe problems to both ecological and human health due to its toxicity and hazard effects even at minute concentrations (Subhanet al., 2018; Li et al., 2019; Wang et al., 2011; Gong et al., 2016). Phenol's toxicity levels are generally in the range of 9 mg/L –25 mg/L for humans and aquatic life (Villegas et al., 2016; Kulkarni, 2013). The Environmental Protection Agency (EPA) determined the toxicity of phenol to saltwater aquatic life at the concentrations lower than 5,800 μg/L for sensitive species and 3.5 mg/L for human (EPA, 1980). Acute exposure to phenol can cause different health problems such as gastrointestinal discomfort and diarrhea, skin irritation, excretion of dark urine, and headaches. It is also toxic to the heart, kidneys, liver, and nervous system. Furthermore, daily exposure to Phenol affects pregnant women's health and fetal growth

(Messerlianet al., 2018; Jamal et al., 2020). Phenol is also toxic for fishes and plants (Kulkarni et al., 2013; Wang et al., 2011).

Till now different processes and methods have been used for phenol removal, degradation, and treating. Various physical, chemical, and biological processes and techniques have been developed to reach the desired sustainable goals which are cost efficiency, simplicity, and environmental friendly (Gong et al., 2016; Shaban et al., 2013; Hoyos-hernandez et al., 2014). Many conventional processes and techniques have been used for the phenol removal from the discharged wastewater such as precipitation, flocculation, adsorption, reverse osmosis, combustion, and chemical oxidation along with the biological degradation methods. However, these methods face several limitations and boundaries regarding cost, effectiveness, and competence (Subhan et al., 2018). Hence, finding an appropriate sustainable method and technique to solve these limitations is vital. Physicochemical processes have been used to treat phenolic wastewater by using ozone, Ultra Violet (UV), and hydrogen peroxide ($H_2O_2$). However, these processes are much more costly and not helpful in treating large volumes of wastewater, besides its harmful to the environment. On the other hand, the biodegradation of phenol is much cheaper and environmentally friendly though it is limited by the salinity of the industrial wastewater. Phenol co-exists with inorganic salts in industrial wastewater (Li et al., 2019). Among these methods and processes of phenol removal, adsorption is the most efficient (Popoola, 2019) due to the ease of operation and cost-effectiveness (Kim, Sing, & Smith, 2020). In addition, several studies resulted in the efficiency of adsorption processes for different concentrations of phenol in aqueous solutions. Hence, different natural and synthetic materials have been used as adsorbents of phenol (Hadi et al., 2016). Oyster shells can be reused as a source of biogenic calcium carbonate to treat industrial wastewater and purify it from toxic

compounds such as Phenol (Wu et al, 2014)

Oysters are typical saltwater bivalve mollusks that live in marine aquatic environments and they commercially used all around the world. Oysters are hermaphrodites and can change their sex through their different life stages. Oysters are vital for the marine ecosystem, they filter out pollutants from the water and easily adapt to new environments. Hence, they are considered a good model species to use for testing the phenolic toxicity impact on invertebrates (Luo et al., 2017; Caplat et al., 2016). Oysters are filter-feeding animals that can cope the harsh and changeable environmental conditions. Oysters can handle both biotic and abiotic pressures and stresses by forming a complex immune system with notable discriminatory properties, which can fight different pathogens and stresses (Wang et al., 2018). Oysters accumulate high concentrations of toxins and have the ability to tolerate the sub-lethal impacts of these toxins. However, they are considered vectors that transfer these toxins to humans through consumption. Vectored toxins from contaminated oysters can cause different diseases such as diarrhetic poisoning, amnesic poisoning, paralytic poisoning and neurotoxic poisoning (Farabegoli et al., 2018; Robledo et al., 2019).

Bivalves filter-feeders such as *Pinctada imbricata radiata* are commercially and ecologically important sentinel species and are used as models in ecotoxicology. Their filtering capacities make them bioindicators of marine pollution and contamination (Khan et al., 2019). Different biological processes in the species bodies result in redox reactions. Biological redox reactions generate potentially harmful reactive oxygen species (ROS), such as peroxide and free radicals. Exposure to toxicants can cause inequity in the concentration of ROS, leading to many oxidative stresses in the tissues which could lead to many diseases; such as cancer, atherosclerotic cardiovascular disease, respiratory system (lung) diseases, chronic inflammatory and

diabetic Mellitus (Lowe, 2014). In general, biomarkers of oxidative stress are categorized by (1) molecules that undergo modification when interacted with ROS in micro-environments and by (2) molecules of the antioxidant system that change due to the increase in redox stress (Ho et al., 2013). Oxidative stress is the main cause of many diseases. Several methods are developed to identify the quantity and nature of oxidative stress of diseases in DNA, proteins, lipids, cabohydrates and amino acids (Frijhoff et al., 2015). The most favorable biomarker analysis is the one correlated with the pathophysiological process of the diseases (Ho et al., 2013). Oxidative stress markers are catalase (CAT), glutamine S-transferase (GST), superoxide dismutase (SOD), peroxidation (LPO), and immunotoxic effects (R. Cao et al., 2018). Oxidative stress in marine bivalve species is influenced by seasonal and environmental conditions. The enzymes play a vital role in protecting the marine bivalve species against the ROS produced during exposure to environmental toxicants or abiotic factors (Concetta et al., 2020).

## 1.2.Objectives

Qatar and its neighbors the Arabian Gulf countries suffer from scarcity of pure drinkable water due to the topography and geological characteristics of the land along with the lack of precipitation (Babiker et al., 2019). Statistical studies indicated significant downward trends in the level of precipitation. This negative trend could continue for the upcoming years due to climate change (Mamoon & Rahman, 2015). The huge industrialization and population growth for the past few years along with the poor water management led to more water calamities, therefore more desalination has been constructed (Ahmad & Al-ghouti, 2020)Al-Ghouti et al, 2017). However, the critical need and demand for other sources of pure water other than desalination of seawater resulted in applying new advanced technologies for improving the reuse of

the treated wastewater effluents in agriculture and industrial sectors (Jasim et al., 2016).

The objectives of this work are as follows:

1) To characterize the Pearl oyster *Pinctada imbricata radiata* biometry, population size-classes distribution and determine the length-weight relationships in the summer season.
2) To investigate phenol ecotoxicity through biomarker analysis and oxidative stress measurements in gills and digestive gland of *Pinctada imbricata radiata* under different Phenol concentrations, namely (0, 1, 2, 5, 10) mg/L.

3) To use oyster shell nanoparticles (OSNP) toward developing the most efficient way of phenol removal from water in a way to reduce the negative environmental impacts and to add valorization to waste material.

4) To impregnate OSNP with silver in terms of using it as a novel technique for detoxification of phenol from water. Furthermore, to find the optimal conditions for phenol removal by OSNP and OSNP-S by investigating the different physicochemical conditions of Phenol such as initial concentration, pH, and temperature.

To achieve these objectives, several specific objectives were carried out:

a) Sampling and laboratory maintnance of the oyster population from Qatar marine environment.
b) Investigating the ecotoxicity and monitoring the variation intake of phenol by oyster shells.
c) Studying the batch adsorption isotherms for the uptake of phenol onto OSNP and OSNP-S under the effect of different conditions such as the initial phenol concentration, pH, and temperature.

d) Studying the physical and chemical characterization of OSNP and OSNP-S by using a scanning electron microscope (SEM) and Fourier-transform infrared spectrophotometer (FTIR) to determine the morphology and the functional groups of the absorbents before and after adsorption. The size and shape of the nanoparticles were analyzed by using a transmission electron microscope (TEM) and Brunauer, Emmett, and Teller (BET). The pH of the solutions was examined. The UV–VIS spectroscopic studies were carried out by using a UV–VIS spectrometer to determine the concentration of the phenol.

e) Applying different isotherm models (Langmuir, Freundlich, Temkin, and Dubinin-Radushkevich) to understand the interactions between the adsorbate and adsorbent.

# CHAPTER 2: LITERATURE REVIEW

## 2.1. Aquatic Marine Ecotoxicology

Aquatic ecotoxicology is considered a multidisciplinary field, which assimilates toxicology, aquatic ecology, and aquatic chemistry (Rand & Petrocelli, 1985). Aquatic ecotoxicology is the study of the effect of different natural and anthropogenic chemicals and activities on aquatic organisms, populations, and ecosystems (Wells, 2020). Furthermore, the increase in the improvement of this knowledge was through establishing new methods in monitoring and measuring the potential hazards and risks associated with human exposure to contaminated aquatic environments and organisms (Jones, 2009). Anthropogenic chemicals and activities pollute the aquatic system with water sewage, metals, pharmaceutical drugs, and pesticides. which cause abiotic and biotic deterioration (Lomartire, 2021). Most organisms that live in aquatic environments are exposed to constant waterborne pollutants, which resulted in a high risk of absorption, bioaccumulation, and toxicity (Chen, 2020). The aquatic marine is considered a dumpster for industrial and domestic wastes. Since the beginning of the 20$^{th}$ century, the dead zones in the oceans have increased fourfold due to pollution and climate change. Human activities are the source of 80% of marine pollutants (Lloyd-smith, 2018).

## 2.2. Types of Marine Toxicants

Toxicants are chemical contaminants with the potential to exert toxicity to the marine environment at certain concentrations. Toxicants are classified as directly toxic to biota or indirectly toxic which could cause changes in the biological diversity and the usefulness of the marine ecosystem to humans (Water & Management, 2000). Many marine toxicants at low concentrations (trace amounts) are considered essential and beneficial for many organisms, populations, and communities of the marine ecosystem.

However, we are just becoming aware of the types and capacity of these toxicants and their harmful effects on the marine ecosystem and human health (Lloyd-smith, 2018). In low concentrations, some elements such as copper, zinc, phosphorus, and nitrogen are essential for functioning the biota (Water & Management, 2000). To understand the effect of the different contaminant types on aquatic organisms and human health, many considerable efforts by researchers have been done (Wells, 2020). The main types of toxicants are:

- Emerging Contaminants
- Microplastics
- Heavy/Toxic Metals
- Organic Pollutants
- Crude Oil Spills

### *2.2.1. Emerging Contaminants*

Emerging contaminants are defined as *"naturally occurring, manufactured or manmade chemicals or materials which have now been discovered or are suspected [to be] present in various environmental compartments and whose toxicity or persistence is likely to significantly alter the metabolism of a living being"* (Sauvé & Desrosiers, 2014). Emerging contaminants are new aquatic pollutants that are recently considered harmful to environmental and human health. Emerging contaminants are still not regulated by environmental laws (Baldwin et al., 2020). Hundred thousands of chemicals that are used commercially enter the aquatic marine ecosystem through the atmosphere, water run-off, and direct disposal. Industrial waste releases tons of hazardous wastes into the environment which eventually go to the marine system (Lloyd-smith, 2018). A wide amount of emerging organic toxicants such as aromatic hydrocarbons, pesticides, pharmaceuticals, and personal products are released into the

marine ecosystem (Lomartire, 2021). Many anthropogenic substances are considered emerging contaminants due to their impact on the environment being ambiguous (Munari et al., 2019). The release of uncontrolled novel pollutants (emerging pollutants) rise an environmental concern (Rathi et al., 2020).

### *2.2.2. Microplastics*

Plastic production globally increased from 1.5 million tons since the 1950s to 335 million tons in 2016. Plastics' massive production resulted in the accumulation of plastic remains in the environment and toxic impacts on biota (Gideon & Faggio, 2019). Plastic waste is entering the aquatic marine environment daily. Plastics undergo weathering and degradation in the marine by breaking down into smaller and smaller pieces and help in removing other toxicants from the seawater by adsorption on their surface (Lloyd-smith, 2018). During the weathering and degradation process, many organic chemicals and toxicants are released, such as polyaromatic hydrocarbons (PAHs), polychlorinated biphenyls (PCBs), dichloro-diphenyl-trichloromethane (DDTs), alkylphenols, and bisphenol A. These hazardous toxicants beside the plastic debris pose ecotoxicological and toxicological risks respectively to the marine ecosystem and human health (Gideon & Faggio, 2019). Microplastics are any plastic that is less than 5 mm. However, plastics of less than 1 μm have been reported and they are easily eaten by zooplankton and transferred through the whole trophic web (Robledo et al., 2019). Many types of research resulted that the presence of plastics and microplastics in the marine environment are eaten mistakenly as food by many species and furthermore, toxicants attached to the microplastics are transferred to other organisms (Baldwin et al., 2020).

### *2.2.3. Heavy/Toxic Metals*

Heavy metals are inorganic toxicants affecting the aquatic ecosystem and humans even in trace quantities. Arsenic, aluminum, cadmium, copper, chromium, lead, iron, zinc, mercury, and nickel are the most concern for aquaculture. Heavy metal is most toxic in its free (hydrated and dissolved) metal ions form in an aquatic ecosystem (Water & Management, 2000). Heavy metals are much concerned due to their toxicity, persistence, non-degradability, and posing potential risks to the environment and human health. Mine tailing (waste leftovers of mineral extraction from rock) is the main source of heavy metals (Häder et al., 2020). Seafood consumption (e.g. fish and shellfish) is the main source of toxicity with heavy metals with the level of concentrations that pose risk to human health (Lloyd-smith, 2018).

### *2.2.4. Organic Pollutants*

Organic pollutants are types of chemicals such as detergents, surfactants, petroleum hydrocarbons, pesticides, polychlorinated biphenyls, and phenolic compounds. Organic pollutants are generated from different human activities such as domestic, agriculture, industrial, and aquaculture activities (Water & Management, 2000). Organic pollutants are toxic compounds that persist in the environment for a long time. Organic pollutants bio-accumulate in different organisms such as aquatic species and can move through the food chains (Lloyd-smith, 2018; Wells, 2020). Many studies reported that different disease developments in humans (cardiovascular, diabetes, and neurodegenerative) could be due to exposure to organic pollutants (Wu et al., 2020).

### *2.2.5. Crude Oil Spills*

Oil spills accidents from tankers, runoffs, boats, and harbors can destroy and harm the marine environment and result in economic losses (Water & Management,

2000; Alameri et al., 2019). Crude oil spills consist of mixtures of thousands of hydrocarbon substances (Alameri et al., 2019; Lloyd-smith, 2018). Polycyclic aromatic hydrocarbons (PAHs) are an important component of crude oil. PAHs accumulate in the marine water and soil for a long time and pose many risks to aquatic organisms (Lloyd-smith, 2018). Researchers have worked on studying seafood contamination with PAHs and their associated human risks for decades. PAHs have been a great environmental concern since they have proto-carcinogenic/ carcinogenic properties (Farrington, 2020). The weathering and degradation processes mainly influence the toxicity of spilled oil on marine organisms. Since weathering processes change the characteristics of the oil components over time ( Singh et al., 2020).

### 2.3. Sources of Marine Toxicants

The main sources of marine pollution are 44% from land via runoffs and wastewater discharges, 33% from the atmosphere via airborne emissions from land, 12% from shipping activities and accidents, 10% from sewage and solid waste dumping, and 1% from offshore mining (Potters, 2013). Demographic expansion along with industrialization especially in coastal areas and river banks increases the anthropogenic pollution generation causing numerous serious environmental problems (El et al., 2018). River networks ease the transport of toxins into the oceans (Lloyd-smith, 2018). Sewage wastewater discharge from industrial, municipal, households are either partially treated or untreated, and they pose many risks to the marine ecosystem. The degree of risks depends on the type of discharged wastewater, the volume, and the predominant hydrographic regime of the sites. Usually freshwater, sediments, nutrients, pathogens, and endocrine disruptors are the main component of sewage discharge (Häder et al., 2020). Mine tailing is the main source of the heavy metals contaminant. Storing the tailing near the coastal areas release metal toxicants contaminant to the

sediments and the marine biota especially in the intertidal zones (Häder et al., 2020). Sediments that are contaminated with heavy metals and hydrophobic organic compounds are hardly remediated (Water & Management, 2000).

### 2.4. Effect of the Toxicants on the Marine Organisms

Many researchers studied the effect of the anthropogenic toxicants on fertilization in marine spawning invertebrates due to that the early life stages of organisms are much more sensitive to toxicants than the adult organisms. Most of the studies proved that there was a high reduction in fertilization due to the toxicants and this led to high concern of the long-term effects on the population of the spawners (Marshall, 2006). Marine mammals affected by toxicants challenge the reduction in individual viability and reproduction, and population persistence is also threatened. Some toxicants such as PAHs bio-accumulate in the blubber and tissues of mammals with different patterns between males and females due to the vertical toxicant transfer from mother to offspring (Noonburg et al., 2010; Kottuparambil & Agusti, 2020). Chemical toxicants are well known for increasing the susceptibility of marine organisms to infections and diseases (Matranga, 2006). Toxicants negatively affect marine organisms causing birth morbidity and many fatalities. Most toxicants disrupt the nervous system whereas other toxicants affect protein phosphorylation and disrupt synaptic transmission (Tubaro et al, 2012).

### 2.5. Consumption of Aquatic Foods and Human Health

Seafood is highly consumed by people all around the world and is well known for its nutrients beneficial. However, the consumption of seafood species stuffed with accumulated toxicants could lead to several devastating diseases (Matranga, 2006). Marine toxicants are cooking and freezing resilient and cause intoxications with different effects which are mostly lethal. Several hazards to human health have been

related to shellfish food poisoning such as paralytic effects, amnesic, neurotoxic, and diarrheic (Daguer et al., 2018). Toxicants such as heavy metals and organic compounds accumulate in many aquatic species' bodies such as in bivalve mollusks; hence the World Health Organization (WHO) considers several codes and measurements to protect consumers. The WHO measurements for aquatic species are based on the Acceptable Daily Intake (ADI) or Acceptable Weekly Intake (AWI). The biological contamination is measured by the concentration of contaminant in water (cells/L) or by the level of consumption of the edible tissue (mg/Kg) (Water & Management, 2000).

### 2.6. Biological Markers (Biomarkers) of Oxidative Stress

The National Institutes of Health defined the term biomarker as "*a characteristic that is objectively measured and evaluated as an indicator of normal biological processes, pathogenic processes, or pharmacological responses to a therapeutic intervention*" (Zhang et al., 2001; Ho et al., 2013). In healthy organisms, different biological processes result in redox reactions that result in generating potential harmful reactive oxygen species (ROS), such as peroxide and free radicals. The ROS is formed and scavenged continuously in cells (Qu et al., 2019). Many studies resulted that living organisms use free radicals, such as the superoxide anion radical ($*O_2$), hydrogen peroxide ($H_2O_2$), peroxyl radicals (*ROO), and nitrogen oxide (*NO) for the advantage of biological effects. However, some of the leached ROS can result in damaging the cellular components of the organism. ROS accumulation can cause damage to cell structure, lipid, proteins, and nucleic acids and furthermore cause dysfunction of the whole immune system. Many enzymatic and non-enzymatic antioxidants mechanisms work as a protective method in the biological systems against oxidative damage. (Valavanidis et al., 2006). In the oxidative phosphorylation process, the leached electrons either reduce molecular oxygen incompletely to active oxygen or

reduce it completely to water. At the same time, many antioxidant enzymes work to stop these reduction processes, such as catalase (CAT) and glutathione peroxidase (GPx), which neutralize $H_2O_2$ to water and lipid peroxides to their corresponding alcohols. Superoxide dismutase (SOD) which neutralizes superoxide radicals to ($H_2O_2$). The glutathione reductase (GR) is used to convert the oxidized glutathione to the reduced glutathione and glutathione-S- transferase (GST) is used for exogenous xenobiotics removal (Bal et al., 2021). Exposure to toxicants can cause inequity in the concentration of ROS, leading to many oxidative stresses in the tissues which could lead to cytotoxicity and genotoxicity and many diseases; such as cancer, atherosclerotic cardiovascular disease, respiratory system (lung) diseases, chronic inflammatory including type 2 diabetes mellitus (Lowe, 2014). In general, biomarkers of oxidative stress are categorized by (1) molecules that undergo modification when interacting with ROS in micro-environments and (2) molecules of the antioxidant system that change due to the increase in redox stress (Ho et al., 2013). Several methods are developed to identify the quantity and nature of oxidative stress of diseases in DNA, proteins, lipids, carbohydrates, and amino acids (Frijhoff et al., 2015). The most favorable biomarker analysis is the one correlated with the pathophysiological process of the diseases (Ho et al., 2013). Oxidative stress markers are catalase (CAT), glutamine-S-transferase (GST), superoxide dismutase (SOD), lipid peroxidation (LPO), and immunotoxin effects ( Cao et al., 2018). Oxidative stress in marine bivalve species is influenced by seasonal and environmental conditions. The enzymes play a vital role in protecting the marine bivalve species against the ROS produced during exposure to environmental toxicants or abiotic factors (Concetta et al., 2020).

### *2.6.1. Superoxide Dismutase (SOD)*

Superoxide dismutase (SOD) is an antioxidant enzyme that exists in all

organisms and plays an important and crucial role in protecting the biological systems against leached free radicals. (SOD) acts as a first-line defense system component against reactive oxygen species (ROS). SOD converts radicals such as superoxide radical ($*O_2$) or singlet oxygen radical ($^1O_2^-$) that are generated in organs through cells metabolism to hydrogen peroxide ($H_2O_2$) and molecular oxygen. However, accumulated $H_2O_2$ is toxic to body cells and tissues. SOD requires a metal cofactor for its activity such as iron (Fe), zinc (Zn), copper (Cu), and manganese (Mn). (Ighodaro & Akinloye, 2018).

### *2.6.2. Catalase (CAT)*

Catalase (CAT) is an antioxidant enzyme that exists in all aerobic organisms. CAT enzyme converts hydrogen peroxide ($H_2O_2$) to water ($H_2O$) and oxygen ($O_2$) in terms of reducing the ROS levels and stopping the death of the cells and tissues. In animals, the *CAT* gene controls CAT enzymes (Raza et al., 2021). In enzymology, CAT is one of the highest and fastest turnover numbers and rates of all enzymes. CAT molecules can turn millions of $H_2O_2$ to water and molecular oxygen ($O_2$)in one second (Nicholls, 2016). CAT uses Iron (Fe) or manganese (Mn).

### *2.6.3. Glutamine-S-Transferase (GST)*

Glutathione transferase (GST) is a protein, which acts as an enzyme and as a binding protein in many detoxication processes. GST is localized in the cytosol and the endoplasmic reticulum (Sandamalika et al., 2019). GST is one of the most important detoxication enzymes. It catalyzes glutathione to electrophilic compounds, which are produced from exogenous xenobiotics through biotransformation and from endogenous substances. (Tsuchida, 1997). GST is induced mostly in the hepatopancreas of shellfish since the hepatopancreas is believed to be a major site of toxins accumulation ( Chen et al., 2011).

### *2.6.4. Glutathione Peroxidase (GPx)*

As mentioned earlier, the antioxidant defense system in tissues and cells consists of antioxidant enzymes. These enzymes play an essential role in cellular homeostasis maintenance and antioxidant defense by removing the excess ROS from the cells (Jo et al., 2008). GPx is well known for its ability to eliminate $H_2O_2$, which is generated by the action of the first antioxidant line (Freitaset al., 2020).

### *2.6.5. Lipid Peroxidation (LPO)*

Lipid peroxidation (LPO) is the main chemical process in the oxidative stress associated with pathogens (Repetto et al., 2012). LPO is a process where oxidants such as free radicals or nonradical species attack lipids which contain unsaturated carbon-carbon double bonds (e.g. polyunsaturated fatty acids) (Ayala et al., 2014). LPO is a marker for oxidative damage of cell membrane in invertebrates and causes the loss of cell function. LPO is commonly estimated as malondialdehyde levels (MDA) or thiobarbituric acid reactive substances (TBARS) and is usually used to study the adverse effects of contaminants on the bivalve mollusks (Zanette et al., 2011).

## 2.7. Ecotoxicology of Oysters

Bivalve mollusks such as oysters have been recently used in many ecotoxicological studies as sensitive bioindicators for aquatic pollutants. Oysters can accumulate pollutants, hence giving scientists a vital bioindicator for phenolic compounds. Variations in pollutant concentrations in bivalves have been related to the bioavailability of pollutant and the biological variables such as sex, weight and reproductive cycle (Valavanidis et al., 2006). Usually oxidative stress occurs due to different seasonal events, nutriants availability, temperature, reproductivity cycle and other environmental factors (Concetta et al., 2020). The digestive glands of oyster are the main organ for toxin accumulation and detoxification (Cao et al., 2018). Hence,

many researchers investigated and measured the physiological and biochemical parameters in this tissue. Oysters have been used in many ecotoxicological studies, in terms of deducing the temporal and spatial contaminations in aquatic environments. They accumulate contaminants through body surfaces and feeding. Hence, they are ideal for ecotoxicological studies (Opiyo et al., 2021).

## 2.8. Phenol Properties and its Potential for Contamination

### *2.8.1. Phenol Properties*

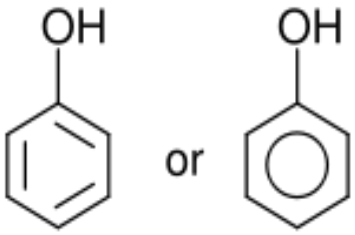


Figure 1: Structure of Phenol.

Phenol (phenic acid or carbolic acid) is a hydroxybenzene compound that is used in many common products such as preservatives, disinfectants, and plasticizers (Meena et al., 2015; Rolland et al., 2020). Natural or anthropogenic phenols are planar organic compounds formed of a six-carbon aromatic (benzene) ring and attached with a hydroxyl group (–O–H) (Stewart et al., 2008). Phenol at normal temperature and pressure is crystalline solid and white when pure. Phenol is highly soluble in ether, ethyl alcohol, hydrocarbons (e.g. benzene), and other polar solvents. However, it is low soluble in water and works as a weak acid. Liquid phenol is corrosive toward plastic, rubber, and coatings. Whereas, hot liquid phenol attack several metals such as lead, aluminum, magnesium, and zinc. Phenol is a combustible compound and is

characterized by a tar-like odor (Busca et al., 2008). The different physicochemical properties are the main cause of the adsorption and extraction difficulties of Phenol. This is mainly occurring at low Phenol concentrations. Many types of sorbents are available but not efficient in Phenol sorption, hence many researchers are working on using and developing new and better materials (Sobiesiak, 2017). Some physical and chemical properties of phenol are shown in Table 1.

Table 1: Chemical and Physical Properties of Phenol ("TOXICOLOGICAL PROFILE FOR PHENOL," 2008)

| Property | Information |
|---|---|
| Molecular weight | 94.111 |
| Color | Colorless to light pink |
| Physical state | Crystalline solid-liquid (w/ 8%$H_2O$) |
| Melting point | 40.89 °C |
| Boiling point | 181.87 °C |
| Density at 20 °C/4 °C | 1.0545 at 45 °C/4 °C |
| Vapor density | 3.24 |
| Odor | Distinct aromatic, somewhat sickening, sweet and acrid odor |
| Solubility: | |
| Water at 25 °C | $8.28 \times 10^4$ mg/L |
| Organic solvent(s) | Soluble in water and ethanol, very soluble in ether, miscible with acetone and benzene |
| Partition coefficients: | |
| Log $K_{ow}$ | 1.46 |
| Log $K_{oc}$ | 1.21-1.96 |
| Vapor pressure at 25 °C | 0.35 mmHg |
| Henry's law constant | $3.0 \times 10^7$ atms $m^3$ mol |
| Autoignition temperature | 715 °C |
| Flashpoint, open cup | 85 °C |
| Flashpoint, closed cup | 79 °C |
| Flammability limits (in air by %v) | 1.7-8.6 % |

atm= atmosphere; v= volume; w= weight

### *2.8.2. Phenol Potential for Contamination*

Phenol along with its derivatives from anthropogenic activities poses negative impacts to human and aquatic ecosystem health. Since phenol (phenylic acid, carbolic acid, and phenic acid) and its derivatives such as nitrophenol, chlorophenol, and bisphenol A are widely used in several industrial sectors (petrochemicals, pharmaceuticals, plastics, steel manufacturing, and food processing) and due to its toxic nature, many reports and studies have addressed the environmental importance of the phenolic pollution (Raza et al., 2019). Many epidemiological studies concluded that the concentration of phenolic compounds is higher in women than men due to the high consumption of cosmetics and care products (Jamal et al., 2020). Hence the toxicity of phenol is mostly concerned due to its significant effects on pregnant women and fetuses (Chao et al., 2020). Phenol is a priority pollutant by US Environmental Protection Agency (USEPA) because it is toxic, carcinogenic, and mutagenic (Agostini et al., 2011). Phenols pose many genotoxic effects to animals and humans such as neurotoxicity, respiratory effects, liver and kidney malfunction and growth retardation. Phenol accumulate in aquatic organisms and transport through the food chain (Agostini et al., 2011).

## 2.9. Presence of Phenol in AquaticEenvironments

Phenol as mentioned earlier is toxic, carcinogenic, and mutagenic. Continuing exposure to phenol affects the central nervous system and damages the lungs and the kidneys. Hence, phenol is classified as class 2 water hazardous pollutants in many countries (Iurascu et al., 2009). Since the concentration of 1 mg/L or above affects the aquatic ecosystem and may result in affecting human health, the release of phenol in the aquatic environment through wastewater discharges is globally restrictive. And the limit of phenolic effluent discharge is limited to less than 0.5 mg/L (Agostini et al.,

2011). The World Health Organization (WHO) reports stated that the total phenol content of water to be chlorinated should not exceed 0.001 mg/L (WHO, 2011). Guidelines for chemical compounds in water that contaminate the fish flesh and other aquatic organisms estimated the phenol threshold level in water by 1.0–10.0 mg/L. Table 2 shows levels of toxicity that affect and cause mortality of some aquatic species. Reports indicate the presence of phenol in aquatic organisms resulting in the food chain bioaccumulation (Water & Management, 2000).

Table 2: Test End-Points Reported in the Literature for Aquatic Organisms Exposed to Phenol.

| Species group | -Common name<br>-Scientific name | -Effect<br>-Test endpoint | Toxic concentrations (mg/L) | References |
|---|---|---|---|---|
| Fish | -Hooknose<br>-Agonus cataphractus | Mortality<br>96 h *LC50 | 10 | (Franklin, 1980) |
| | -Minnow<br>-Phoxinus phoxinus | Mortality<br>96 h LC50 | 9.5 | (Oksama & Kristoffersson, 1979) |
| | -Mozambique tilapia<br>-Oreochromis mossambicus | Mortality<br>96 h LC50 | 19 | (Burbank, 1970) |
| | -European flounder<br>-Platichthys flesus | Mortality<br>96 h LC50 | 20.94 | (Smith, Furay, Layiwola, & Filho, 1994) |
| Crustaceans | -Sand Shrimp<br>-Crangon crangon | Mortality<br>48 h LC50 | 10-33 | (Franklin, 1980) |
| | -Scud<br>-Gammarus duebeni | Mortality<br>96 h LC50 | 89.5-183.2 | (Oksama & Kristoffersson, 1979) |
| Mollusks | -Marine bivalve<br>-Katelysia opima | Mortality<br>48 h LC50<br>96 h LC50 | 128<br>117 | (Duan et al., 2018)<br>(Dange and Masurekar, 1985) |

*LC: Lethal concentration 50

### *2.9.1. Sources*

Phenol is mostly generated from the distillation of fossil fuels and the degradation of pesticides (Water & Management, 2000). Phenol genotoxic effects are frequently observed in areas of the petroleum industry (Agostini et al., 2011). The main natural sources of phenol in the aquatic marine ecosystem are animal wastes and organic wastes from anthropogenic activities, mostly wastewater from manufacturing industries such as plastic, adhesives, resins, rubber,…etc. and wastewater discharges from synthetic fuel industries ("TOXICOLOGICAL PROFILE FOR PHENOL," 2008).

### *2.9.2. Phenol as Potential Contaminant of Marine Oyster*

Oysters as part of the bivalves' family accumulate toxicants in their tissues. Hence, they are considered dependable references for marine toxicant concentration and used in environmental risk assessment (Acosta et al., 2015). Oysters are exposed to several organic toxicants from different chemical families. Some of these toxicants are regulated and have been found at far lower concentrations than the regulatory thresholds. However, there is a lack of data for some other organic toxicants from several sources such as toluene, xylene, ethylbenzene, and phenols from offshore oil industries, accidental spills, water process, mine tailing process, and illegal discharges (Amiard et al., 2011).

## 2.10. Phenol Removal Technologies

The technologies used for phenol removal from industrial wastewater are classified as conventional and advanced techniques. Steam distillation, adsorption, liquid-liquid extraction, solid-phase extraction, biodegradation, wet air oxidation, and catalytic wet air oxidation are the conventional techniques used for phenol removal. Whereas, electrochemical oxidation, membrane processes, photo-oxidation, Fenton

reaction, ozonation, UV/$H_2O_2$, and enzymatic treatments are advanced technologies used for phenol removal (Villegas et al., 2016). The dvantages and disadvantages of some of these technologies are listed in Table 3.

Table 3: Advantages and Disadvantages of Some Phenol Removal Technologies.

| Removal Technologies | Advantages | Disadvantages | References |
|---|---|---|---|
| Distillation | High enthalpy<br>High activity<br>Economical<br>Ecofriendly | High energy demand | (Villegas et al., 2016) |
| Adsorption | Simple<br>Wide range of adsorbents<br>High removal efficiency | High cost for *AC adsorbent<br>Low adsorptive capacity for AC alternatives | (Kulkarni, 2013)<br>(Le et al., 2020)<br>(Khraisheh et al., 2020) |
| Solvent extraction | Simple technique | High Cost<br>Hazardous by-products<br>High solvent consumption | (Shaban et al., 2013)<br>(Gharaati, 2019) |
| Membrane separation | Reliable<br>Economically feasible<br>Low Energy demand<br>High quality effluent | Membrane fouling | (Villegas et al., 2016) |
| Reverse Osmosis | Low energy demand<br>High packing density<br>Low thermal damage | Pressure fluctuation<br>Clogging | (Mujtaba, 2017)<br>(Anwar et al., 2021) |
| Enzymatic methods | High efficiency<br>Low cost | Non- reusability<br>Instability in harsh conditions | (N. Singh & Singh, 2007) |

*AC: Activated carbon

### *2.10.1. Adsorption Technology*

Adsorption is considered a surface phenomenon and is also known as adsorbent-adsorbate interaction. Amongst numerous water purification and recycling technologies, adsorption is considered the fastest, cheapest, and most common method.

Inexpensive adsorbents are available in nature and they can be used for the removal of pollutants with a removal efficiency of 90–99% (Ali & Gupta, 2006). Adsorption can be applied for water purification and many industrial purposes. In the adsorption process interaction of pollutant (adsorbate) by adhering to the solid surface (adsorbent) occurs. This interaction is affected by many parameters such as temperature, nature of adsorbate and adsorbent, pH, size of the particle, and many other experimental conditions (Dotto & Mckay, 2020).

### *2.10.2. Adsorbents*

Adsorbents are the key elements of the adsorption process. Choosing, developing, and characterization of the adsorbent control the adsorption process. Hence, it is vital to find the most suitable adsorbent with specific criteria such as (low cost and availability, chemical and mechanical stability, good textural and physicochemical characteristics, high adsorption capacity, high efficiency, fast kinetics, and potential for regeneration and reuse) (Dotto & Mckay, 2020). Table 4 summarizes some adsorbents used in phenol removal with their % Removal.

Table 4: Comparative Adsorption % Removal of Phenol by Different Adsorbents.

| Adsorbent | Substrate | % Removal | Reference |
|---|---|---|---|
| Biochar (Pin wood) | α-FeOOH | 100 | (Zhao et al., 2022) |
| Silica nano particles (from rice straw) | Peroxidase (from rice straw) | 99.92 | (Naguib & Badawy, 2020) |
| Clay mineral (Kaolinite) | Sphingomonas sp. GY2B | 96 | (Gong et al., 2016) |
| Clay (Diatomit) | Aluminum chloride/ Cationic surfactants | 99 | (Musleh et al., 2014) |
| Natural phosphate ore (hydroxyapatite) | Aluminum oxide | - | (Bouiahya et al., 2019) |
| Activated Carbon | Iron | 98 | (Majid et al., 2019) |
| Pumice (raw) | - | 89.14 | (Heydari & Karimyan, 2018) |
| Pumice (Activated) | Manganese | 100 | (Heydari & Karimyan, 2018) |
| Nano-zeolite | Iron | 82.5 | (Le et al., 2020) |
| Calcium carbonate | Catechol | 70 | (Shan et al., 2007) |
| Calcium carbonate (Pearl oyster shell) | - | 36.98 | Current study |
| Calcium carbonate (Pearl oyster shell) | Silver | 25.89 | Current study |

## 2.11. Nanotechnology

According to the definition of the “National Nanotechnology Initiative”, the term nanotechnology can be applied for any maneuvering of materials possessing at least one dimension sized 1 to 100 nm (Ganji & Kachapi, 2015). Therefore, all sorts of studies that deal with the properties of matter below the stated size are described as nanotechnology. Dealing with such a tiny size, (approaching the molecular scale), enhances the ability to manufacture highly functioning products from the bottom up by using new techniques and tools. Nanotechnology is a revolutionizing and interesting technology with great benefits to human beings (Cruz et al., 2020). The scale of nanotechnology covers several science fields such as organic chemistry, physics, medical diagnostic, molecular engineering, molecular electrons, surface science…etc.

These days, nanotechnology dominated plentiful sectors such as food, medicine, electronics, solar and fuel cells, chemical sensors, sporting products …etc. (Dutta & Das, 2020)

### *2.11.1. Nanomaterials (nanoparticles, NPs)*

Nanoparticles, and as per the previous definition are materials that have one of the dimensions being less than 100 nm (Ganji & Kachapi, 2015) (Subramani et al., 2019). Nanomaterials with these nanoscale dimensions, thus, have specific properties (e.g. photoemission, optical, catalytic activity, and antimicrobial activities). These properties have the capability of improving characteristics such as permeability, hydrophilicity, selectivity and mechanical properties. This issue, in turn, would expand the potential applications of NPs in many fields, like biomedical purposes, electronics, communications, and other fields. Nanoparticles made of metal or metal oxides are commonly used for this purpose (Chung et al., 2015). It has been estimated that there will be an increase in global nanomaterials production by half a million tons. These nanomaterials will be developed with specific characteristics and will be used in different applications and sectors (Albuquerqueet al., 2020).

### *2.11.2. Oyster Shell Adsorbent for Phenol Rremoval From Wastewater*

The most important mollusks used commercially are the ones that belong to the classes Bivalvia, Gastropoda, and Cephalopoda (Duncan & Coast, 2003). Edible (true) oysters are the type of oysters that have a central adductor muscle. The adductor muscle is the soft part (flesh) that is eaten with the visceral mass. The outer shell of the oyster is composed of several layers of foliated microstructure and lenses of calcium carbonate (chalk) (Checa et al., 2018). Bivalves such as clams, oysters, mussels, scallops, and cockles are the most known class in the food market. Bivalves' structure consists of paired shell controllers that are joined at a dorsal hinge and a sessile filter-feeding way

of life characterizes them. Bivalves' internal body contains adductor muscles (edible parts) for shell closure (Duncan & Coast, 2003), gills, a visceral mass including the digestive gland, the digestive and circulatory system and the gonads. Biogenic carbonates such as the oyster shell have been known for their advantages over the geological carbonate (Wu et al., 2014). Oyster shells consist of aragonite (natural crystal form of carbonate) which is very tough and strong but very light. Oyster shell composition is also high in magnesium and calcium carbonate phase and easily found since it is produced and consumed in thousands of tons yearly all around the world. An oyster shell can be used in different environmental and industrial applications because they have several geochemical and mineral properties. Oyster shell properties include high reactive surface area, absorbability, and exchange capacity (Wu et al., 2014; Lee et al., 2011). Many research studies applied waste oyster shells to remove different pollutants from wastewater such as dissolved cations: copper (Wu et al., 2014), fluoride (Chang et al., 2019), arsenic (Fan et al., 2015), natural organic matters (humic acids) (Alipour et al., 2014), boron (Tsai et al., 2011), and other anthropogenic pollutants. Although the different methods of oyster shell recycling used in these studies showed great efficiency in wastewater pollutant removal nevertheless, the methods used to generate many spent adsorbents, which are considered secondary pollutants. Hence, more effective methods needed to be investigated for the reusing and recycling of oyster shell waste (Tsai et al., 2011). Oyster shell composed of biogenic calcium carbonates ($CaCO_3$), which considered a great substituted to geological CaCO3 as an adsorbent. The main advantage of oyster biogenic $CaCO_3$ over the geological $CaCO_3$ is that it does not need mining and exploitation. Oyster shell biogenic carbonate has a twisted open aragonite structure and consists of three layers: the outer cuticle layer, which is composed of cutin and organic matter, the middle prismatic layer that forms the most

of the shell and finally the inner nacreous layer (Figure 2). Both prismatic and nacreous layers are made of >80% of $CaCO_3$ (Helm & Bourne, 2004; Wu et al., 2014). Oyster Shell is used in many environmental and industrial applications due to its mineralogical and geochemical properties. Oyster shell properties include high absorbability, reactive surface and exchange capacity (Wu et al., 2014).

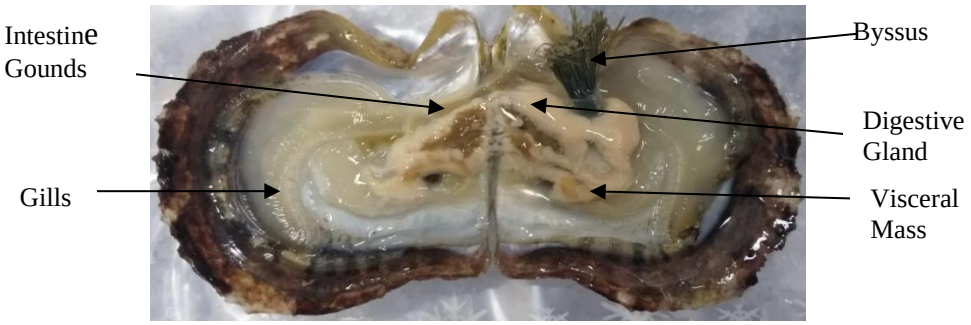


Figure 2: Internal features of shell valve of hard shell

*2.11.3. Why Calcium Carbonate/Silver (OSNP-S) is a Nanocomposite?*

Silver nanoparticles (Ag NPs) are metallic nanoparticles are considered feasible adsorbents with great chemical and physical characteristics. Ag NPs have high catalytic activity, biocompatibility, and high adsorption capacity, which is due to their high surface area. Ag NPs, can be easily separated and reused (El-tawil et al., 2019). Ag NPs have fascinated extensive researchers due to their countless beneficial applications. Ag NPs are used in surface-enhanced Raman scattering substrates (SERS), optical sensors, catalysts, and biomarkers. Ag NPs could reduce the environmental risks and potential adverse effects of chemical-based methods on the environment (Rahimi et al., 2020). To attain better performance and higher adsorption capacity, different techniques such as fabrication of metal/metal oxides, surface functionalization, and magnetic induction are used to modify adsorbents' surfaces. In this research, Silver ions were used to

modify calcium carbonate (oyster shell) due to the previous reasons and due to it is considered eco-friendly and cost-effective with no need for high pressure, temperature, energy, and toxic chemicals.

# CHAPTER 3: METHODOLOGY

## 3.1. Wild Pearl Oyster Sampling Site.

The wild Pearl oyster population investigated in this research was sampled in Al-Wakra oyster- beds in the subtidal zone between 5 and 7 meters depth (Figure 3).

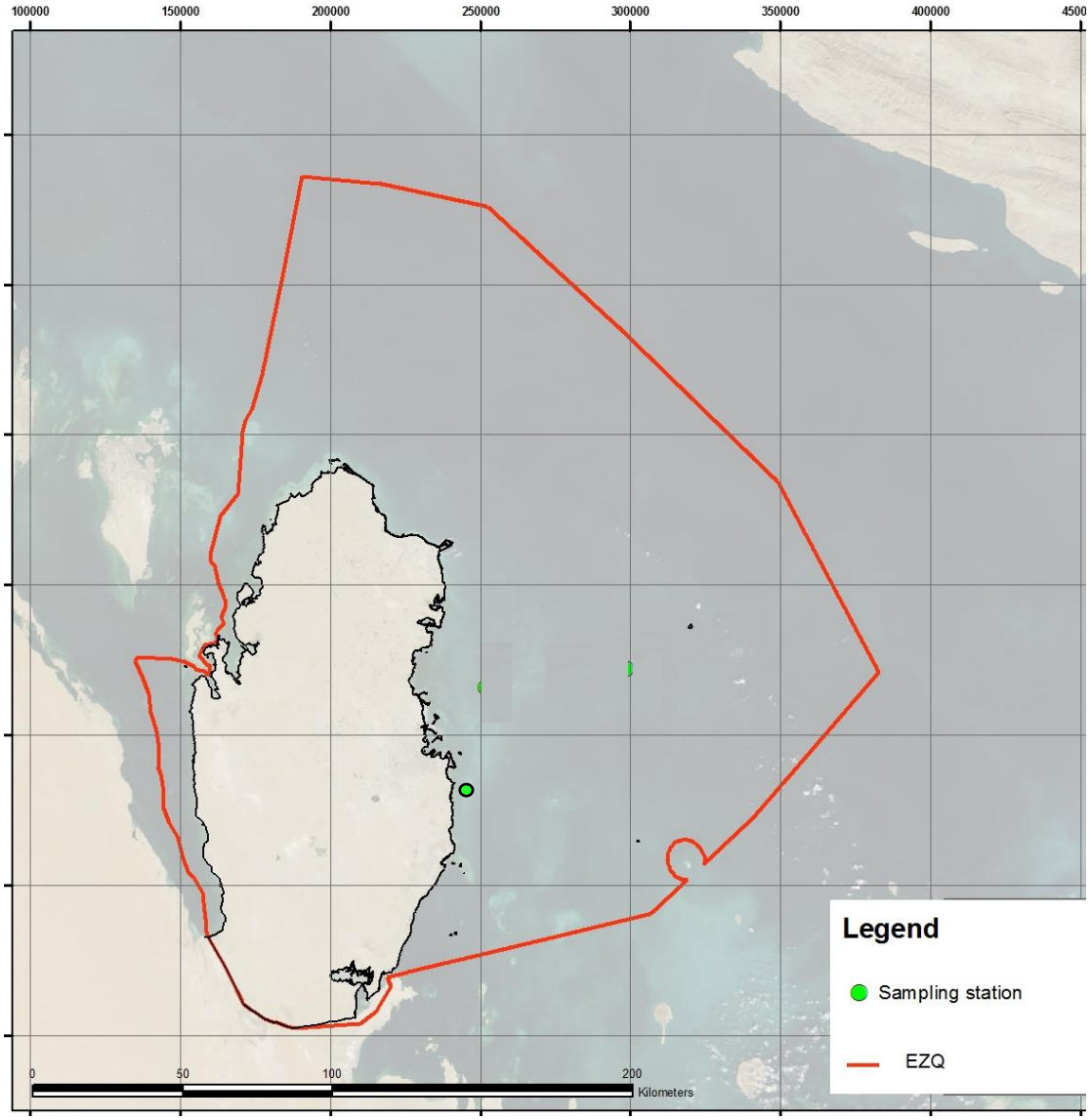


Figure 3: Marine map of Qatar showing the Economic Exclusive Zone (EEZ) and the Pearl oyster sampling site at Al-Wakra.

## 3.2. Chemicals and Materials

All chemicals were analytical grade and used without further purification. Phenol, silver nitrate ($AgNO_3$), ethanol and Sulfuric acid ($H_2SO_4$), sodium phosphate buffer, Triton X-100, and ultra-pure $H_2O$. Hydrochloric acid (HCl), and sodium hydroxide (NaOH) were used for the pH adjustment. For the ecotoxicology part, 15 aerated aquaria with dimensions of 60 ×40 × 30 cm, adigital Vernier caliper for the biometry analysis and ultratorax for homogenizing the tissues with buffer were used.

## 3.3. Ecotoxicology Part

### *3.3.1. Oyster Cultivation and Experimental Design*

Random samples of 300 oysters of the same sizes ranging from 50 and 70mm were transferred to the laboratory after removing the epiphytes attached to them and preparing them for cultivation. The oysters were prepared by adding running seawater for one day until the specimens were adapted to the laboratory conditions. The specimens were used for the phenol toxicity test. The specimen's culture was carried on by randomly placing 15 oysters in 5 individual aquarium tanks in triplicates as shown in the experimental design (Figure 4). Five treatments were used, control (seawater at 40 psu), 1 mg/L, 2 mg/L, 5 mg/L and 10 mg/L phenol. Seawater temperature, salinity, and pH of the tanks were maintained at 24 – 25 $^{o}$C (sampling temperature), 40 $\pm$ 1 psu salinity (Qatar water salinity), and pH 8.2 $\pm$ 0.1 (normal seawater pH). The seawater in the tanks was aerated. Prior to biomarker analysis, the adult oysters have been exposed to different concentrations of phenols during 96h in triplicates versus a control. Daily, three random oyster samples from each aquarium were anesthetized in ice at 0 $^{o}$C for 5-10 minutes, in terms of reducing the stress on the oysters and preserving their metabolic characteristics and activity. Each oyster was weighed by semi-analytical balance (0.01 g). The biometry (height, length, and width) of each sample was measured by using a Digital Vernier caliper (0.01 mm) before any

dissection and analysis.

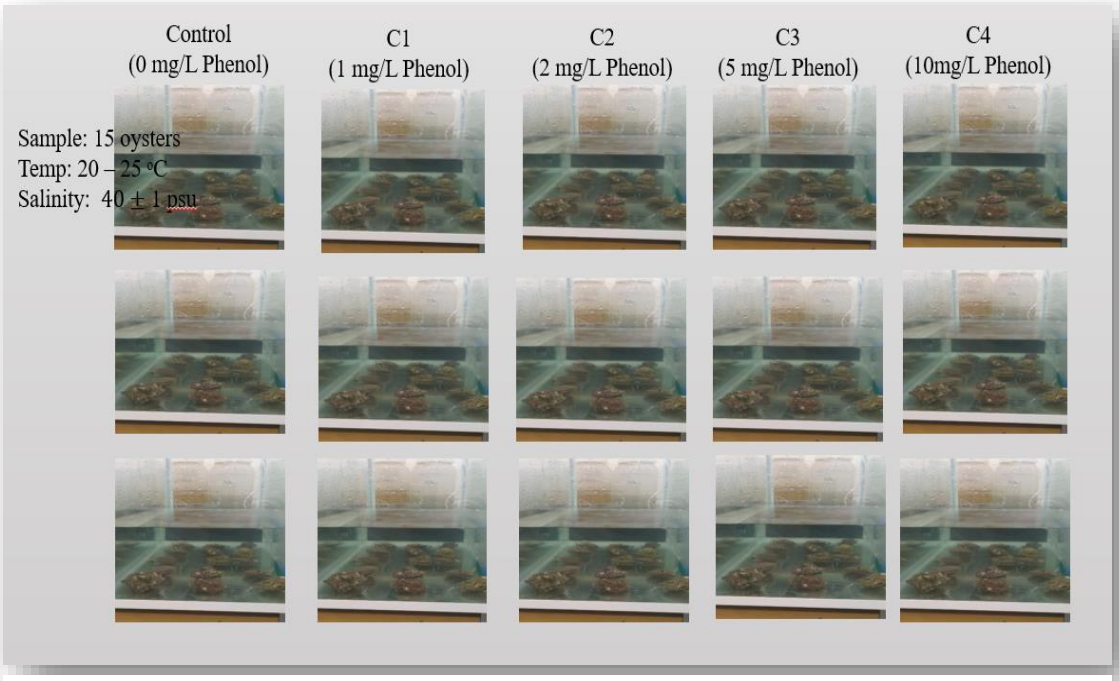


Figure 4: Oyster cultivation and experimental design.

### *3.3.2. Biometric Analysis of Oyster Population*

The biometry (height, length, and width) of each sample was measured by using a Digital Vernier caliper (0.01 mm). The biometry data was used for the analysis of the oyster population. Biometric relationship analyses were done on the length, width, and height of the oyster shell. Length-weight, width-weight, and height-weight relationships were analyzed through quadratic equations with the formula:

$$Y = aX^b$$

Where: Y = weight (g), X = the length or width or height (thickness) of the shell (cm), a (intercept) and b (slope) parameters.

The biometric data analysis was performed by using Microsoft Excel 2016. The growth model of the oyster samples (isometric or allometric), was determined by the value of

(b). Oyster growth is considered isometric if ($b = 3$) and allometric if ($b \neq 3$). If the value of ($b < 3$), then there is negative allometric and if ($b > 3$) there is positive allometric (Kalesaran et al., 2018). The composite of the Pearl Oyster *Pinctada imbricata radiata* was distributed into four separate size classes with lengths of 3.5-4.5; 4.5-5.5; 5.5-6.5, and 6.5-7.5 cm, respectively.

### *3.3.3. Biomarker Analysis and Oxidative Stress*

During the experiment, the gills and digestive glands of each oyster sample were weighed and were kept for biomarker and oxidative stress analysis. The gills and digestive glands tissues from each *Pinctada imbricate radiata* sample were taken and homogenized at 4 °C using an ultratorax in a phosphate buffer solution (100mM) containing: Solution (A): 35.8 g of $Na_2HPO_4$ .$12H_2O$ (358 g.mol-1) in 1 liter of ultrapure distilled water and solution (B): 3.4g of $KH_2PO_4$ (136 g.mol-1) in 250 ml of ultrapure water. Then, solution (A) was adjusted to pH 7.8 with solution (B). Finally, 0.1% of Triton X-100 (e.i: for 50 mL add 50µL) is added to the Phosphate Buffer Solution and mixed well with a magnetic bar. The homogenate was centrifuged at 9000 g for 30 min at 4 °C. Furthermore, the resulting supernatant was divided into several aliquots and was stored at -80 °C until total protein and biomarker analysis.

#### *3.3.3.1. Total Protein*

The protein content of all samples was analyzed according to the Bradford method (Bradford, 1976), by using 50 µL sample protein and bovine serum albumin as a standard. The measured parameters were normalized for the total protein concentration of each sample. The assay was analyzed in a microplate reader using 96 well plates and concentration proteins were expressed in mg/g wet weight.

#### *3.3.3.2. Catalase (CAT) Activity Measurement*

Catalase (CAT)is an enzyme that catalyzes the decomposition of $H_2O_2$ formed by Superoxide dismutase (SOD) in molecular water ($H_2O$) and molecular oxygen ($O_2$). CAT activity was estimated through the quantification and the rate of disappearance of $H_2O_2$ at 240 nm for 20 min (Claiborne, 1985). 50 µL of the sample was added to 50 µL of 30% $H_2O_2$ and 950 mL of 75 mM phosphate buffer at pH = 7: the results are expressed as CAT activity in U/mg protein

#### *3.3.3.3. Superoxide Dismutase (SOD) Activity Measurements*

SOD activity was measured according to (McCord & Fridovich, 1969) as follow: 10 µL of sample sample was combined with 1960 µL of $Na_2CO_3$/$NaHCO_3$ buffer (50 mM) at a pH = 10.2 and 10 µL of catalase bovine with 20 µL of epinephrine. The SOD activity was measured at 480 nm using a spectrophotometer and expressed as SOD activity in U/mg protein.

### *3.3.4. Statistical Analysis*

Excel 2016 was used for all statistical analyses. All data were expressed as means ± standard deviation (SD) of duplicate experiments (n = 2). The statistical analysis of data to test the effects of phenol concentrations were performed by two-way ANOVA in term of verifying the significant differences between the dose concentrations (ppm) and time (hr) versus controls. Data were log-transformed to meet the ANOVA assumption significant when $p \leq 0.001$.

## 3.4. Adsorption Part

### *3.4.1. Oyster Shells Collection and Preparation for Adsorption*

To prepare the adsorbent for the phenol adsorption experiment, oyster shells intended for waste disposal were collected from a local pearl diver. The fresh organic part (flesh) of the oyster was removed and the shell was soaked in 50% sulfuric acid to dissolve any organic matters attached. Then the shells were scrubbed cleaned and washed several times with alcohol and ultra-pure water to remove sand and other impurities. Finally, the oyster shells were air-dried at 60 $^{o}$C overnight. The raw oyster shell was then powdered grinned and sieved through 0.125 mm (125 μm) mesh particle size then dried again at 60 $^{o}$C overnight, stored, and kept for ball milling (type of the instrument).

### *3.4.2. Preparation of Oyster Shell Nanoparticle, OSNP*

Ball milling was used as a physical process to prepare the nanoparticles. The row oyster shell was ball milled in CryoMill grinder for 48 h at 800 RPM by using mixed agate balls (15×6 mm and 7×8 mm) in 4×50 ml agate jars.

### *3.4.3. Modification of OSNP With Silver*

The silver-activated oyster shell nanoparticles OSNP-S were prepared by reacting 10 g of OSNP and 5.7 g KOH with 100 mL distilled water for 1 h at a temperature of 60 °C in term of changing the OSNP surface to negative charge . Then, 1.695 g of $AgNO_3$ was added to the solution for another 1 h. After that, the resulting solid was again reacted with 5.7 g KOH for another 1 h and then the formed brown solid (OSNP-S) was left overnight for further oxidation. The OSNP-S was washed with plenty of water to remove the excess alkaline, centrifuged for 15 min at 4000 RPM,

dried at 60°C for overnight, and stored in glass bottles for analysis and further experiments (Alhaddad et al., 2021).

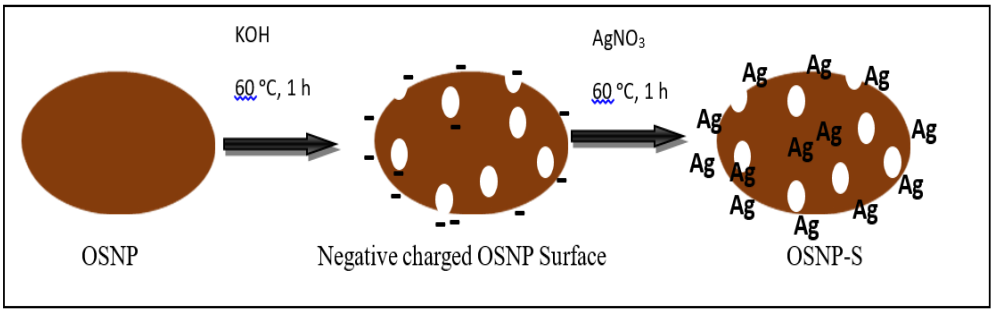


Figure 5: Proposed mechanism of OSNP-S formation.

### *3.4.4. Characterization of OSNP and OSNP-S*

The physical and chemical characterization of OSNP and OSNP-S were determined by using different instruments (SEM, BET, FTIR, and TEM). SEM is a multipurpose instrument used for the characterization of 2D and 3D materials. It is used to characterize the physical properties of different materials by measuring the particle size and describing the morphology and the aspect ratio (Hassan et al., 2020). In this research paper, images of OSNP and OSNP-S before and after adsorption were taken by using Nova nanoSEM 450 at a 5kV voltage and 5–100 microns to characterize their physical properties. In this research paper, OSNP and OSNP-S adsorbents were prepared; and to determine their pore surface area distribution along with the particle size before and after phenol adsorption, Brunauer–Emmett–Teller (BET) model Aim Sizer-AM301 was used. BET Theory seeks to explain the physical adsorption of gas molecules onto solid surfaces. The BET equation was applied to the P/Po ranges of the $N_2$ isotherms.

$$\frac{1}{V\left[\left(\frac{P_\circ}{P}\right)-1\right]}=\frac{C-1}{VmC}\left(\frac{P}{P_\circ}\right)+\frac{1}{VmC}$$

Where $V$ = adsorbed gas quantity, $P_\circ$ = saturation pressure of adsorbate, $P$ = equilibrium pressure of adsorbate and $C$ = BET constant.

To study morphology and functional groups of the adsorbents OSNP and OSNP-S before and after adsorption, Fourier-transform infrared spectrophotometer (FTIR) was used. The spectra were collected from 4000 to 400 $cm^{-1}$ with a Spectrum 400 FTIR PerkinElmer- UATR. The size and shape of the nanoparticles were analyzed by using a transmission electron microscope (TEM) Make-FEI; Model-Tecnai G2 FEG 200 KV. The pH of the solutions was examined.

### *3.4.5. Phenol Solutions Preparation*

For the adsorption experiment part, phenol stock solution (1000 ppm) was prepared in ultra-pure distilled water. Then different experimental solutions were prepared by diluting the stock solution to the different concentrations, namely 5, 10, 15, 20, 30, 40, 50, 60, 80, 100 mg/L. The final phenol concentrations were measured by using UV-1900i UV/Vis spectrophotometer.

### *3.4.6. Batch Adsorption Experiments*

A batch system was used to carry out the adsorption study by using a 100 mL lab bottle under different pH values, temperature, and initial phenol concentrations. For each bottle experiment, 50 mL phenol stock solution and 0.1 N HCl or 0.1 N NaOH were used to adjust the pH, and then the OSNP or OSNP-S adsorbent was added (0.05 g). Two trials and a blank of each batch experiment were conducted to ensure quality control. The samples of each batch experiment were stirred under a constant speed of 165 rounds per minute (rpm) for 24 hrs. After each batch experiment, filtration was carried out. The filtered solutions were analyzed under a UV/VIS spectrophotometer to determine the final concentration. The filtrate (adsorbents) was kept at room temperature for dryness and further analysis using SEM, FTIR, surface area, porosity,

and bulk density techniques. The adsorption process was studied as a pH (2, 4, 6, 8 and10), temperature (25°C, 35℃ and 45℃), initial phenol concentration (5, 10, 15, 20, 30, 40, 50, 60, 80 and 100 mg/L) and adsorbent dose (0.05 g/L) for 24 h. The adsorption capacity (q, mg/g) and percentage removal was calculated by using the following equations:

$$q_e = \left[\frac{C_0 - C_e}{M}\right] \times V$$

$$\%\, removal = \left[1 - \frac{C_e}{C_0}\right] \times 100\%$$

Where Co and Ce (mg/L) are the concentration of liquid phase adsorbate at an initial time and at equilibrium before and after adsorption (mg/L), V is the experimental volume (L) and M is the adsorbent mass (g). The concentration of phenol in an aqueous solution was analyzed by UV analysis performed on a UV–visible spectrophotometer (at wavelength = 270 nm)(Adebayo & Areo, 2021; Hadi et al., 2016).

### *3.4.7. Adsorption Isotherms*

Equilibrium isotherms are essential keys for designing an adsorption experiment. Constructing an adsorption isotherm can estimate the adsorption characteristics of an adsorbent (Hadi et al., 2016). The isothermal models explain all the data related to the concentration, and their parameters give an understanding of the adsorption ability and explain characteristics of the overall adsorption process (Adebayo & Areo, 2021). Isotherms are performed by fixing the mass of an adsorbent (OSNP or OSNP-S) and changing the concentration of the adsorbate (phenol) over a suitable range. The four isotherm models used in this study were Langmuir, Freundlich, Temkin, and Dubinin–Radushkevich. To understand the equilibrium study of adsorption process and the adsorption behavior of phenol molecules onto OSNP and OSNP-S, the isotherm models equations were used. For all results of the experiments,

the double factor two way ANOVA was done by the use of the Microsoft excel. The two-way ANOVA test is conducted to determine the differences between samples means and whereas these differences are significant or not. Furthermore, to determine the interactions between the dependent and independent variables.

*3.4.7.1. Langmuir Isotherm Model*

The Langmuir isotherm model is used to describe the formation of the monolayer uniform adsorption on the outer surface of the adsorbent (Chang et al., 2019). The adsorption was plotted by using $\frac{C_e}{q_e}\ Vs\ \ Ce$ , whereas $q_m\ and\ K_l$ parameters were calculated.

$$\frac{C_e}{q_e} = \frac{1}{q_m . K_l} + \frac{C_e}{q_m}$$

Here, $q_e$ is the amount of adsorbed to the solid (mg/g), $q_m$ is the maximum monolayer uniform coverage capacity (mg/g), b ($K_l$)is the Langmuir constant (L/mg) and $C_e$ is the equilibrium concentration.

The separation factor ($R_L$) of the Langmuir isotherm model for all concentrations was determined by using the following equation:

$$R_L = \frac{1}{1 + \ K_L C_\circ}$$

Were $C_\circ$ is the initial concentration of Phenol before the adsorption process. For a favorable process, $R_L$ should be between 0 and 1 (Majid et al., 2019).

*3.3.7.2. Freundlich Isotherm Model*

The Freundlich isotherm model is used for heterogeneous surfaces and envisages that an increase in the concentration of substances in the liquid phase result in an increase in the concentration of the ions substances adsorbed on the surface of the solid (Léon & Matos, 2018) and its linear equation is:

$$\log qe = \log k_f + \frac{1}{n}\log Ce$$

OR

$$\ln q_e = \ln k_f + \frac{1}{n}\ln C_e$$

$K_f$ and n are Freundlich constants. Moreover, they represent the adsorption capacity and intensity. Higher the $K_f$ value greater the heterogeneity. Larger the value of n (n > 1), the more spontaneous the adsorption process. The adsorption was plotted by using $\ln q_e \; Vs \; lnCe$ , whereas $\frac{1}{n} \; and \; k_f$ parameters were calculated.

*3.4.7.3. Temkin Isotherm Model*

The Temkin isotherm model is used to study the interactions occurring between the adsorbent surface molecules and the adsorbate molecules. This model neglects concentrations values that are extremely low or high. It also assumes that due to the adsorbent-adsorbate interaction on the surface, the heat of adsorption of the molecules is likely to decrease linearly (Ugraskan et al., 2022; Léon & Matos, 2018). In this paper, the following Temkin isotherm equation was used:

$$q_e = \left(\frac{RT}{b_T}\right)\ln K_T + \left(\frac{RT}{b_T}\right)\ln C_e$$

The R is the universal gas constant, and T is the temperature in Kelvin. The $K_T$ is the Temkin adsorption potential (L/g), while $b_T$ is constant. The plot $q_e \; Vs \; lnCe$ used to show the uniform distribution of the binding energies. The calculated parameters were $b_T \; and \; K_T$ (Al-trawneh et al., 2021; Léon & Matos, 2018).

*3.4.7.4. Dubinin–Radushkevich Isotherm Model*

D-R model is mainly used to determine the mechanism of adsorption that occurs on heterogeneous surfaces (Fathy et al., 2020). Hence it is superior to the Langmuir isotherm model, which assumes a homogeneous surface. The isotherm model is

commonly used to determine the type of adsorption, whether it is physical, chemical, or ion exchange (Ugraskan et al., 2022). The isotherm model explains the structure of the adsorbent porous and assumes that the adsorption happens by filling the pore walls layer by layer (adsorption potential theory) (Hu & Zhang, 2019). The D-R isotherm model parameters are calculated by using the following equations:

$$lnq_e = lnq_{(D-R)} - \beta\varepsilon^2$$

$$\varepsilon = RTln\left(1 + \frac{1}{C_e}\right)$$

$$E = {1}\Big/{\sqrt{-2\,\beta}}$$

The $q_e$ is the phenol adsorbed amount per unit mass of adsorbent (mg/g), $q_{(D-R)}$(mg/g) is the maximum theoretical adsorption capacity obtained from the D-R isotherm model, ε (kJ mol−1 ) is the adsorption potential and β (mol$^2$ /KJ$^2$) is the D-R isotherm constant related to the adsorption energy E. The adsorption was plotted by using ln $q_e Vs\ \varepsilon^2$ , whereas $-\beta\ and\ q_{(D-R)}$ parameters were calculated.

### *3.4.8. Adsorption Thermodynamics*

The thermodynamics are vital for investigating the nature of the temperature-dependent adsorption process to find if it is spontaneous or not and if the adsorption nature is endothermic or exothermic. This process of Phenol adsorption at different temperatures was investigated by calculating the Gibbs free energy change (ΔG°) (kJ/mol), by Van't Hoff equation:

$$\Delta G^{\circ} = -RTlnK_e^{\circ}$$

$T$ is the temperature (Kelvin), $R$ is the universal gas constant (8.314 J K$^{-1}$ mol$^{-1}$), and $K_e^{\circ}$ is the thermodynamic equilibrium constant of adsorption or Langmuir constant (L/mg).

The relation between free energy change (ΔG°), enthalpy (ΔH°) (kJ/mol), and

entropy change (ΔS°) (J/Kmol) is shown in the following equation:

$$\Delta G^{\circ} = \Delta H^{\circ} - T\Delta S^{\circ}$$

To plot the graph between $\Delta G^{\circ}$ vs. T(K) in terms of determining the values of $\Delta H^{\circ}$and $\Delta S^{\circ}$respectively, the $\Delta G^{\circ}$ is calculated from the equation (Tang et al., 2015; Lima et al., 2020). If $\Delta H^{\circ}$is positive, then the adsorption process is endothermic and if it is negative, then the process is exothermic. While for $\Delta S^{\circ}$, positive sign indicates the spontaneousity of the adsorption process (Hassan et al., 2020).

### *3.4.9. Reusability of Adsorbent - Desorption Studies*

Desorption and the reuse ability of the spent adsorbent were investigated. To regenerate the adsorbent (OSNP-S), 10 ml of 0.1 M sodium hydroxide and 0.1 M hydrochloric acid solutions were added to 0.01g of the spent adsorbent from the adsorption experiment (100 ppm, pH10, 35 ◦ C). This was done in duplicate. The mixtures were stirred at 165 RPM and room temperature for 24 h. Then filtrated and their absorbance values were measured using a UV–Visible spectrophotometer at 270 nm.

### *3.4.10. Real Wastewater Sample Evaluation*

To examine the feasibility of OSNP and OSNP-S adsorption, a real phenol-containing wastewater sample generated from olive was used. Olives were soaked in water, the phenol content was measured by using UV-spectrophotometer, the concentration was calculated and the real sample was used for the adsorption process. OSNP/OSNP-S adsorbents (0.05 g) were added to 50 ml of the real wastewater sample in two trials. The samples of each batch experiment were stirred under a constant speed of 165 rounds per minute (rpm) for 24 hrs. After each batch experiment, filtration was carried out. The filtered solutions were analyzed under a UV/VIS spectrophotometer to determine the final concentration.

# CHAPTER 4: RESULTS AND DISCUSSION

## 4.1. Ecotoxicology Part

### *4.1.1. Biometric Analysis of Oyster Population*

Pearl Oyster *Pinctada imbricate radiata* collected in the oyster bed of Al-Wakra seawaters, varied from 3.55 to 7.11 cm long with a mean shell length of 5.08 cm. As shown in Table 5, the length size was separated into four classes with a class interval of 1.0 cm. Figure 6 indicates that Pearl Oyster *Pinctada imbricate radiata* of Al-Wakra waters was dominated by size class (4.5-5.5 cm) with 70.64% of the total samples measured. Then the following results of size class (5.5-6.5) with 17.43%, size class (3.5-4.5) with 10.09%, and size class (6.5-7.5) with 1.84%. The biometry (size) analysis does not show distinct length/ age groups (Aideed et al., 2015). Nevertheless, in this study, the biometry of the size analysis of the samples shows that the population of Pearl Oyster *Pinctada imbricata radiata* was dominated by samples of (4.5-5.5 cm) length, which probably represent the mature population. The small individuals (3.5-4.5 cm) seem to cover the population of Pearl Oyster *Pinctada imbricata radiata* that belong to the relatively young population. In the current study, it was noticed that three classes (4.5-5.5, 5.5-6.5, and 6.5-7.5 cm) match the age groups (classes) reported by (Mohammed, 2003), who distributed the composite of the Pearl Oyster *Pinctada imbricata radiata* in Qatari water into four separate age groups with the mean lengths of 5.68, 6.58, 7.75, and 8.47 cm respectively. Moreover the unimodal distribution of the pearl size-classes confirm that the Al-Wakra oyster bed zone is dominated by an unique population of *Pinctada imbricata radiata*.

Table 5: Population's Size Classes of Pearl Oyster *Pinctada Imbricata Radiata* from the Oyster Bed of Al-Wakra.

| Class of shell length (cm) | Number of Individuals | % Percentage |
|---|---|---|
| 3.5-4.5 | 22 | 10.09 |
| 4.5-5.5 | 154 | 70.64 |
| 5.5-6.5 | 38 | 17.43 |
| 6.5-7.5 | 4 | 1.84 |
| Total | 218 | 100 |

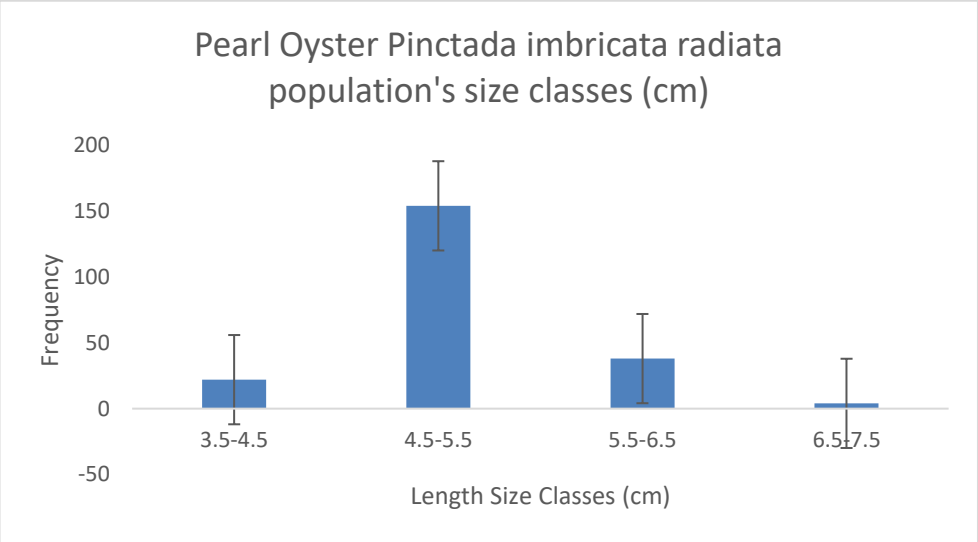


Figure 6: Length frequency distribution of Pearl Oyster *Pinctada imbricata radiata* from oyster bed of Al-Wakra.

### *4.1.2. Biometric Relationships*

Biometric relationships are used to differentiate between size classes, where the length-weigh, width-weight, and length-weight relationships are required in population dynamics and to predict the growth patterns of aquatic organisms. Furthermore, the rate of increase in weight shows how the ecological parameters affect the living organism in specific habitat (Mohammed, 2003). Figure 7 show the relationships between the length-weight, width-weight and height-weight of *Pinctada imbricata radiata* from

Qatari waters with the resultant respective formulas:

$y= 0.5099x^{2.4522}$ and a regression coefficient $R^2 = 0.5457$

$y= 0.8739x^{2.135}$ and $R^2 = 0.3802$

$y= 14.038x^{1.0235}$ and $R^2 = 0.4316$

All the relationships indicate negative allometric growth of the *Pinctada imbricata radiata* oyster, due to that the slope (b) values were less than three (Kalesaran et al., 2018). It is obvious that the oyster samples were growing faster in their shell sizes rather than their weight (Aideed et al., 2015). The results showed that there is a strong correlation between length, width, height versus weight.

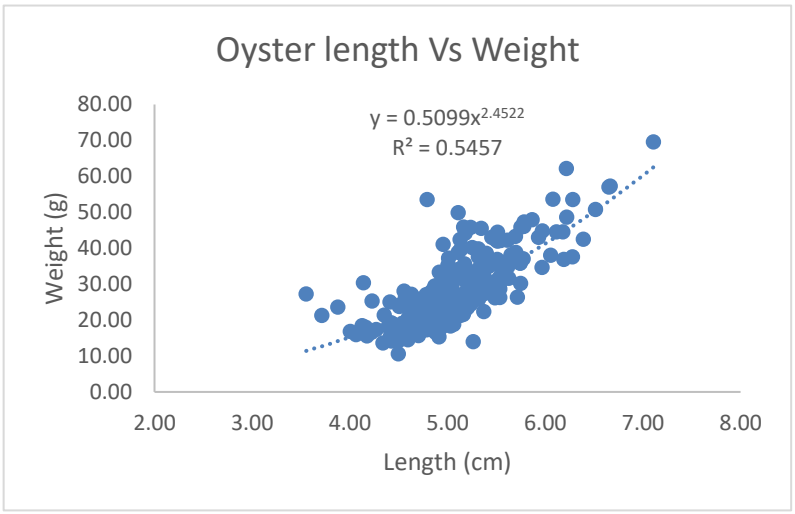


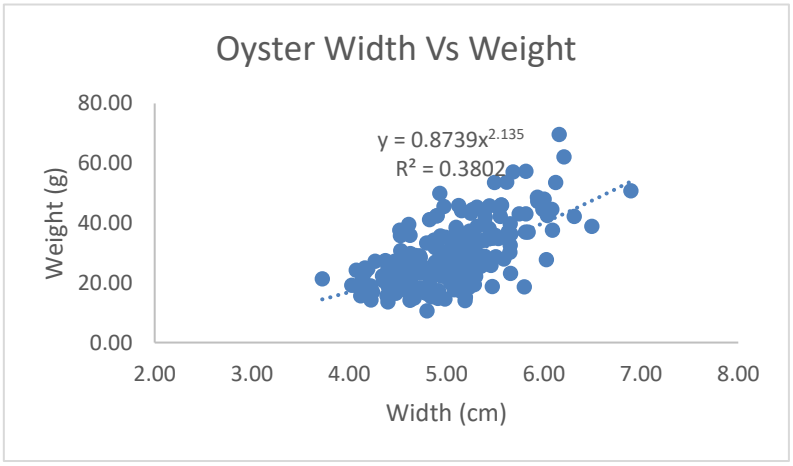


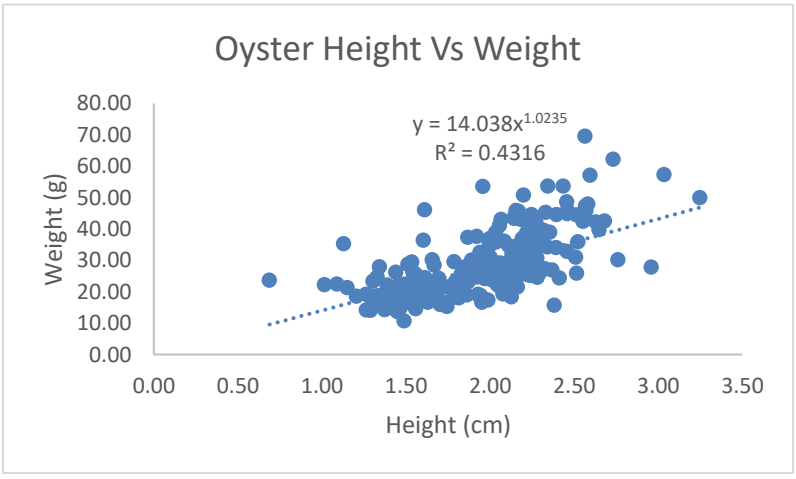


Figure 7: Length, width and height-weight relationship of the pearl oyster *Pinctada imbricata radiata* (N = 218 ).

### *4.1.3. Biomarker Analysis and Oxidative Stress*

The total protein and antioxidant enzymes (CAT and SOD) analysis were performed on cytosolic fractions of gills and digestive gland of *Pinctada imbricata radiata* exposed to different phenol concentrations at different times. The CAT and SOD enzymatic activities and analysis from both gills and digestive glands increased compared to the control organisms. Whereas, the total protein slightly decreased over time. Table 6 and Figure 8 show the results for gills. At 0 hr the total protein was the highest for all samples and the lowest was at 96 hr time. However, there were no significant differences between the total proteins averaged values ($p > 0.001$) as commonly there are no big changes for this parameter. The results for CAT and SOD analysis of gills showed that Treatment (concentration of phenol), the Time of Treatment, and also Treatment × Time have all a positive impact and there is a significant difference with ($p < 0.001$) in all cases. The activity of CAT in gills increased until the 4th day in 1 and 10 ppm Phenol exposure and the difference was significant ($p < 0.001$). The SOD activity in gills showed increasing through the whole treatment period with a significant difference.

Table 6: Pearl Oyster *Pinctada imbricata radiata* Gills Total Protein and Antioxidant Enzymes (CAT and SOD) Analysis.

| Oyster Gills Total Protein (mg/g wet weight) | | | | | | | |
|---|---|---|---|---|---|---|---|
| Phenol Concentration | 0 Hours | 24 Hours | 48 Hours | 72 Hours | 96 Hours | Mean | Standard Deviation |
| 0 ppm | 21.23 | 20.58 | 19.82 | 17.47 | 15.18 | 18.86 | 2.50 |
| 1 ppm | 21.23 | 20.72 | 19.77 | 17.28 | 15.00 | 18.80 | 2.61 |
| 2 ppm | 21.48 | 20.88 | 20.25 | 16.93 | 14.98 | 18.91 | 2.81 |
| 5 ppm | 20.99 | 20.73 | 20.10 | 16.85 | 14.67 | 18.67 | 2.78 |
| 10 ppm | 21.33 | 21.30 | 20.07 | 17.17 | 14.77 | 18.93 | 2.88 |
| CAT Activity in the Gills (U/mg protein) | | | | | | | |
| Phenol Concentration | 0 Hours | 24 Hours | 48 Hours | 72 Hours | 96 Hours | Mean | Standard Deviation |
| 0 ppm | 57.10 | 57.28 | 57.62 | 57.33 | 58.00 | 57.47 | 0.35 |
| 1 ppm | 58.33 | 57.75 | 60.08 | 65.58 | 70.08 | 62.37 | 5.31 |
| 2 ppm | 59.50 | 60.37 | 62.78 | 68.33 | 73.40 | 64.88 | 5.88 |
| 5 ppm | 58.42 | 60.45 | 64.60 | 71.15 | 76.08 | 66.14 | 7.39 |
| 10 ppm | 57.77 | 59.58 | 63.63 | 71.70 | 76.43 | 65.82 | 8.00 |
| SOD Activity in Gills (U/mg protein) | | | | | | | |
| Phenol Concentration | 0 Hours | 24 Hours | 48 Hours | 72 Hours | 96 Hours | Mean | Standard Deviation |
| 0 ppm | 28.78 | 29.03 | 29.68 | 30.45 | 30.83 | 29.76 | 0.88 |
| 1 ppm | 30.23 | 30.80 | 34.98 | 35.85 | 37.68 | 33.91 | 3.25 |
| 2 ppm | 30.90 | 32.38 | 38.65 | 39.98 | 42.68 | 36.92 | 5.06 |
| 5 ppm | 31.10 | 33.18 | 40.02 | 43.53 | 47.38 | 39.04 | 6.86 |
| 10 ppm | 30.64 | 31.70 | 42.98 | 48.07 | 52.12 | 41.10 | 9.63 |

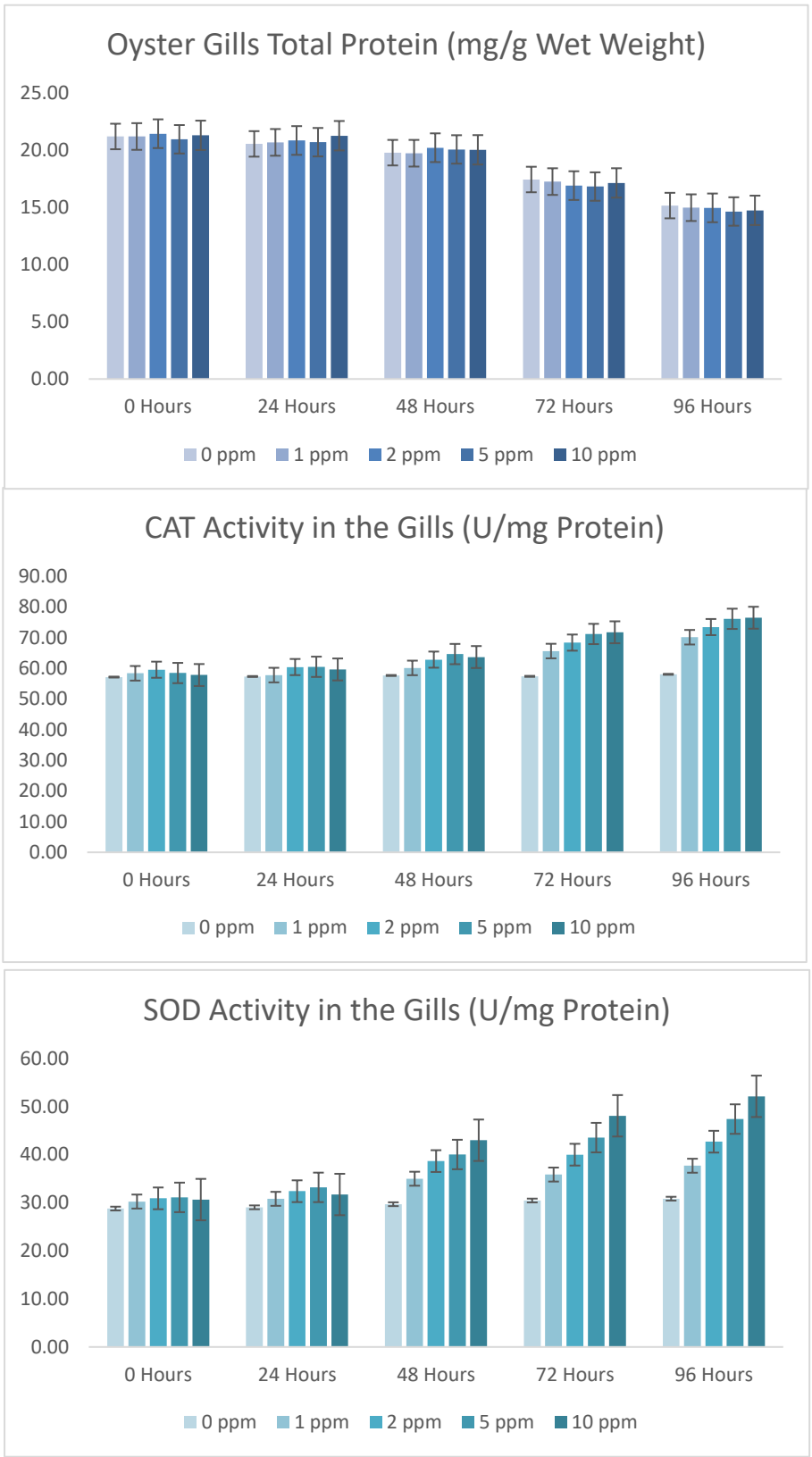


Figure 8: Pearl Oyster *Pinctada imbricata radiata* Gills Total protein, CAT and SOD analysis.

Results of Total proteins and enzymatic activities for the digestive gland are shown in Table 7 and Figure 9. The results showed that the activity of total protein decreased over time but there were no significant differences between the total proteins averaged values (p-value > 0.001). This decrease can be explained by the fast imposed on the pearl oysters during our experiment. The results for CAT and SOD analysis showed that Treatment (concentration of phenol), the Time of Treatment, and also Treatment × Time interaction have all a positive impact and there is in all cases a significant difference compared to the control (p-value < 0.001). The activity of CAT and SOD in digestive glands increased with a significant difference (p-value < 0.001). Furthermore, the results showed that CAT analysis of gills and digestive glands gives the highest mean values of 66.14 and 63.32 U/mg protein after 4 days period of 5 ppm and 10 ppm treatments respectively. The difference and variation in all enzymatic activities and analysis are related to the phenol concentration, exposure time, and the interaction between treatment concentration and time.

Table 7: Pearl Oyster *Pinctada imbricata radiata* Digestive Glands Total Protein and Antioxidant Enzymes (CAT and SOD) analysis.

| Oyster Digestive Gland Total Protein (mg/g wet weight) | | | | | | |
|---|---|---|---|---|---|---|
| Phenol Concentration | 0 Hours | 24 Hours | 48 Hours | 72 Hours | 96 Hours | Standard Deviation |
| 0 ppm | 48.11 | 48.27 | 48.27 | 43.28 | 41.52 | 3.25 |
| 1 ppm | 48.84 | 47.00 | 47.00 | 43.60 | 41.50 | 2.97 |
| 2 ppm | 48.36 | 48.32 | 48.32 | 44.00 | 41.98 | 3.01 |
| 5 ppm | 48.24 | 47.94 | 47.94 | 43.70 | 41.05 | 3.24 |
| 10 ppm | 46.83 | 47.80 | 47.80 | 42.72 | 40.67 | 3.27 |
| CAT Activity in the Digestion Gland (U/mg protein) | | | | | | |
| Phenol Concentration | 0 Hours | 24 Hours | 48 Hours | 72 Hours | 96 Hours | Standard Deviation |
| 0 ppm | 50.94 | 51.62 | 52.13 | 52.18 | 52.72 | 0.67 |
| 1 ppm | 50.97 | 51.80 | 53.25 | 52.67 | 54.60 | 1.39 |
| 2 ppm | 50.74 | 51.82 | 54.85 | 53.83 | 57.60 | 2.68 |
| 5 ppm | 51.02 | 52.13 | 55.65 | 56.07 | 60.07 | 3.58 |
| 10 ppm | 51.01 | 53.38 | 57.47 | 58.80 | 63.32 | 4.80 |
| SOD Activity in Digestion Gland (U/mg protein) | | | | | | |
| Phenol Concentration | 0 Hours | 24 Hours | 48 Hours | 72 Hours | 96 Hours | Standard Deviation |
| 0 ppm | 18.99 | 19.58 | 20.03 | 20.82 | 21.20 | 0.90 |
| 1 ppm | 20.58 | 21.72 | 23.70 | 26.40 | 27.17 | 2.86 |
| 2 ppm | 20.28 | 23.77 | 26.90 | 29.42 | 31.67 | 4.51 |
| 5 ppm | 20.86 | 22.08 | 29.44 | 32.27 | 34.88 | 6.20 |
| 10 ppm | 20.80 | 22.22 | 32.08 | 35.95 | 40.32 | 8.53 |

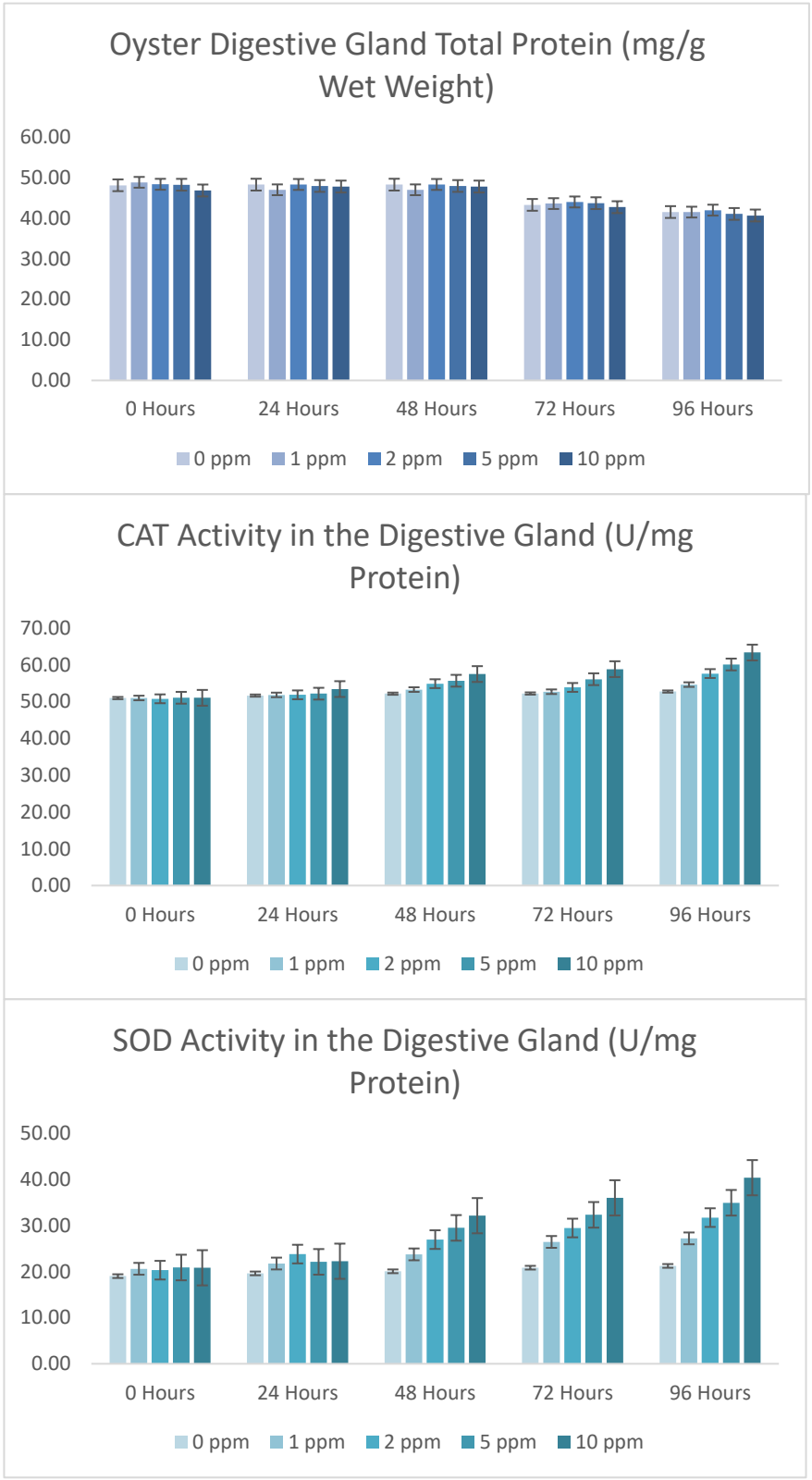


Figure 9: Digestive gland Total protein, CAT and SOD analysis.

## 4.2. Adsorption Isotherm Part

### *4.2.1. The Possible Mechanism of OSNP-S Formation*

The oyster shell is made of layers of the microstructure of calcium carbonate (Checa et al., 2018). The formation of OSNP-S starts by reducing the size of the oyster shell to nanoparticles by ball milling technique. Reducing the size of oyster shell particles to nano-size increases the surface area, allowing for more silver deposition. Adding alkaline solution turns the OSNP surface to negative charge, which interacts with the positively charged silver ion and forms the OSNP-S as shown in Figure 5.

### *4.2.2. Adsorbent Characterization*

To identify the physical and chemical characterization properties of the OSNP and OSNP-S, several analyses such as BET, SEM, TEM, and FTIR techniques were adopted.

#### *4.2.2.1. BET isothermal analysis*

The physical characterization and structural properties such as surface area and pore volume, which were determined by BET help in determining the activity of the adsorbents (Dehmani et al., 2020). The results of nitrogen adsorption-desorption isotherm analysis for both OSNP and OSNP-S are shown in Table 8 and Figure 10. The analysis indicated that OSNP is an IV type of adsorption isotherms with an H1 hysteresis loop that is according to IUPAC is characteristic of typical mesoporous material. The desorption isotherm curve on top of the adsorption curve went along with the production of the hysteresis loop (Wang, 2018). The OSNP mesoporous structure makes it a highly efficient candidate for activation with many different cations. The BET and Langmuir Surface Area of OSNP were 40.339 and 44.063 $m^2/g$ respectively, while the Total Pore Volume was 0.1823 $m^3/g$ and the average pore radius was 90.4 $A^o$. For OSNP-S, the BET and Langmuir surface areas were 15.917 $m^2/g$ and 20.198 $m^2/g$,

respectively, while the total pore volume was 0.1157 $m^3/g$ and the average pore radius was 145.4 $A^o$.

Table 8: BET Isothermal Analysis of OSNP and OSNPS.

| Adsorbent | BET Surface Area ($m^2/g$) | Langmuir Surface Area ($m^2/g$) | Total Pore Volume ($m^3/g$) | Average Pore Radius ($A^o$) |
|---|---|---|---|---|
| OSNP | 40.339 | 44.063 | 0.1823 | 90.4 |
| OSNP-S | 15.917 | 20.198 | 0.1157 | 145.4 |

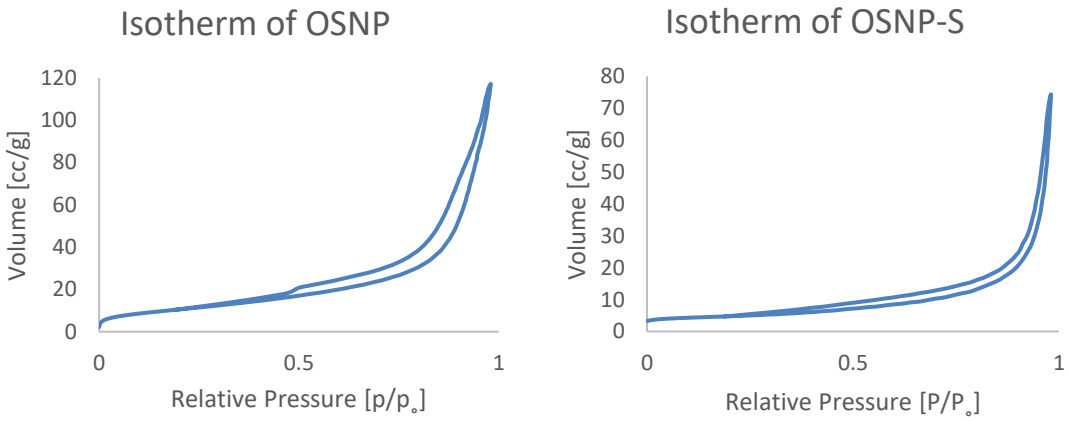


Figure 10: BET isothermal analysis of OSNP and OSNP-S.

*4.2.2.2.SEM analysis*

To find the microstructure of both OSNP and OSNP-S (Morphology characterization), high resolution scanning electron micrograph SEM was used in both 25000× and 50000×. Figure 11 (a -d) shows the SEM photomicrograph for row and activated oyster shells and indicates that there is a high concentration of heterogeneous distribution of fine particles along with some larger particles. The shape of OSNP-S (Figure 11c, d) is more irregular than the OSNP (Figure 11a, b). The irregularity of the particles could be related to the unreacted OSNP with silver. It is always favorable to

have irregular and imperfect surface since pollutants can be trapped, hosted, and interacted with the active adsorption sites (Navarro et al., 2016).

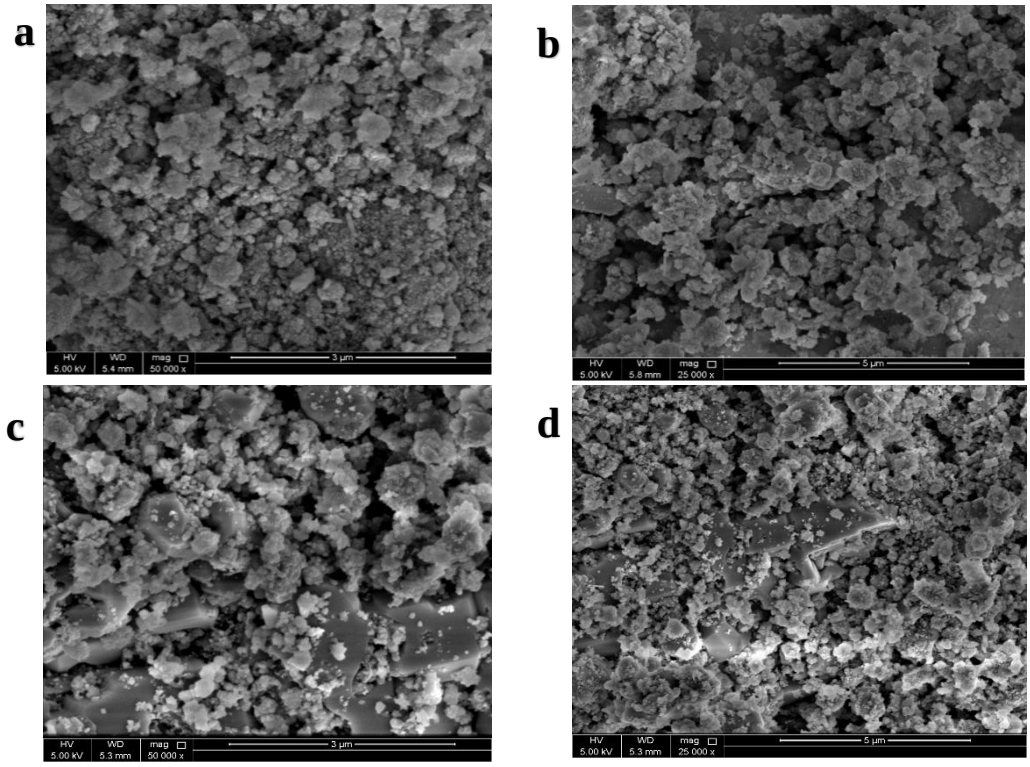


Figure 11: SEM figures of OSNP (a,b) and OSNP-S (c,d).

*4.2.2.3. TEM analysis*

To determine the microstructure of OSNP (Figure 12a-c) and OSNP-S (Figure 12d-f), the compounds were observed by TEM. The TEM images of OSNP-S (figure 6d, f) show spheroidal and chain-like particles of calcite along with spherical uniform distributed Silver particles covering its surface with notable agglomeration. The high resolution of OSNP and OSNP-S (Figure 6c, f) shows the lattice plane.

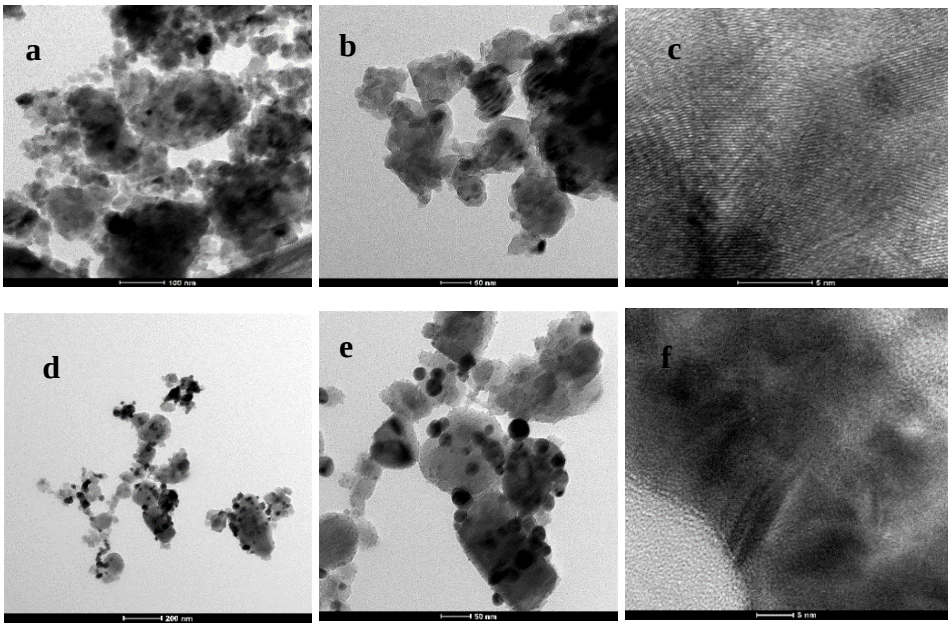

Figure 12: TEM figures OSNP (a, b, c) and OSNP-S (e, f, g).

*4.2.2.4. FTIR analysis*

The Fourier Transform Infrared Spectroscopy FTIR provides some useful information on the chemical composition and structure of the adsorbents. The functional groups of OSNP and OSNP-S are represented in Figure 13. The FTIR spectrums were attained over the region 400 $cm^{-1}$ to 4000 $cm^{-1}$. The spectrums indicate a decrease in the peak intensity of OSNP-S due to amendment with silver. The OSNP spectrum shows eight main characteristic peaks at 2500, 1788, 1446, 1157, 858.98, 712, 676.85 and 597.48 $cm^{-1}$. The OSNP-S spectrum shows six main characteristic peaks 2500, 1788, 1408, 1083, 856, and 712 $cm^{-1}$. These peaks represent the stretching carbon functional groups in calcite (Hajji et al., 2017; Rodriguez-blanco et al., 2010). The Silver metal interactions are observed at region bands 500 to 900 $cm^{-1}$. The peaks in this region were disappeared in OSNP-S (Chang et al., 2019). Region bands 700- 900 $cm^{-1}$ represent Ca-O whereas 1300- 1500 $cm^{-1}$ represent C-O bands.

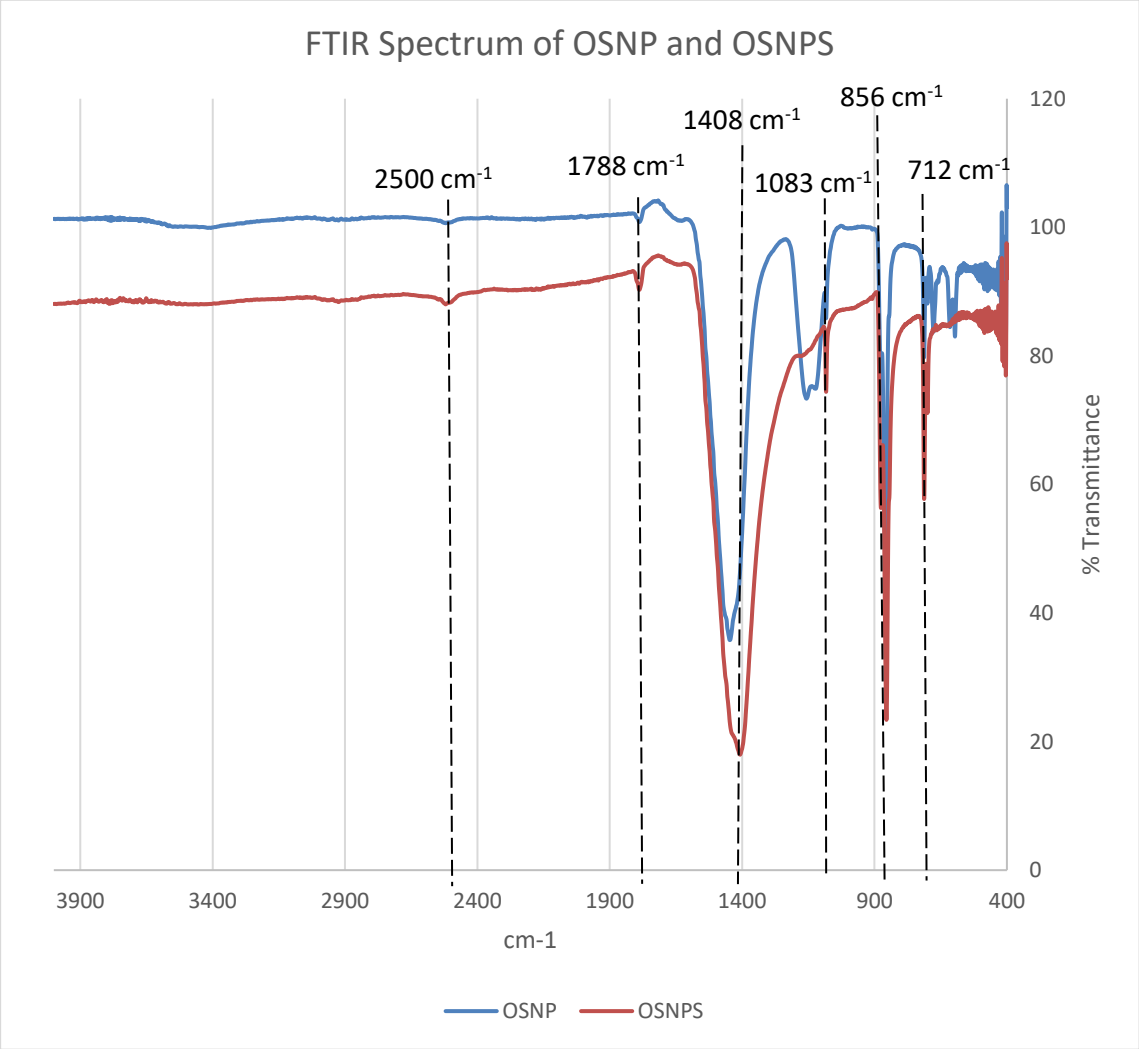


Figure 13: FTIR sprctrum of OSNP and OSNP-S.

### *4.2.3. Adsorption Process*

The adsorption process mainly occurs on the surface of a solid substance. Adsorption occurs when a soluble substance in an aqueous solution is transfer onto the bulk of a solid substance. The solid substance is called adsorbent whereas the soluble substance is called adsorbate. Studying the adsorption process and finding its optimal conditions is very important due to its role in purifying aqueous solutions such as wastewater and gas streams. Adsorption is an effective method with low infrastructure and operating costs, mainly when recyclable and sustainable materials are used. Hence,

it is broadly used in industry. As a result, it is critical to do further studies and research in this field to develop and design optimal adsorption systems (Guo & Wang, 2019; Azizian et al., 2018). The adsorption mechanism depends on the mass transport process and the different physiochemical characteristics of the adsorbent. Generally, adsorption undergoes different main processes where the molecule of adsorbate transfer from the solution to the surface of the adsorbent and diffuse through the surface layers and go into the pores of the adsorbent. Furthermore, it accumulate in the active sites of the adsorbent. The mechanism of phenol adsorption undergoes many interactions such as hydrogen bonding, dispersion, Van der Waals, hydrophobic bonding, electron donor-acceptor complex, and polar interaction (Adebayo & Areo, 2021). In Figure 14 the proposed adsorption mechanism of phenol adsorption on OSNP surface is most likely to undergo hydrogen bonding, whereas it is electrostatically bonded to OSNP-S.

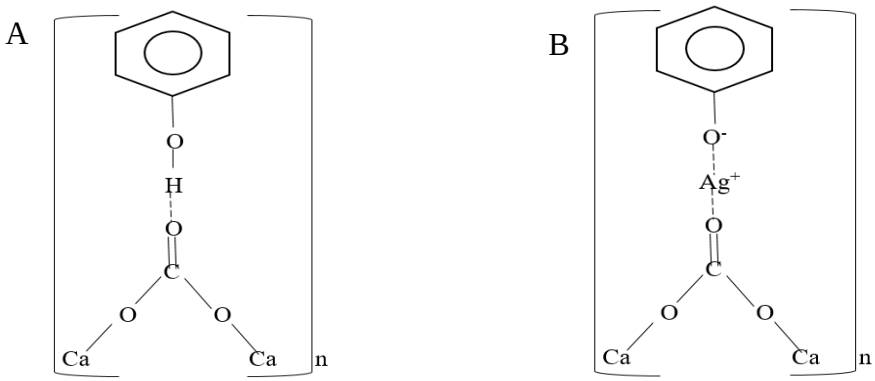


Figure 14: Proposed adsorption mechanism of phenol on (A) OSNP surface and (B) OSNP-S.

### *4.2.4. Adsorption Parameters*

#### *4.2.4.1. Effect of pH*

Removal of phenol from an aqueous solution is highly affected by pH. The adsorption strength is changed by changing the pH, this is mostly due to the changes in

the surface properties of the adsorbent along with the ionization state and ionic forms of Phenol (Dehmani et al., 2020). The point of zero charges (pHpzc) is very important for knowing the processes taking place at the mineral-water interface, counting adsorption dissolution, precipitation, and colloid formation. Minerals display a negative surface charge above the pHpzc, whereas a positive charge occurs below the pHpzc. The amount of surface charge in different pH conditions for different minerals depends on the nature of the surface reaction. Whereas the occurrence of pHpzc indicates a change in surface electrochemical properties. The measurements of calcite surface interaction forces propose that pHpzc equals 9.5 ± 0.1 (Hurchill et al., 2004). The effect of pH on the adsorption was studied over the range of pH 2-10. The analysis result is shown in Figure 15. The highest percentage removal was at the lower pH 2 for both OSNP and OSNP-S. The acidic media increase the electrostatic attraction with the phenolate ions which leads to high Phenol adsorption (Bwatanglang et al., 2021) (Ouallal et al., 2019). The interaction of minerals and water has an important impact on the adsorption properties of Phenol. Hence the high phenol adsorption at low pH could be due to π-π interactions along with hydrogen bonding interaction between the prepared adsorbate and phenol molecules (Hurchill et al., 2004). By increasing to pH 4 the adsorption dropped heavily, due to the weak electrostatic attraction force between the positively charged surface of adsorbate and the negatively charged phenol (Sahu et al., 2017). Since Phenol is acidic with pH around 5-6 and relatively well water-soluble, hence at pH 6 intermolecular hydrogen bond between Phenol molecules dominates in the aqueous leading to low Phenol adsorption. The decrease in Phenol adsorption in higher pH values is related to the presence of a huge amount of positive Hydrogen ions ($H^+$) which contest the Silver positive ions on the surface of the adsorbate in OSNP-S (Dehmani et al., 2020). It was also reported that the $OH^-$ in the aqueous solution

compete for the phenol molecules for the sorption sites changing the OSNP-S surface to negative charge, hence resulting in repulsion with phenolate ions ($C_6H_5O^-$) and decreasing the phenol uptake (Sharan et al, 2009; Ouallal et al., 2019). At pH 10, the phenol removal decrease due to the that both phenolate ions and the surface of the adsorbent are negatively charged producing an electrostatic repulsion (Sobiesiak, 2017). Several types of research reported that the removal of phenol decreases by an increase of pH value. This was related to the positive oxonium ions on the surface of the adsorbent, resulting in an increase in water adsorption and cluster formation. Thus, decreasing in the availability of active sites on the adsorbent surface occurs along with the blocking of the entrance of fine pores with the adsorbed molecules of phenol (Sobiesiak, 2017). Two pH values were adapted in the current adsorption experiment, pH 6 and10. This is to study and compare the uptake of Phenol in typical wastewater pH value and in the basic pH value.

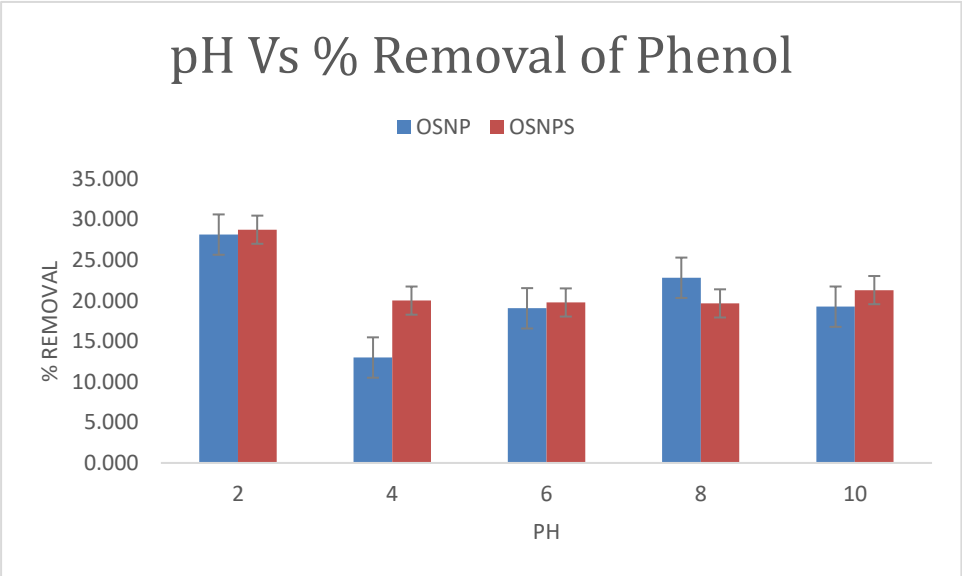


Figure 15: Effect of pH on % removal of phenol.

*4.2.4.2. Effect of Concentration and Temperature*

In this study, the adsorption capacity by the OSNP and OSNP-S initial concentration at both pH 6 and 10 are shown in Table 9, Figures 16 and 17. For pH 6, at room temperature, the results show that OSNP is a higher adsorbent than OSNP-S. The highest phenol removal by OSNP was at the concentration of 10 ppm (36.98%). Whereas OSNP-S showed less uptake in all concentrations (< 30%). At 35$^{o}$ C, the uptake was almost the same for both OSNP and OSNP-S at all concentrations and almost less than 20% removal except for OSNP-S at 10 ppm (20.71%). At 45$^{o}$C, the highest uptake was at 5 ppm for both OSNP and OSNP-S (33.73%) and (28.40%) respectively. There was a notable reduction from the lowest concentration all the way to the highest concentration of the adsorbates. The sum of the results indicate that there are variations in the removal percent of phenol by both adsorbents at different initial concentrations and temperature, but it was indicated that the adsorption reduces with higher temperature. The highest phenol removal at pH 10 was dominated by OSNP-S. The results of the analysis indicated that the highest adsorption at all assigned temperatures was at 20 ppm and 10 ppm for OSNP-S and OSNP, respectively, and verified that adsorption of phenol reduces with higher temperature due to the mass transfer, since higher temperature cause higher kinetic movement and result decrease in the phenol uptake. Hence, it is recommended to do the experiment at room temperature. At pH 10, the removal was higher for OSNP-S than at pH 6. Phenol removal by 20 ppm OSNP-S at room temperature, 35$^{o}$C, and 45$^{o}$C was 25.89%, 23.22%, and 21.01% respectively whereas the removal by 10 ppm OSNP at the same temperatures was 20.12%, 21.30%, and 19.53% respectively.

Table 9: Highest Percentage Removal of Phenol by OSNP and OSNP-S at pH(6, 10) and Temperatures (25$^{o}$, 35$^{o}$, 45$^{o}$ C).

| | | Temperature | | | | | |
|---|---|---|---|---|---|---|---|
| | | 25$^{o}$ C | | 35$^{o}$ C | | 45$^{o}$ C | |
| pH | | OSNP | OSNP-S | OSNP | OSNP-S | OSNP | OSNP-S |
| 6 | Ci, ppm | 10 | 100 | 30 | 10 | 5 | 5 |
| | %Removal | 36.98 | 17.90 | 18.05 | 20.71 | 33.73 | 28.4 |
| 10 | Ci, ppm | 10 | 20 | 10 | 20 | 10 | 20 |
| | %Removal | 20.18 | 25.89 | 21.3 | 23.22 | 19.53 | 21.01 |

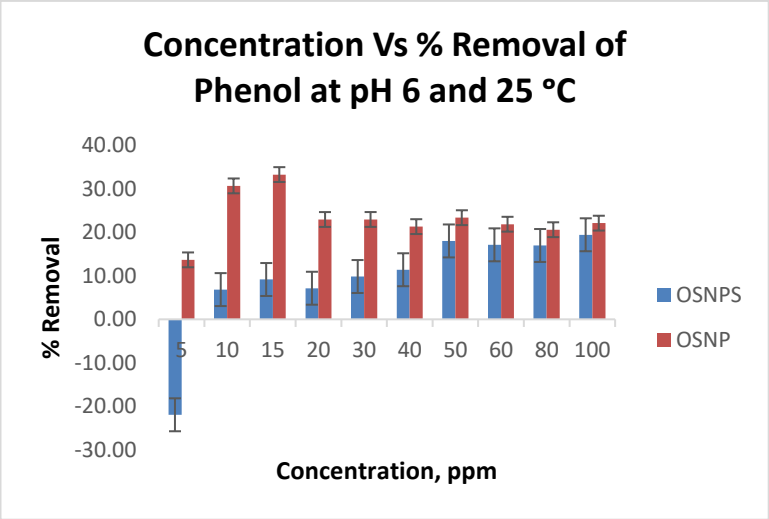


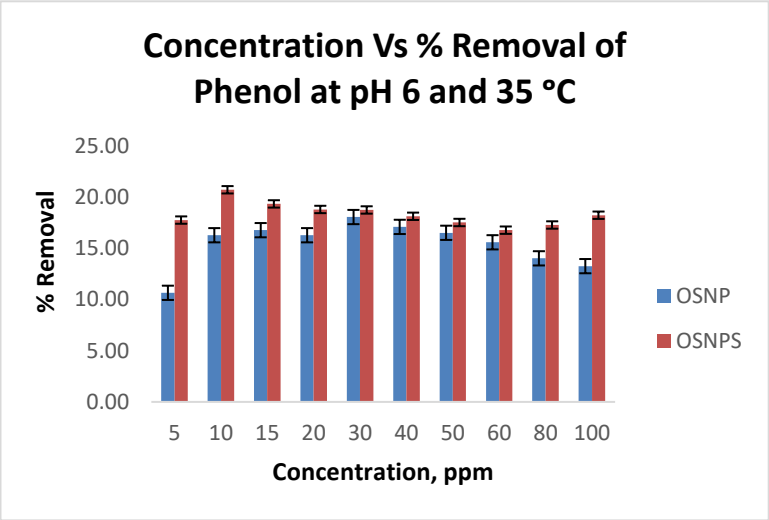


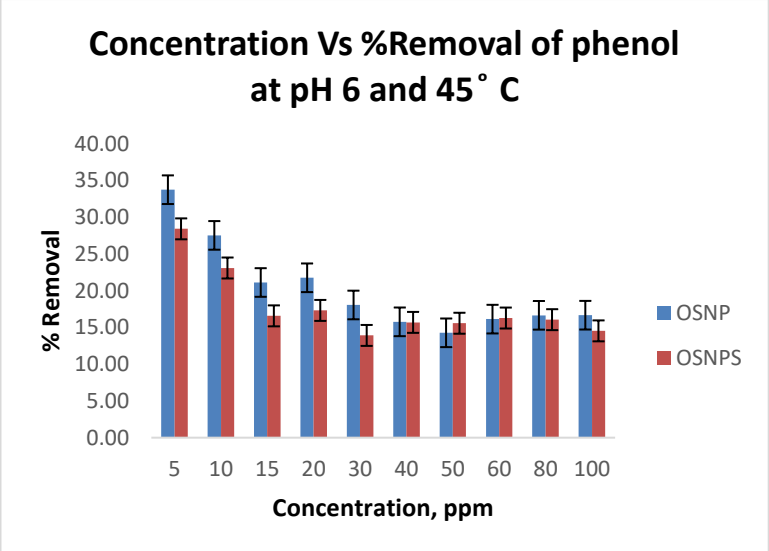


Figure 16: Adsorption capacity by the OSNP and OSNPS initial concentration at pH 6 at different temperatures.

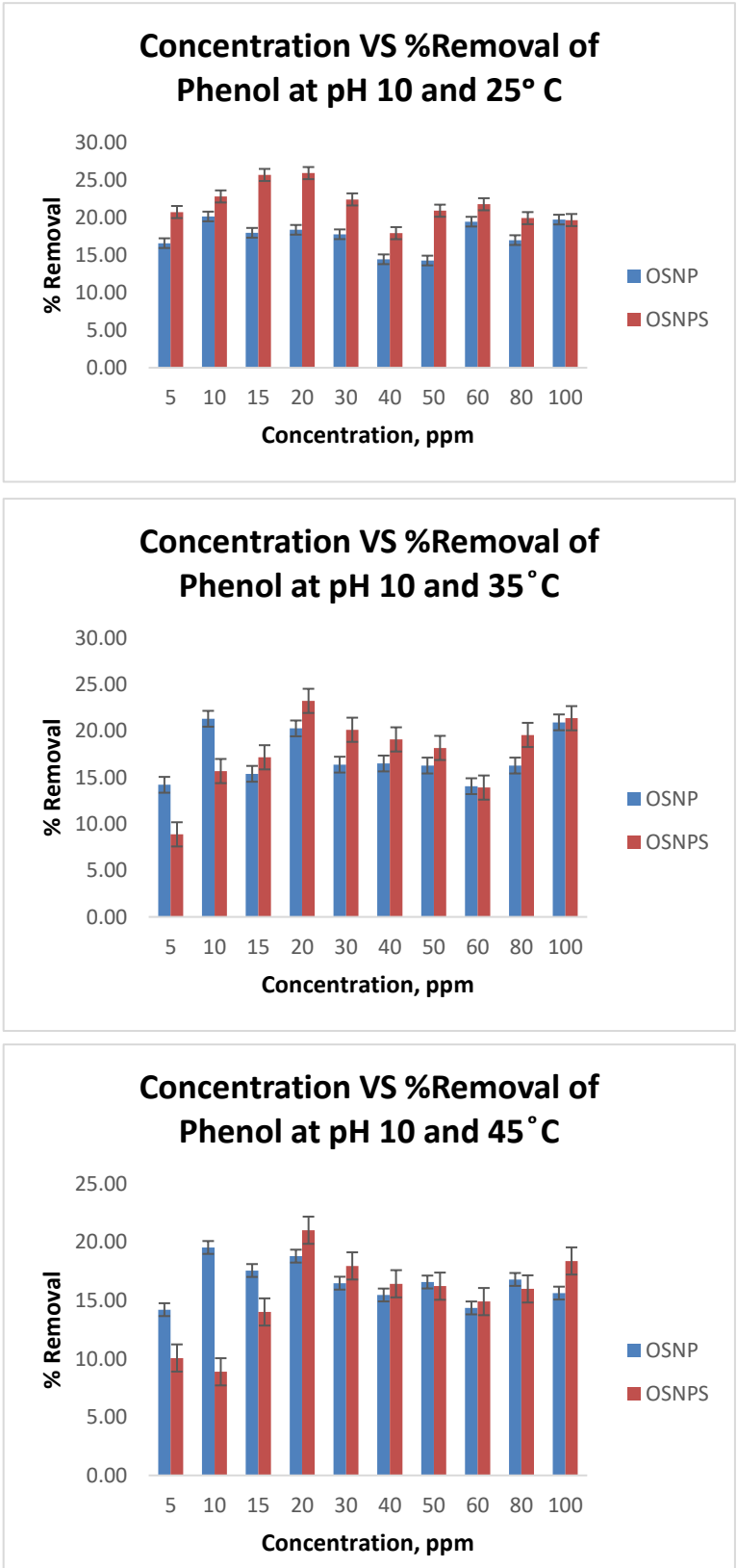


Figure 17: Adsorption capacity by the OSNP and OSNPS initial concentration at pH 10 at different temperatures.

*4.2.4.3. SEM of Adsorbent After Phenol Adsorption*

SEM micrograph of OSNP and OSNP-S after phenol adsorption at different pH values and temperatures are shown in Figure 18. From the SEM analysis can be seen changes in the adsorbents morphology after adsorbing phenol. The micrographs show many nonbonding agglomerates and voids, which increase in parallel with temperature. The agglomerates and nonbonding are due to strong particle-particle (electrostatic) interaction occurring on OSNP causing the detachment of unembedded particles (Cao et al., 2016; Eletta et al., 2020). In the OSNP-S micrograph at pH 10 and 25$^{o}$C, regular particles with less nonbonding and voids were observed. The de-agglomeration of OSNP-S was due to surface modification, which reduces the surface energy along with a reduction in electrostatic forces of attraction. This indicates that at these conditions more adhesion of phenol on the surface of the OSNP-S occurs due to its physical characteristics, which facilitate the interaction of phenol in the active sites. Furthermore, it is recommended to accomplish this experiment at high basic pH and at room temperature.

| Temperature | | |
|---|---|---|
| 25°C | 35° C | 45°C |

OSNP, pH 6

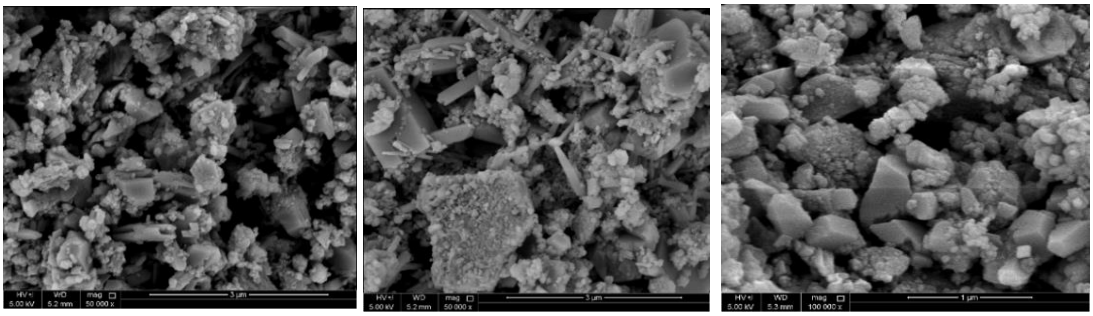

OSNP-S, pH 6

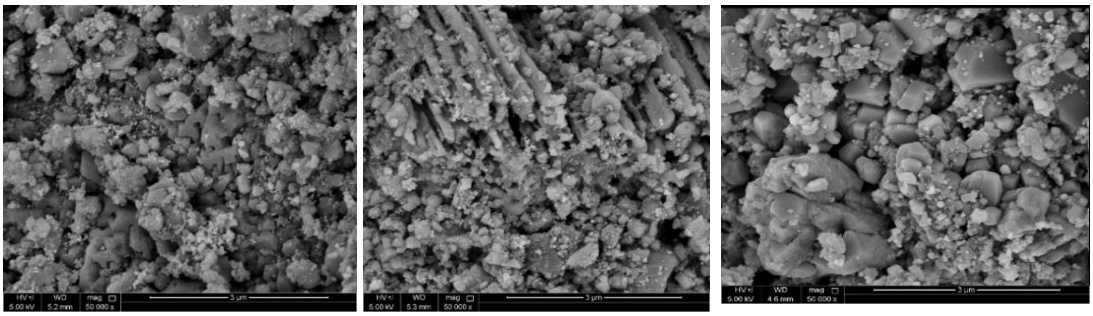

OSNP, pH 10

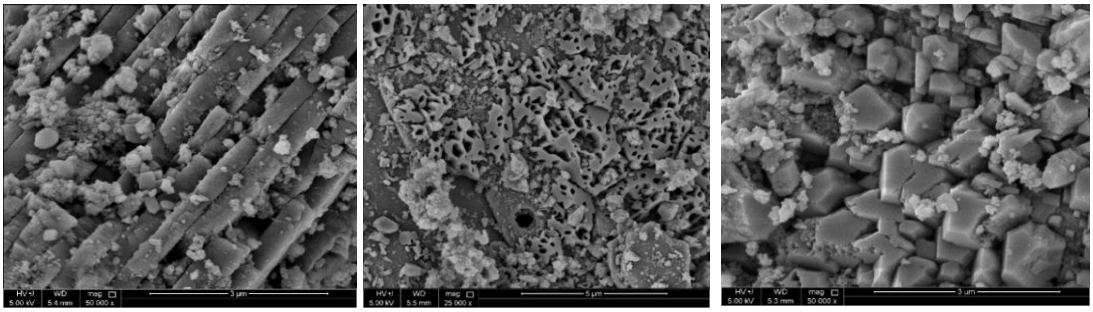

OSNP-S, pH 10

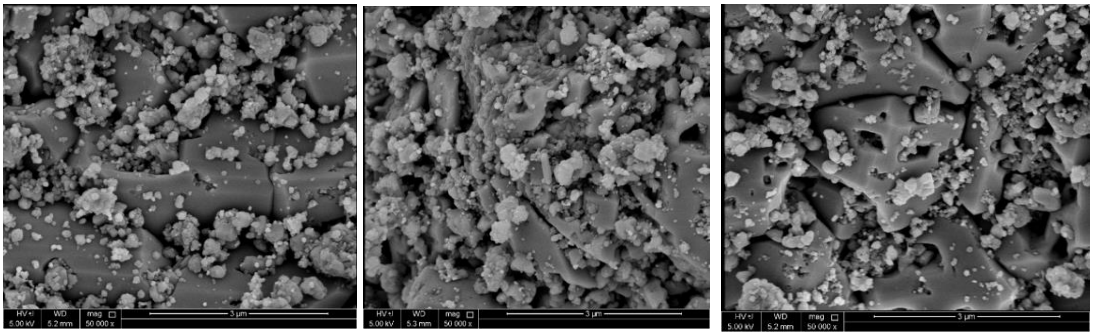

Figure 18: SEM images of higher phenol adsorption at different concentrations.

*4.2.4.4. TEM of Adsorbents After Phenol Adsorption*

The microstructure of OSNP and OSNP-S after phenol adsorption at pH6 and pH 10 was further observed by TEM. The images in Figures 19 and 20 show the deposit of phenol on the surface of adsorbents. The low magnification (500 nm) of TEM images indicated that OSNP-S is successfully coated with phenol more than what is seen in OSNP images, this result was proved by enlarged TEM images. To get the optimum result, it is recommended to carry on with the phenol adsorption process at high basic pH and room temperature.

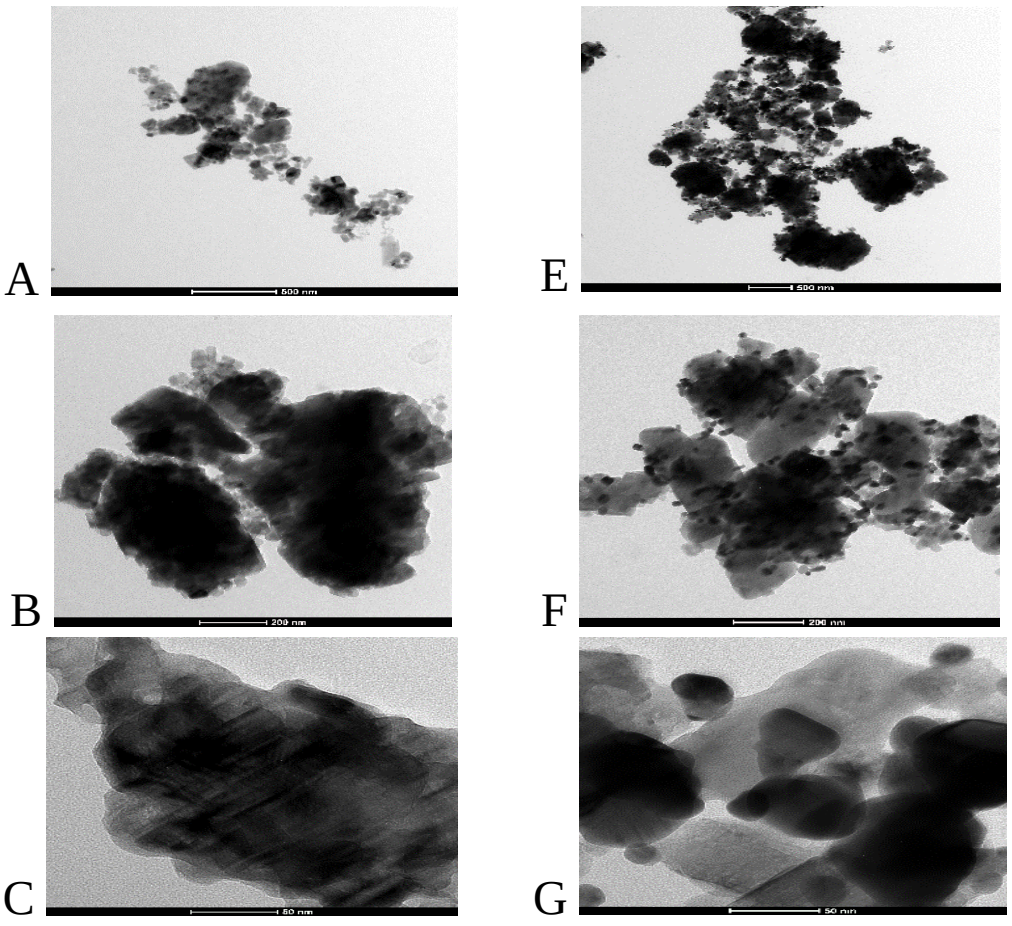

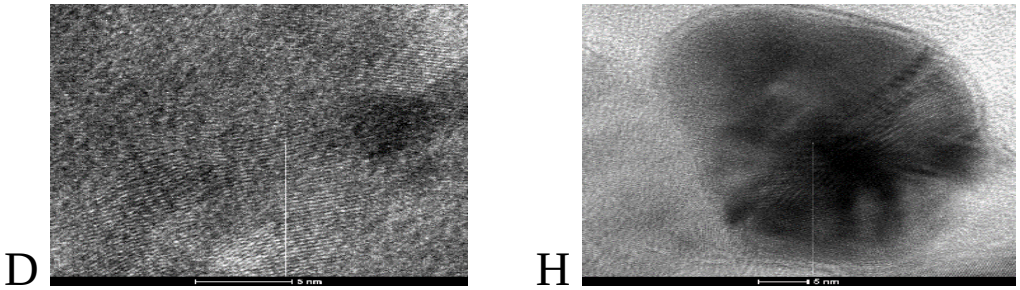


Figure 19: Low and high magnification TEM images of OSNP(A-D) and OSNP-S (E-H) at pH6 and room temperature.

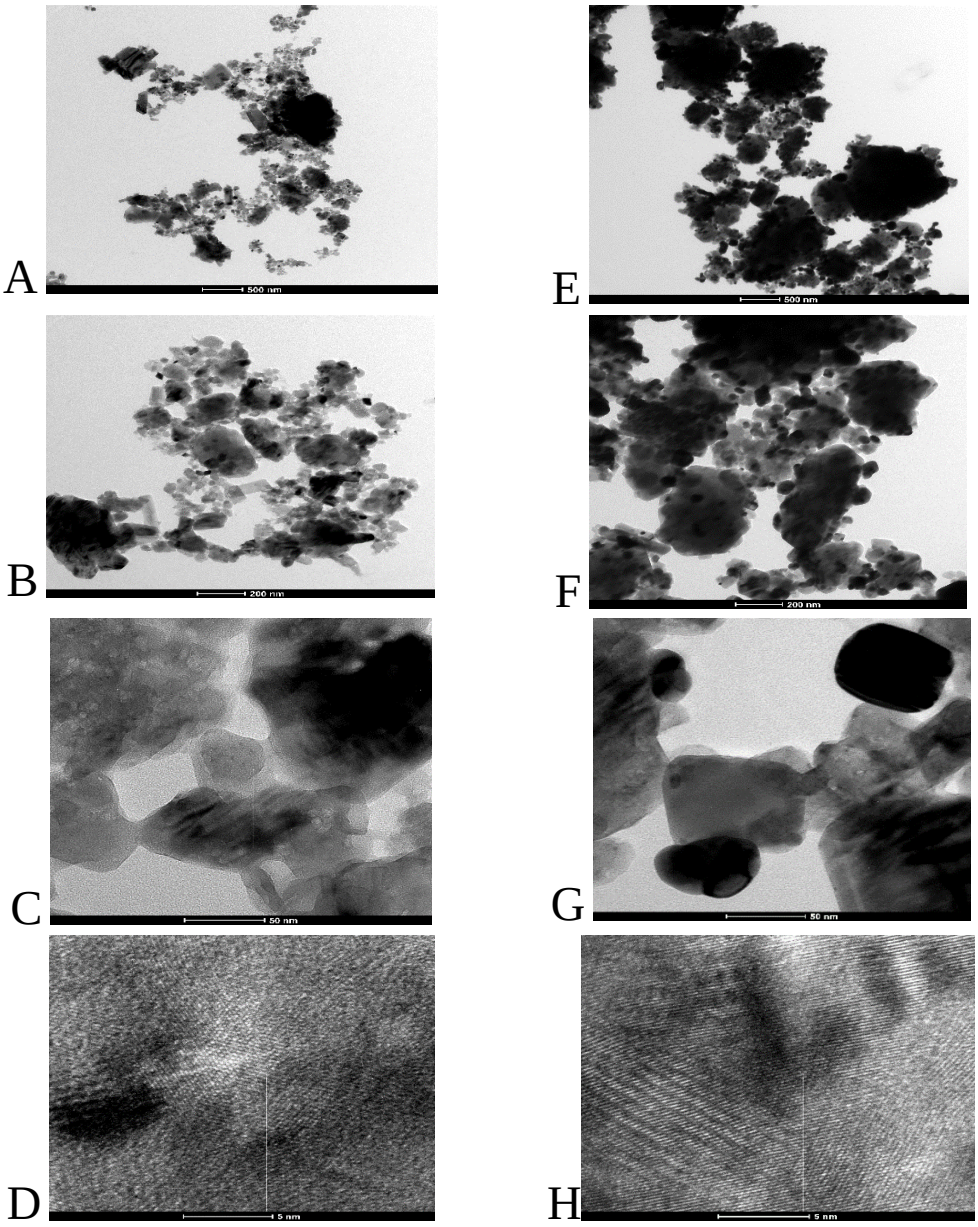

Figure 20: Low and high magnification TEM images of OSNP(A-D) and OSNP-S (E-H) at pH10 and room temperature.

*4.2.4.5. FTIR of adsorbents after Phenol adsorption*

To confirm the adsorption of phenol on the surface of OSNP and OSNP-S, FTIR analysis was conducted. The results in Figures 21 showed the appearance of vibration of -OH broad peak from 3000 $cm^{-1}$ - 3700 $cm^{-1}$ with low intensity. This range indicates the presence of an intermolecular bonded hydroxyl group (Adebayo & Areo, 2021). The -OH band is larger intensity in OSNP compared to OSNP-S due to the adsorption of phenol on OSNP was more. The appearance of very low and minute intense bands was notable between 2800 $cm^{-1}$ -3000 $cm^{-1}$, which indicates the presence of –CH bond (Piazza et al., 2019). From the FTIR spectra, the intensity of whole bands increased after phenol adsorption.

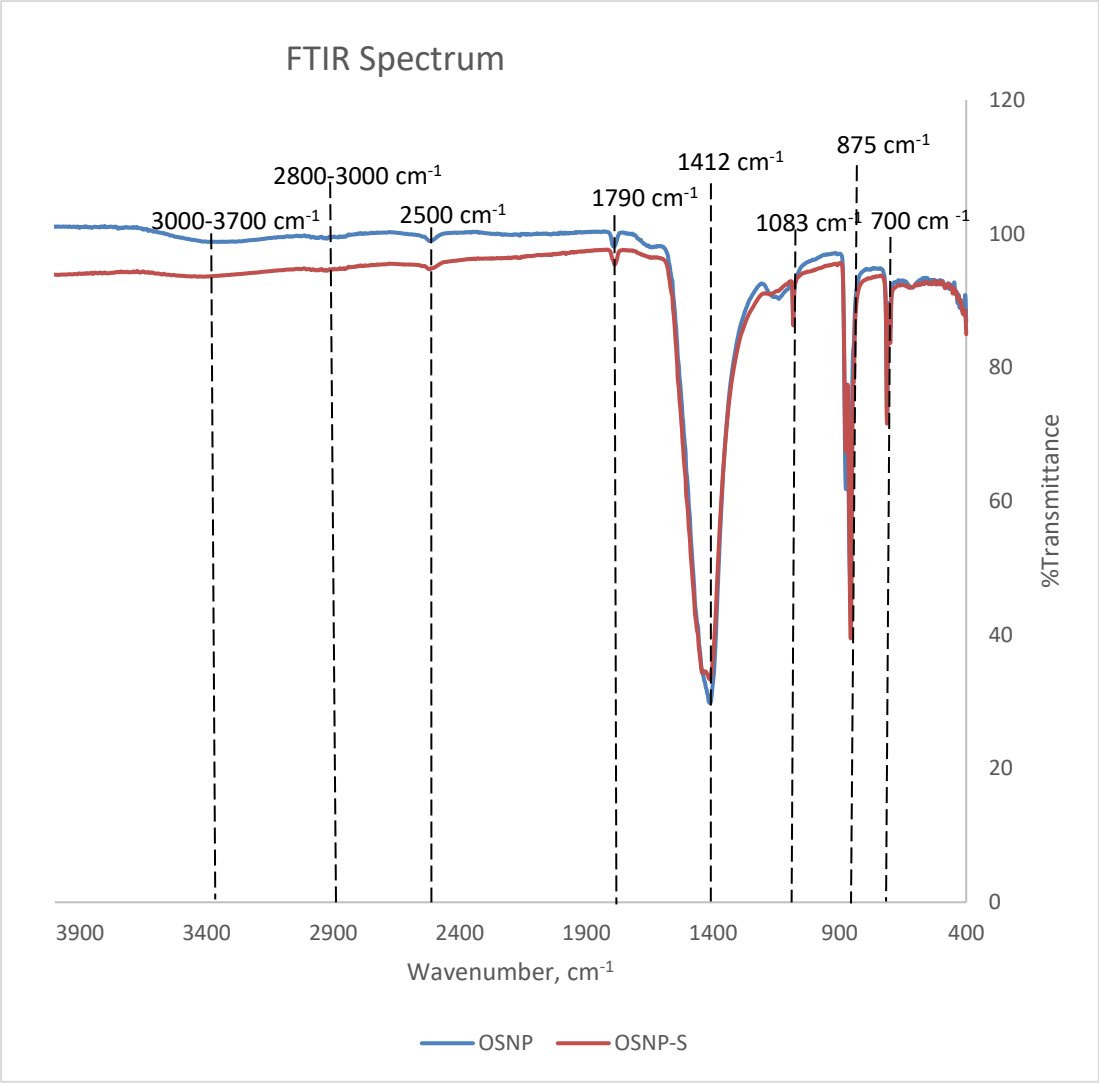


Figure 21: FTIR spectrum of OSNP and OSNP-S after phenol adsorption.

### *4.2.5. Adsorption of Real Phenol sample*

A batch adsorption experiment was carried on for phenol removal from a real sample of olive wastewater at room temperature by using 0.05 g of OSNP and OSNP-S, 50 mL of the real sample, and shaking at 165 RPM for a duration of 24 h. The filtrate was measured by UV-spectrophotometer. Since the UV absorbance value was very high (4), hence the wastewater was diluted by dilution factor $D_F$ = 10. There was no indication of phenol removal at pH 6. Hence, the experiment was conducted at pH 10 and the calculation resulted in the percent phenol removal by 16.22% and 56.78% for

OSNP and OSNP-S respectively. For OSNP-S, the removal percentage of phenol was much higher than the removal in the batch adsorption experiment. This could be due to other parameters that were available in wastewater, which enhanced the attachment of phenol to OSNP-S and furthermore made the adsorption process more effective. There are several components in olive wastewater such as sugars, phenolics, nitrogenous compounds, and organic acids along with tannins, pectins, and carotenoids (Campaniello et al., 2021). The wide range of phenolic compounds in olive wastewater is phenolic alcohols, secoiridoid derivatives, phenolic acids, lignans, flavonoid and hydroxytyrosol (La et al., 2017). (Apalangya et al., 2014) reported that calcium carbonate/Ag nanocomposite exhibits high antimicrobial activity due to its hydrophilic nature and the dispersion of +ve silver ions in an aqueous solution. This could be the reason that no phenol was removed by OSNP-S at pH 6, since the surface was occupied with the bacteria and microorganisms in the real sample. However, at pH 10, the high alkalinity leads to denaturation of the bacteria and the microorganisms, causing it to detach from the OSNP-S surface. Furthermore, allowing phenol to be absorbed on OSNP-S surface. (Tanget al., 2020) indicated that reduction of the bacteria adsorption onto the mineral surface was seen at high pH.

### *4.2.6. Adsorption Isotherm*

To understand the adsorption mechanism of phenol by OSNP and OSNP-S, the adsorbate- adsorbent interaction should be understood in addition to the paratmeters of the Langmuir, Freundlich, Temkin, and Dubinin-Radushkevich isotherm models. These models are useful in understanding the adsorption behavior of phenol molecules onto OSNP and OSNP-S. In the case of finding the best model for phenol adsorption on the surface of OSNP and OSNP-S, these models were tested by using the experimental data obtained from the batch adsorption experiment at different initial concentrations and

temperatures. Figures 22, 23, 24, and Table 10, show the different isotherm models used at different initial concentrations of phenol along with different temperatures and pH 6. Furthermore, Figures 25, 26, and, 27 along with Table 12, show the results at pH 10. These adsorption parameters were calculated from the slopes and intercepts of the linear plots.

*4.2.6.1. Adsorption Isotherms at pH 6*

Based on the results of the Langmuir model, the adsorption capacity (Qm) of phenol on the OSNP and OSNP-S decreases with temperature. The $K_L$ large values indicate that there is a strong interaction between adsorbate and adsorbent while a smaller value implies a weak interaction. The separation factor ($R_L$) value for almost all the concentrations of phenol in the Langmuir model was between 0 and 1 as shown in Table 11. This indicates that the isotherm adsorption is favorable for phenol. The $R_L$ values were between -0.00048 and 0.968. The decrease in adsorption could be due to the diminution of the adsorptive interaction between the active sites of adsorbate and adsorbents. If $0 < R_L < 1$, the adsorption process is favorable, if $R_L = 0$, the process is irreversible, if $R_L = 1$ then the process is linear (depends on the amount and the concentration adsorbed), if $R > 1$, then the process is unfavorable and most desorption occur (Gouamid et al., 2013). On other hand, the coefficient of determination $R^2$ of the Freundlich adsorption isotherm model showed the best equilibrium data for Phenol adsorption on the surfaces of OSNP and OSNP-S. The results of 1/n were less than one in most of the data calculated, indicating and proving the surface heterogeneity. The closer to zero the more heterogeneous (Inthapanya et al., 2019). The favorable adsorption process in Freundlich adsorption isotherm is when $0 < 1/n < 1$, and a cooperative adsorption process occurs when $1/n > 1$. Furthermore, if $n = 1$ then there is a linear adsorption process occurring, if $n > 1$, then physical interaction adsorption

process occurring, and if $n < 1$, then chemical interaction adsorption processing (Ragadhita et al., 2021). The results of almost all the concentrations indicated $n > 1$, which is evidence of a favorable adsorption process with physical interaction. In Temkin isotherm, the adsorption heat constant ($B_T$) is positive and less than 8 KJ/mol for all samples, which proves that the adsorption process is endothermic and occurs physically (Ragadhita et al., 2021; Ugraskan et al., 2022).

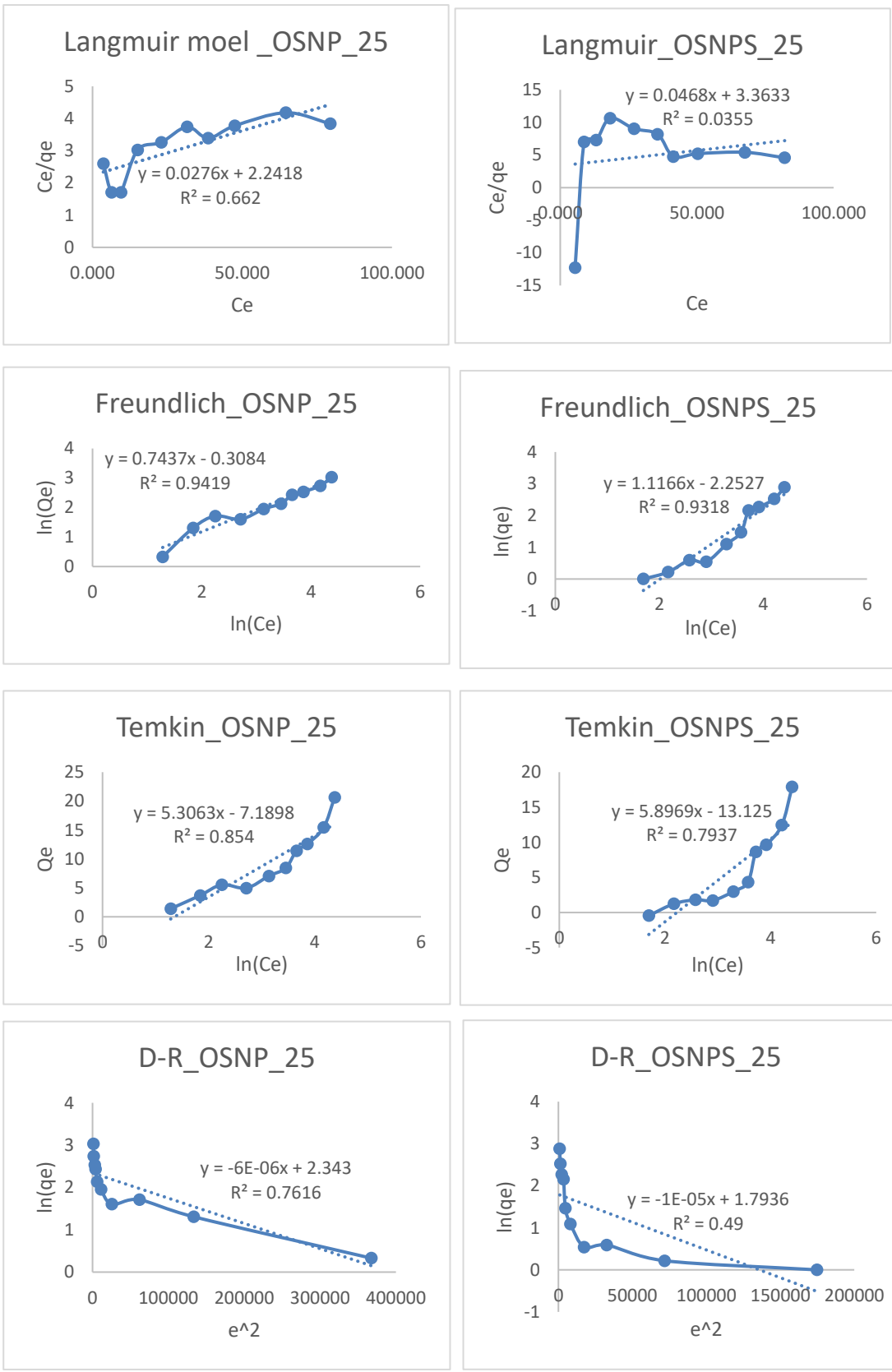


Figure 22: Adsorption isothermal graphs for OSNP and OSNP-S at initial concentrations, 25°C and pH 6.

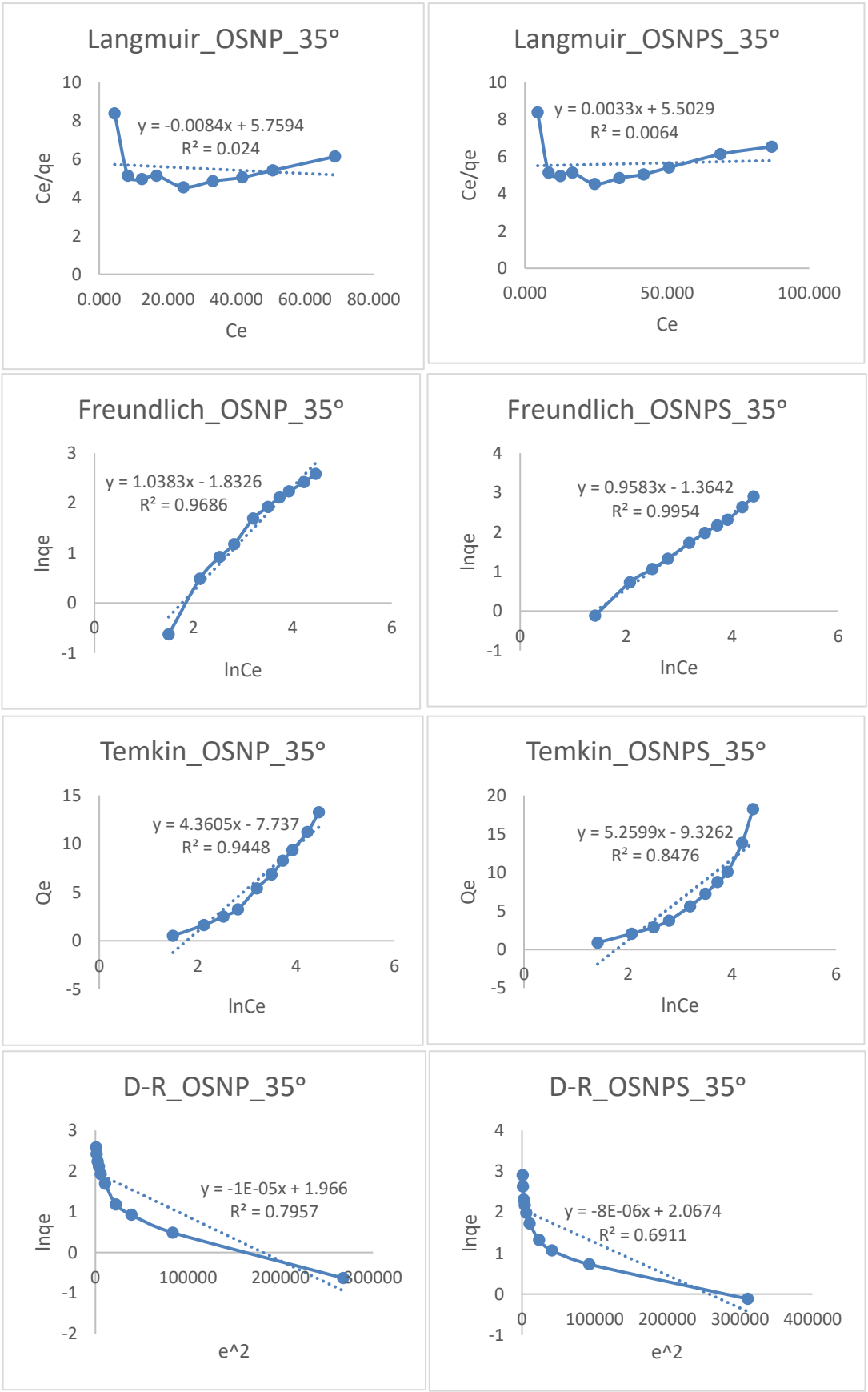


Figure 23: Adsorption isothermal graphs for OSNP and OSNP-S at initial concentrations, 35°C and pH 6.

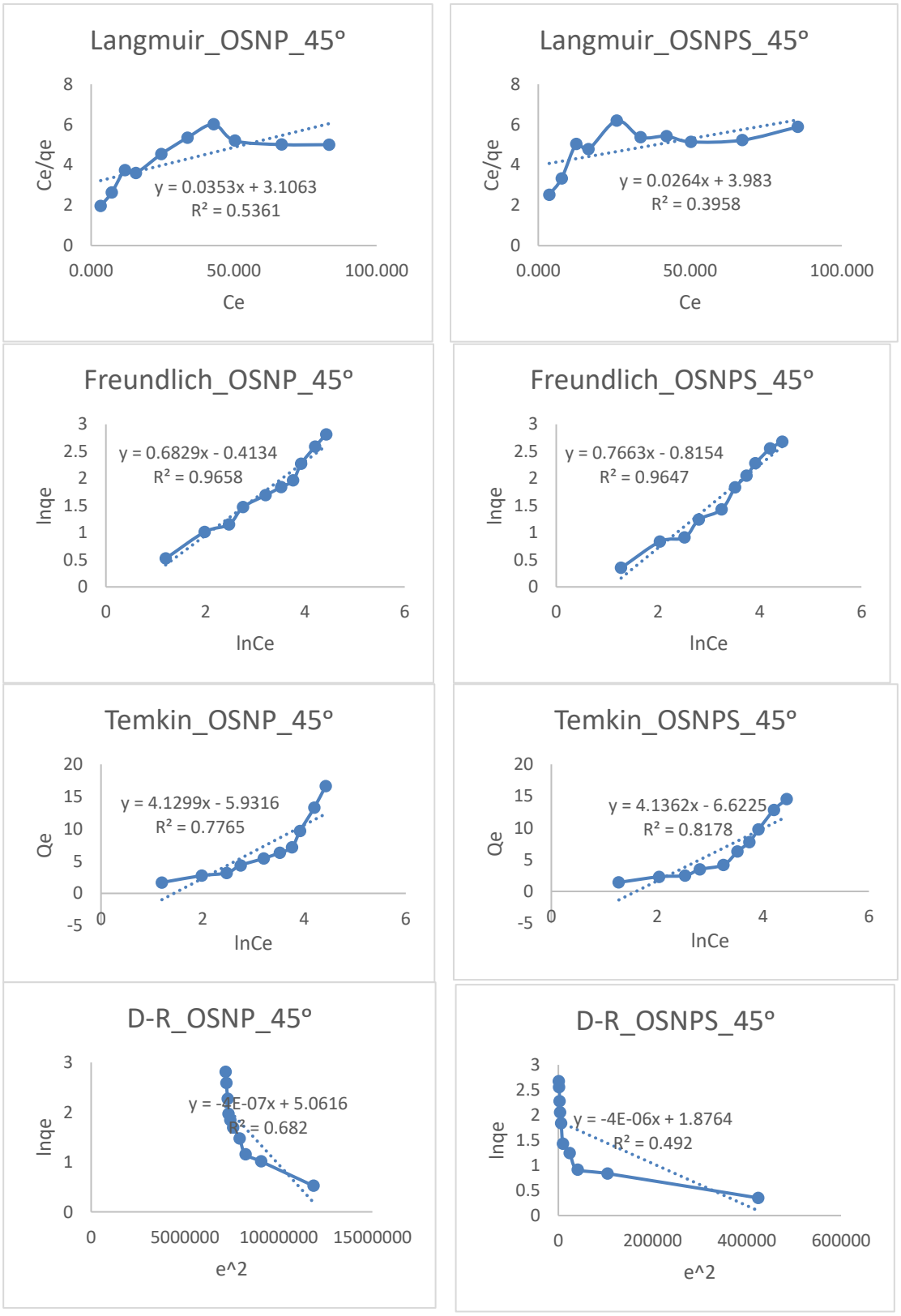


Figure 24: Adsorption isothermal graphs for OSNP and OSNP-S at initial concentrations, 45°C and pH 6.

Table 10: Different Isotherm Parameters of the Phenol Adsorption onto OSNP and OSNP-S at 25 °C, 35 °C and 45 °C (w = 0.05 g, V = 50 mL, pH 6, 165 rpm, agitation time 24 hr).

| Model | Parameter | 25°C | | 35°C | | 45°C | |
|---|---|---|---|---|---|---|---|
| Langmuir | | OSNP | OSNPS | OSNP | OSNPS | OSNP | OSNPS |
| | $Q_m$ (mg/g) | 0.4461 | 0.2973 | 0.1736 | 0.1817 | 0.3219 | 0.2511 |
| | $K_L$ (L/mg) | 16.162 | 6.3531 | -20.670 | 55.067 | 9.1197 | 9.5101 |
| | $R^2$ | 0.662 | 0.0355 | 0.024 | 0.0064 | 0.5361 | 0.3958 |
| Freundlich | | | | | | | |
| | $K_F$ ($mg^{(1-1/n)}*L^{(1/n)}/g$) | 1.3613 | 0.1051 | 6.2501 | 0.2556 | 0.6614 | 0.4425 |
| | 1/n | 0.7437 | 1.1166 | 1.0383 | 0.9583 | 0.6829 | 0.7663 |
| | n | 1.3446 | 0.8956 | 0.9631 | 1.0435 | 1.4643 | 1.3050 |
| | $R^2$ | 0.9419 | 0.9318 | 0.9686 | 0.9954 | 0.9658 | 0.9647 |
| Temkin | | | | | | | |
| | Bt(J/mol) | 5.3063 | 5.8969 | 4.3605 | 5.2599 | 4.1299 | 4.1362 |
| | At(L/mg) | 0.2580 | 0.1080 | 0.1696 | 0.1698 | 0.2378 | 0.2017 |
| | $R^2$ | 0.854 | 0.7937 | 0.9448 | 0.8476 | 0.7765 | 0.8178 |
| Dubinin-Radushkevich | | | | | | | |
| | $Q_{D-R}$ (mg/g) | 10.4124 | 6.01105 | 7.14205 | 7.90425 | 157.843 | 6.5300 |
| | $E_{D-R}$ (KJ/mol) | 288.675 | 223.607 | 223.607 | 250.000 | 1118.03 | 353.553 |
| | $R^2$ | 0.7616 | 0.49 | 0.7957 | 0.6911 | 0.682 | 0.492 |

Table 11: Separation Factor ($R_L$) at Different Initial Concentrations, Temperatures and at pH 6.

| $C_\circ$ (ppm) | $R_L$ | | | | | |
|---|---|---|---|---|---|---|
| | 25°C | | 35°C | | 45°C | |
| | OSNP | OSNPS | OSNP | OSNPS | OSNP | OSNPS |
| 5 | 0.012223 | 0.030520 | -0.00977 | 0.597688 | 0.021460 | 0.020597 |
| 10 | 0.006149 | 0.015496 | -0.00486 | 0.747034 | 0.010846 | 0.010406 |
| 15 | 0.004108 | 0.010385 | -0.00324 | 0.815518 | 0.007257 | 0.006961 |
| 20 | 0.003084 | 0.007809 | -0.00242 | 0.854821 | 0.005453 | 0.005230 |
| 30 | 0.002058 | 0.005219 | -0.00162 | 0.898198 | 0.003642 | 0.003493 |
| 40 | 0.001544 | 0.003920 | -0.00121 | 0.921617 | 0.002734 | 0.002622 |
| 50 | 0.001236 | 0.003138 | -0.00097 | 0.936277 | 0.002188 | 0.002099 |
| 60 | 0.001030 | 0.002617 | -0.00081 | 0.946317 | 0.001824 | 0.001749 |
| 80 | 0.000773 | 0.001964 | -0.00061 | 0.959180 | 0.001369 | 0.001313 |
| 100 | 0.000618 | 0.001572 | -0.00048 | 0.967070 | 0.001095 | 0.001050 |

*4.2.6.2. Adsorption Isotherms at pH 10*

At pH 10 and as shown in Table 12, the results of the Langmuir model showed that the adsorption capacity ($Q_m$) of phenol on the surface of OSNP was almost constant whereas, for OSNP-S decreases in $Q_m$ with temperature was noticed. At higher $K_L$ a strong interaction between adsorbate and adsorbent is indicated while a smaller value indicates a weak interaction. The separation factor ($R_L$) value for almost all the concentrations of phenol in the Langmuir model was less than one ($R_L < 1$). Hence, the isotherm adsorption is favorable for phenol (Gouamid et al., 2013). The coefficient of determination $R^2$ of the Freundlich adsorption isotherm model showed the best equilibrium data for Phenol adsorption on the surfaces of OSNP and OSNP-S. The $R^2$ Freundlich adsorption isotherm model ranged from 0.9468 to 0.9832 and the second best $R^2$ value was in the Temkin model (0.7301-0.8854). Furthermore, the results of 1/n

were less than one in most of the data calculated, indicating and proving the surface heterogeneity and favorability of the adsorption process (Inthapanya et al., 2019). For n values, the results of almost all the concentrations indicated $n > 1$, which is evidence of a favorable adsorption process with physical interaction (Ragadhita et al., 2021). In Temkin isotherm, the adsorption heat constant ($B_T$) is positive and less than 8 KJ/mol for all samples, which proves that the adsorption process is endothermic and occurs physically (Ragadhita et al., 2021; Ugraskan et al., 2022). As far as the OSNP-S as an adsorbent, we have not found any study that embedded silver on oyster shell surface for phenol removal. However, the maximum adsorption capacity of phenol on OSNP and OSNP-S at both pH values 6 and 10 were low compared to other adsorbents used in different studies presented in Table 14. Furthermore, the Qm results were close to a previous study done on the Oyster shell (Chitosan)/TiO2 nanocomposite which, had a low adsorption capacity of 1.699 mg/g for phenol at $25^{o}$ C (Etimet al., 2015).

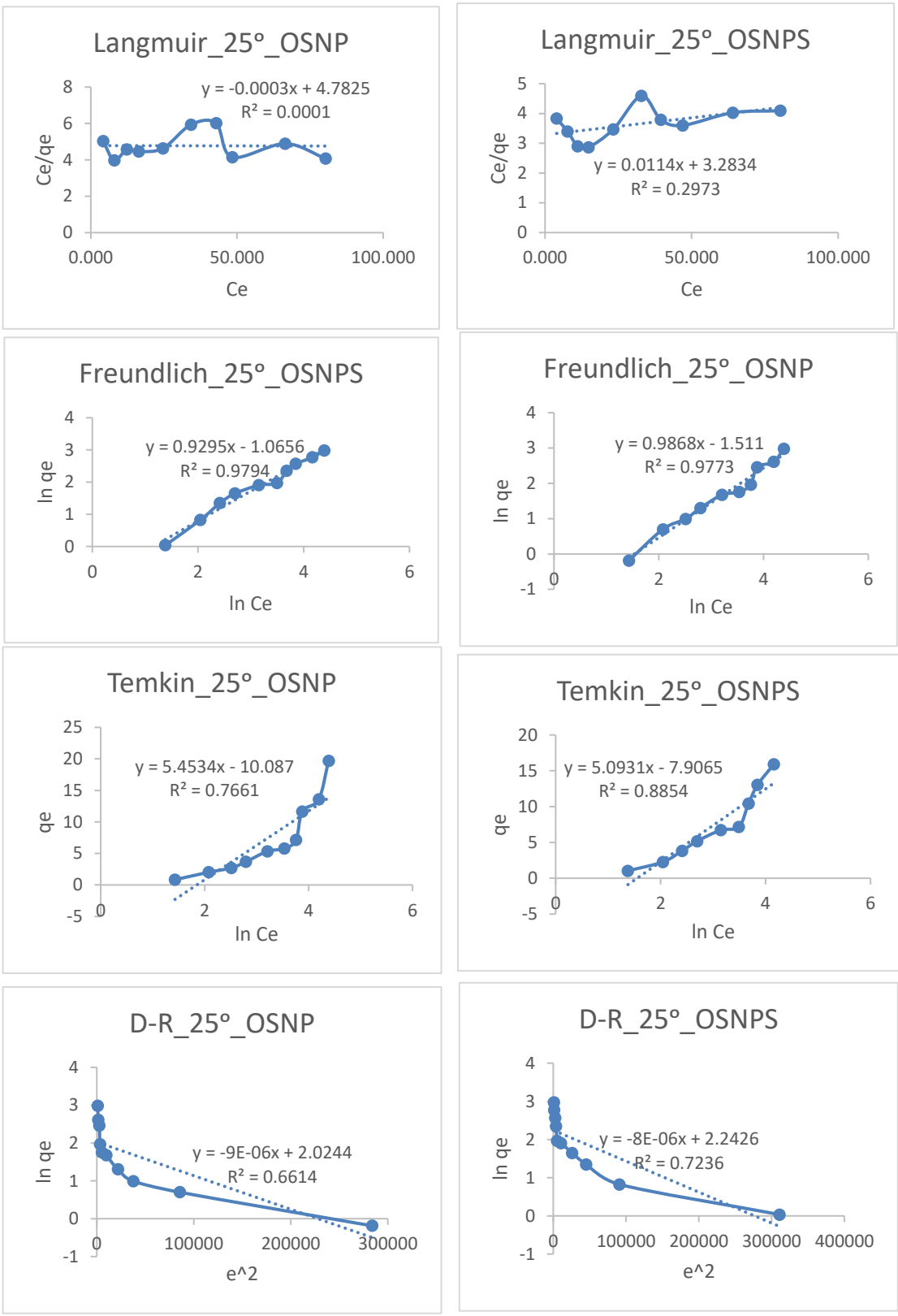


Figure 25: Adsorption isothermal graphs for OSNP and OSNP-S at initial concentrations, 25°C and pH 10.

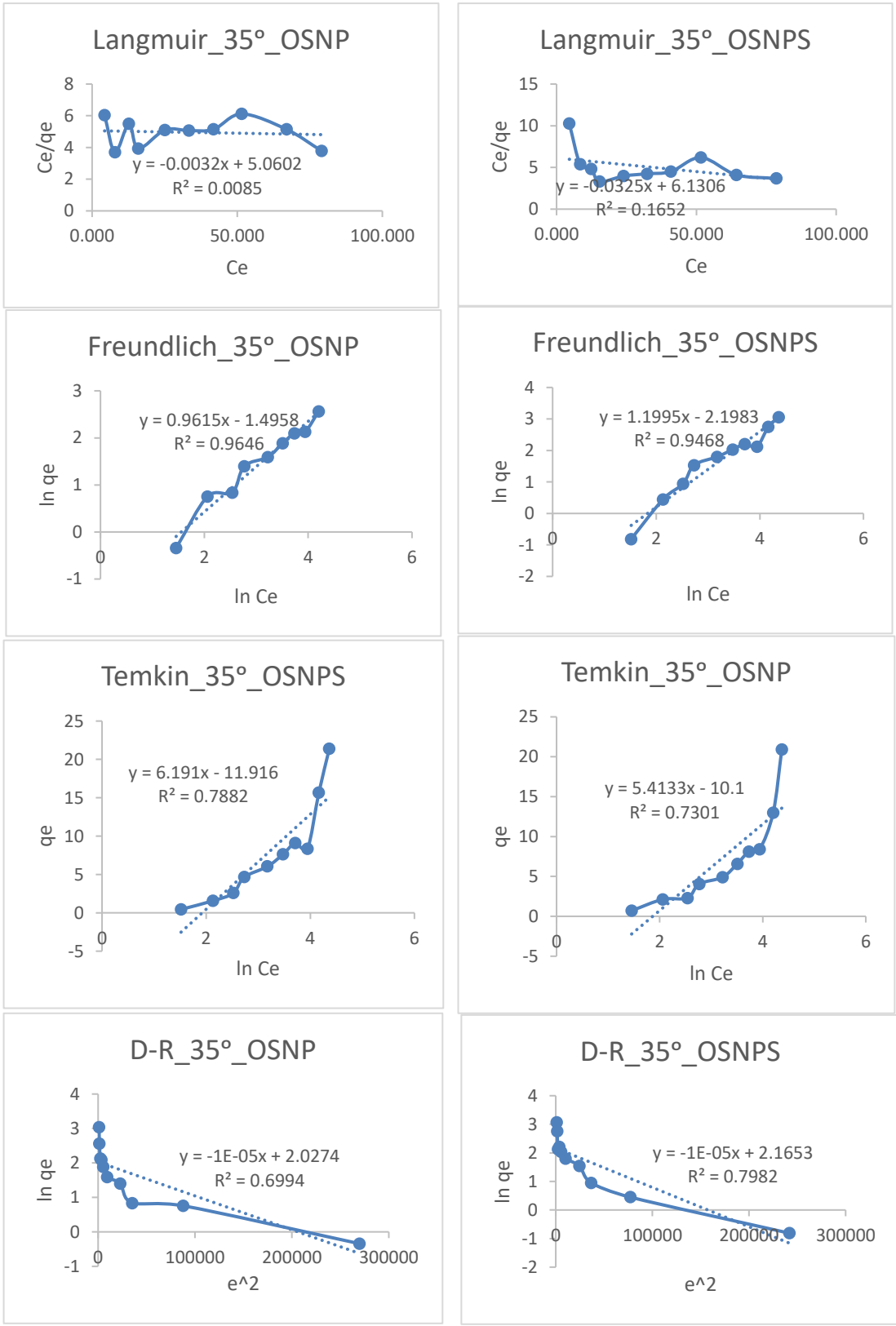


Figure 26: Adsorption isothermal graphs for OSNP and OSNP-S at initial concentrations, 35°C and pH 10.

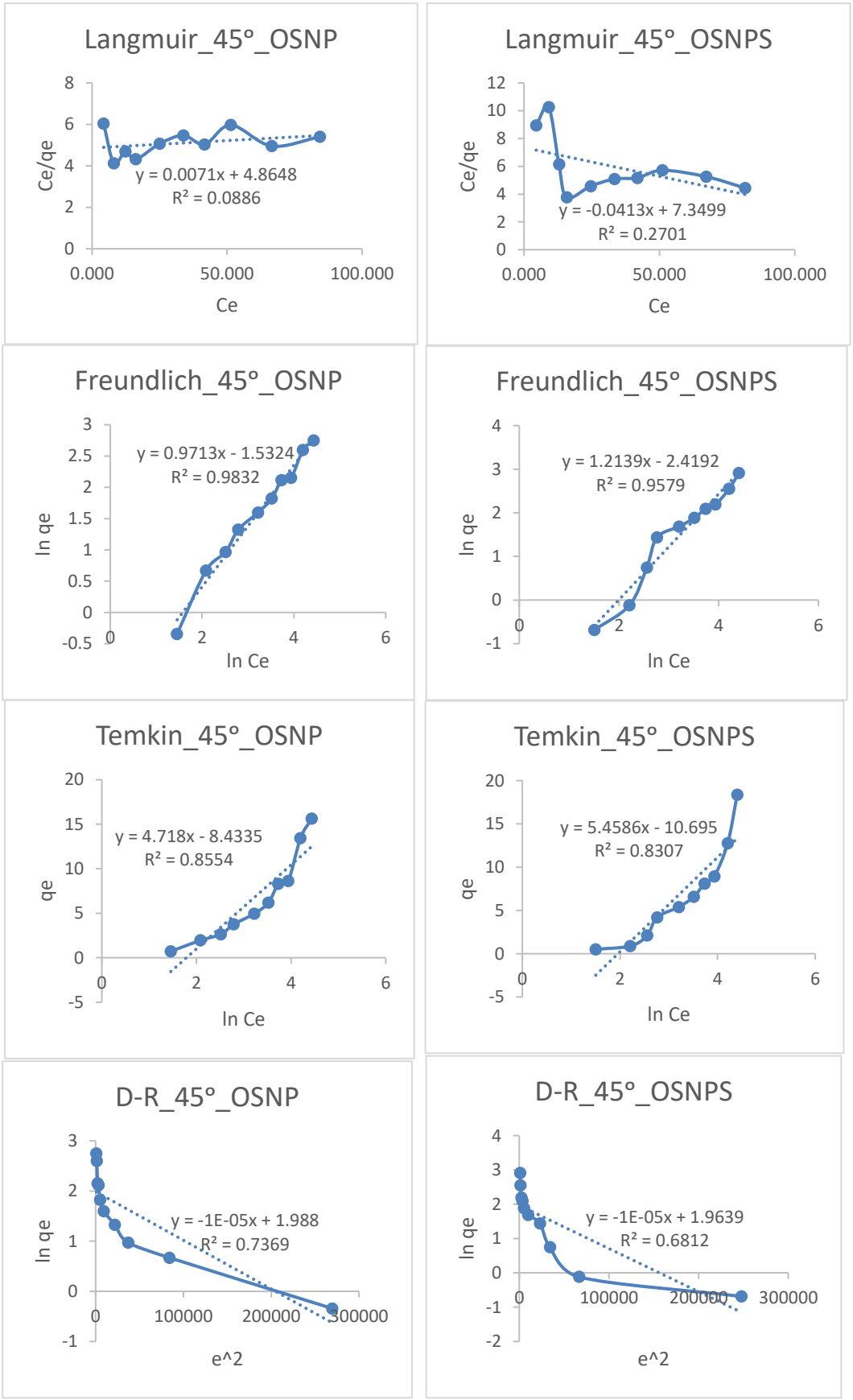


Figure 27: Adsorption isothermal graphs for OSNP and OSNP-S at initial concentrations, 45°C and pH 10.

Table 12: Different Isotherm Parameters of the Phenol Adsorption onto OSNP and OSNP-S at 25 °C, 35 °C and 45 °C (w = 0.05 g, V = 50 mL, pH 10, 165 rpm).

| Model | Parameter | 25°C | | 35°C | | 45°C | |
|---|---|---|---|---|---|---|---|
| Langmuir | | OSNP | OSNPS | OSNP | OSNPS | OSNP | OSNPS |
| | $Q_m$ (mg/g) | 0.2091 | 0.3046 | 0.1976 | 0.1631 | 0.2056 | 0.1361 |
| | $K_L$ (L/mg) | -696.986 | 26.716 | -61.757 | -5.019 | 28.952 | -3.294 |
| | $R^2$ | 0.0001 | 0.2973 | 0.0085 | 0.1652 | 0.6886 | 0.2701 |
| Freundlich | | | | | | | |
| | $K_F$ ($mg^{(1-1/n)}*L^{(1/n)}/g$) | 0.2207 | 0.3445 | 0.2241 | 0.1110 | 0.2160 | 0.0890 |
| | 1/n | 0.9868 | 0.9295 | 0.9615 | 1.1995 | 0.9713 | 1.2139 |
| | n | 1.0134 | 1.0759 | 1.0409 | 0.8337 | 1.0296 | 0.8238 |
| | $R^2$ | 0.9773 | 0.9794 | 0.9646 | 0.9468 | 0.9832 | 0.9579 |
| Temkin | | | | | | | |
| | Bt(J/mol) | 5.4534 | 5.0931 | 5.4133 | 6.1910 | 4.7180 | 5.4586 |
| | At(L/mg) | 0.1573 | 0.2117 | 0.1548 | 0.1459 | 0.1674 | 0.1410 |
| | $R^2$ | 0.7661 | 0.8854 | 0.7301 | 0.7882 | 0.8554 | 0.8307 |
| Dubinin-Radushkevich | | | | | | | |
| | $Q_{D-R}$ | 7.5716 | 9.4178 | 7.5943 | 8.7172 | 7.3009 | 7.1271 |
| | $E_{D-R}$ | 235.702 | 250.000 | 223.607 | 223.607 | 223.607 | 223.607 |
| | $R^2$ | 0.6614 | 0.7236 | 0.6999 | 0.7982 | 0.7369 | 0.6812 |

Table 13: Separation Factor ($R_L$) at Different Initial Concentrations, Temperatures and at pH 10.

| | $R_L$ | | | | | |
|---|---|---|---|---|---|---|
| $C_o$,(ppm) | 25° | | 35° | | 45° | |
| | OSNP | OSNPS | OSNP | OSNPS | OSNP | OSNPS |
| 5 | -0.00029 | 0.007431 | -0.00325 | 0.998561 | 0.006861 | -0.06463 |
| 10 | -0.00014 | 0.003729 | -0.00162 | 0.99928 | 0.003442 | -0.03131 |
| 20 | -7.2E-05 | 0.001868 | -0.00081 | 0.99964 | 0.001724 | -0.01541 |
| 30 | -4.8E-05 | 0.001246 | -0.00054 | 0.99976 | 0.00115 | -0.01022 |
| 40 | -3.6E-05 | 0.000935 | -0.0004 | 0.99982 | 0.000863 | -0.00765 |
| 50 | -2.9E-05 | 0.000748 | -0.00032 | 0.999856 | 0.00069 | -0.00611 |
| 60 | -2.4E-05 | 0.000623 | -0.00027 | 0.99988 | 0.000575 | -0.00508 |
| 80 | -1.8E-05 | 0.000468 | -0.0002 | 0.99991 | 0.000432 | -0.00381 |
| 100 | -1.4E-05 | 0.000374 | -0.00016 | 0.999928 | 0.000345 | -0.00304 |

Table 14: Comparison of Maximum Adsorption Qapacity (Qm) of Phenol on Different Adsorbents.

| Adsorbent | Qm (mg/g) | Temperature (°C) | pH | Reference |
|---|---|---|---|---|
| OSNP | 0.4461 | 25 | 6 | Current study |
| OSNP-S | 0.2973 | 25 | 6 | Current study |
| OSNP | 0.2091 | 25 | 10 | Current study |
| OSNP-S | 0.3046 | 25 | 10 | Current study |
| Activated Clay | 15.00 | 23 | 5 | (Djebbaret al., 2012) |
| Diphenyldiquinoline | 15.15 | 25 | 4 | (Al-trawneh et al., 2021) |
| Activated carbon/Iron | 20 | 25 | 7 | (Majid et al., 2019) |
| Fly ash | 142.86 | 25 | 8 | (Sharan et al., 2009) |
| Coconut shell -clay | 1665 | 25 | 2 | (Adebayo & Areo, 2021) |
| Oystershell (Chitosan)/$TiO_2$ | 1.699 | 25 | 6 | (Etim et al., 2015) |
| Seaweed (Saragassum sp.) (Chaetomorpha) | 82.1 17.7 | 25 | 10 | (Navarro et al., 2016) |

### *4.2.7. Thermodynamics*

Adsorption thermodynamics were plotted in graphs representing temperature (Kelvin) Vs $\Delta G^o$ (KJ/mol) (Figure 28). The values of energy change ($\Delta G^o$), standard enthalpy ($\Delta H^o$), and standard molar entropy ($\Delta S^o$) at pH 6 and pH 10 are given in Table 15. $\Delta G^o$ was calculated from van't Hoff equation whereas; $\Delta H^o$ and $\Delta S^o$ were indicated from the intercept and slope of the graphs respectively. The $\Delta G^o$ values were in negative sign, indicating that the adsorption process is thermodynamically feasible, spontaneous, and chemically controlled in all temperatures and pH conditions 6 and 10. The $\Delta H^o$ and $\Delta S^o$ values for OSNP at pH 6 were -20.42 and 0.0525 KJ $mol^{-1}$ respectively. The negative sign of $\Delta H^o$ indicates that the nature of the adsorption process is exothermic while the positive value of $\Delta S^o$ indicates the increase in disorder at the adsorbate-adsorbent interface during the adsorption process. At pH 6 values of the thermodynamic parameters of OSNP-S, $\Delta H^o$ and $\Delta S^o$ were 14.23 and -0.0687 KJ $mol^{-1}$ respectively. The adsorption process was endothermic due to the positive $\Delta H^o$ value whereas, the negativity of $\Delta S^o$ represents the decrease in the adsorption process randomness and the reduced confusion at solid-solution interface (Dehmani et al., 2020). At pH 10, the thermodynamic parameters for OSNP and OSNP-S had opposite signs of the values indicated in pH 6. For OSNP, $\Delta H^o$ and $\Delta S^o$ were 134.1 and -0.4449 KJ $mol^{-1}$ respectively and for OSNP-S, the values were -128.1 kJ $mol^{-}$ and 0.4070 kJ $mol^{-1}$. The results showed scattered points due to the non stable bonding accuring during the adsorption and desorption process. In (Daraei et al., 2013) study, the thermodynamic parameters results for the adsorption of phenol on eggshell (calcium carbonate) at different temperatures indicated that the adsorption was spontaneous, feasible and undergoes an exothermic process. Furthermore, the adsorption was indicated physical in nature.

Table 15: Thermodynamics Parameters Results of OSNP and OSNP-S at pH 6 and pH 10.

| Adsorbent | pH | T (K) | $\Delta G^o$(KJ $mol^{-1}$) | $\Delta H^o$ (KJ $mol^{-1}$) | $\Delta S^o$(KJ $mol^{-1}$) |
|---|---|---|---|---|---|
| OSNP | 6 | 298 | -6.894 | | |
| | | 308 | 0 | -20.42 | 0.0525 |
| | | 318 | -5.844 | | |
| OSNP-S | 6 | 298 | -4.581 | | |
| | | 308 | -10.265 | 14.23 | -0.0687 |
| | | 318 | -5.955 | | |
| OSNP | 10 | 298 | 0 | | |
| | | 308 | 0 | 134.1 | -0.4449 |
| | | 318 | -8.898 | | |
| OSNP-S | 10 | 298 | -8.140 | | |
| | | 308 | 0 | -128.1 | 0.4070 |
| | | 318 | 0 | | |

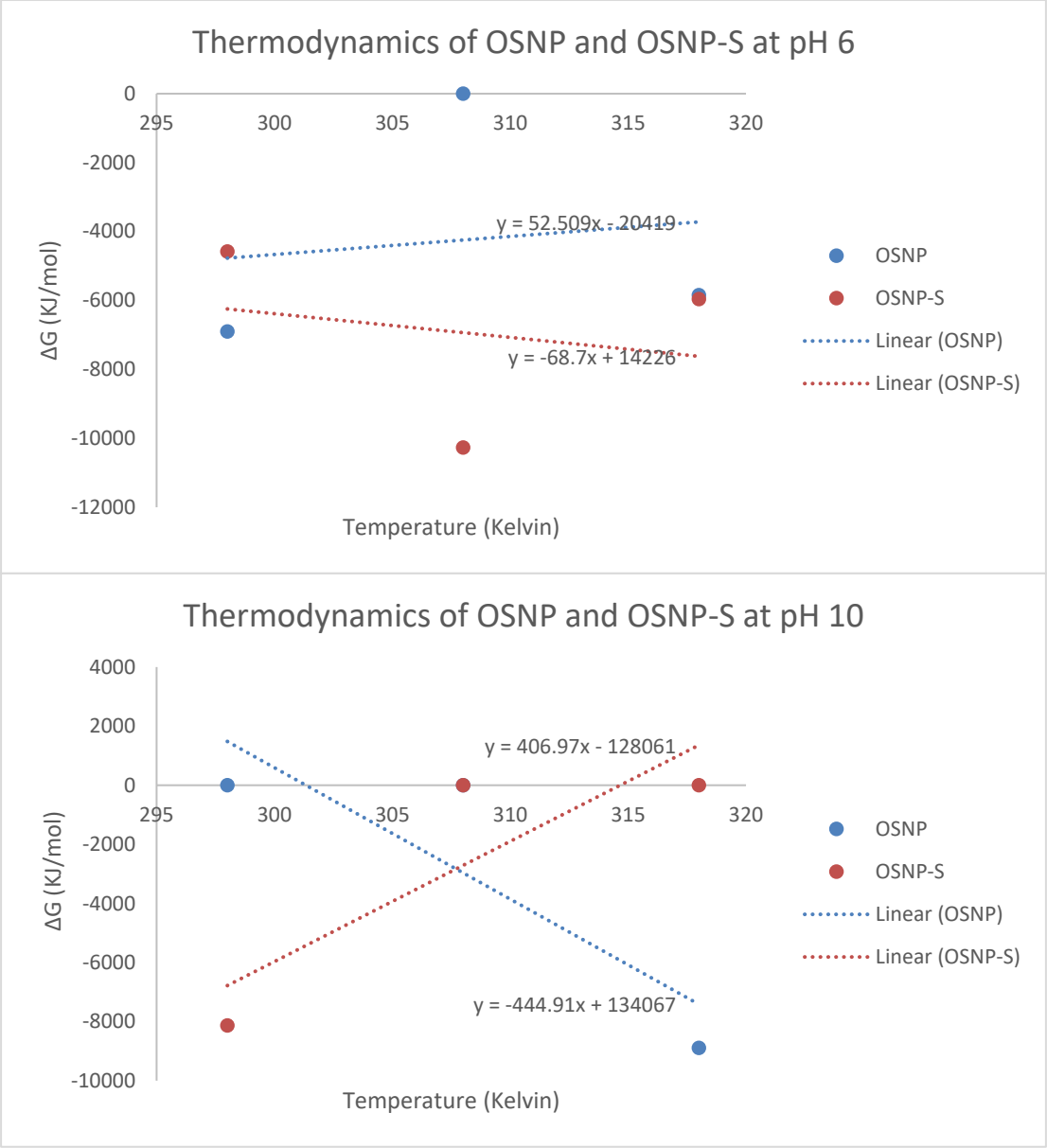


Figure 28: Thermodynamics graphs of OSNP and OSNP-S at pH 6 and pH 10.

### *4.2.8. Reusability of Adsorbent - Desorption Studies*

The desorption phenomenon is the release of a substance from or through a surface. The process is the opposite of sorption (adsorption or absorption). The adsorbents used in adsorption processes get saturated by time due to occupying all adsorption sites, hence, the adsorption reaches equilibrium, gets totally inactive, and is stated as exhausted and spent. To overcome the spent adsorbent problem, the

regeneration process is used. Desorption breaks the bond between adsorbent-adsorbate in ease to liberate adsorbate from solution. (Patel, 2021). Desorption should be compared to adsorption performed under the same parameters and conditions of solution composition and ionic strength in term to predict fixation, which adsorbate equate with non-exchangeability (Baveye & Steenhuis, 2004). In phenol desorption, phenol is released from loaded OSNP-S by contact with NaOH or HCl solutions. The results of desorption of phenol with 0.1 M NaOH and 0.1 M HCl were 97.44% and 98.64% respectively. The high phenol removal by NaOH and HCl solutions indicates that by converting phenol molecules into phenolate anions, the adsorbed phenol would be easily desorbed (Aklet al., 2014). As mentioned earlier, we have not found any study regarding oyster shell/silver nanocomposite for phenol removal. However, in an adsorption study of phenol on polymer surface (Ghafariet al., 2019), the phenol desorption with NaOH was 86% recovery. Whereas (Mojoudi et al., 2019), reported that the NaOH solution had better regeneration performance compared to the HCl solution and this was explained by the fact of formation of soluble salt $C_6H_5O^-Na^+$ which, eases the desorption of phenol from the adsorbent.

### *4.2.9. Statistical Analysis*

The statistical analysis results of data two-way ANOVA without replication for testing the phenol concentrations and temperature effect on the adsorption process showed that at pH 6 the temperature significant effect for both OSNP and OSNP-S ($p < 0.05$) whereas, the concentration was not significant ($p > 0.05$). At pH 10, concentration had a significance effect on both adsorbents and temperature had a significant effect only on OSNP-S.

# CHAPTER 5: CONCLUSION

In this paper and for the first time in the Arabian Gulf region, the Pearl oyster *Pinctada imbricata radiata* was used as a bio-indicator of phenol pollution.

The first objective was to investigate the ecotoxicity and monitor the activity of some biomarkers of oxidative stress such as Catalase (CAT) and Superoxide Dismutase (SOD) for the Pearl oyster *Pinctada imbricata radiata* organs such as the gills and the digestive gland under different increasing concentrations of phenol. Hence, fresh adult Pearl oysters *Pinctada imbricata radiata* were maintained in the laboratory in 15 aquaria in natural conditions of permanent aeration, at 25°C, 40 psu salinity, and 12:12 photoperiod. Then, after acclimation, the oysters were exposed to different concentrations of phenols (1, 2, 5, and 10 ppm), during 96h in triplicates versus control (0 ppm). To characterize our pearl oyster population from Al-Wakra oyster beds, the biometric analysis of individual shell size and weights, showed that the dominated size class was (4.5-5.5 cm) length with 70% of the population. Furthermore, the biometric relations (length, width, and height versus weight) between size classes of *Pinctada imbricata radiata* showed negative allometric growth. The Total proteins values decreased over time but there were no significant differences between the total proteins averaged values (p-value > 0.001) as commonly there are no big changes for this parameter due to the fast imposed to the pearl oyster during the 96h experiment. CAT and SOD enzymatic activities for both gills and digestive glands showed an increase in values compared to the control organisms with positive impact and there is a significant difference with a p-value < 0.001 in all cases when we consider the phenol treatment (concentration) the time of exposure and both treatment and time combined. These results indicated that Pearl oyster *Pinctada imbricata radiata* is an excellent bioindicator of phenol pollution and should be used for other pollutants indicator and

in marine environmental pollution monitoring programs as other bivalves such as the mussels, *Mytilus galloprovincialis* and the Pacific giant oyster, *Cassostrea gigas* (Opiyo et al., 2021; Vilhenaet al., 2021).

The second objective was to use silver-impregnated oyster shell nanoparticles OSNP-S as a novel technique for the detoxification of phenol from water. Pearl oyster shell nanoparticles (OSNP) were prepared by a simple Ball-milling process and then impregnated with silver. A Batch system was used to carry out the adsorption study at different pH values, temperature, and initial phenol concentrations. The Phenol intake level was measured by the Ultra Violet-Visible spectroscopy method. The physical and chemical characterization of both OSNP and OSNP-S were determined with Scan Electron Microscopy (SEM) and Fourier transform infrared spectrophotometer (FTIR). To study the surface area, pore radius, and pore volume, Brunauer, Emmett, & Teller (BET) and Transmission electron microscope (TEM) were used. Batch adsorption isotherms (Langmuir isotherm, Freundlich isotherm, Temkin isotherm, and Dubinin-Radushkevich isotherm models) were used to study the efficiency of the adsorbents in removing phenol and to describe the adsorbent-adsorbate interaction system. The results indicated that BET surface area, Langmuir surface area, and pore volume of the OSNP was the highest. The batch analysis that was conducted at pH 6 were in favor of OSNP in term of adsorbing the highest amount of phenol from the aqueous solutions at different concentrations. However, at pH 10, the removal results were in favor of OSNP-S. The highest phenol removal occurred at room temperature. Furthermore, the highest phenol removal of real olive wastewater was at pH 10 and the room temperature was by OSNP-S (56.78%). Based on adsorption isotherm models, the values of the coefficient of determination $R^2$ of the Freundlich adsorption isotherm model showed the best equilibrium data for Phenol adsorption on the surfaces of OSNP and OSNP-S.

The results of 1/n were less than one in most of the data calculated, indicating and proving the surface heterogeneity and favorability of the adsorption process whereas, the n values ($n > 1$) indicated the physical interaction adsorption process. The adsorption thermodynamics parameter $\Delta G^o$ values, were in negative sign, indicating that the adsorption process is thermodynamically feasible, spontaneous, and chemically controlled in all temperatures and both pH conditions 6 and 10. At pH 6 values of the thermodynamic parameters of OSNP-S, indicated that the adsorption process was endothermic due to the positive $\Delta H^o$ value whereas, the negativity of $\Delta S^o$ represents the decrease in the adsorption process randomness and the reduced confusion at solid-solution interface. At pH 10, the thermodynamic parameters for OSNP and OSNP-S had opposite signs of the values indicated in pH 6. The statistical analysis results of data two-way ANOVA showed that at pH 10 both concentration and temperature had a significant effect on the phenol removal by OSNP-S ($p < 0.05$). Since the current study indicated an increase in oxidative stress that could affect peal oysters *Pinctada imbricata radiata* that could lead to their disease or mortality, it is recommended to conduct more studies to further examine the effects of phenol on *Pinctada imbricata radiata*. Moreover, the endemic pearl oyster should be considered as a key species in marine pollution coastal monitoring programs and ecotoxicological studies in Qatar seawaters and at a regional scale in the Arabian Gulf. Furthermore, since there are minute studies regarding the phenol removal by the oyster shell nanoparticles and oyster shell/silver hence, more studies on the adsorption of phenol by oyster shell are needed.

REFERENCES

Acosta, A. L., Bustamante, P., Budzinski, H., Huet, V., Acosta, A. L., Bustamante, P., … Thomas-guyon, H. (2015). Persistent Organic Pollutants in a marine bivalve on the Marennes-Oléron Bay and the Gironde Estuary ( French Atlantic coast ) -Part 2 : Potential biological effects To cite this version : HAL Id : hal-01223660.

Adebayo, M. A., & Areo, F. I. (2021). Resources , Environment and Sustainability Removal of phenol and 4-nitrophenol from wastewater using a composite prepared from clay and Cocos nucifera shell : Kinetic , equilibrium and thermodynamic studies. *Resources, Environment and Sustainability*, *3*(March), 100020. https://doi.org/10.1016/j.resenv.2021.100020

Agostini, E., Talano, M. A., Laura, A., & Oller, W. (2011). *Phytoremediation of phenolic compounds: Recent advances and perspectives*.

Ahmad, A. Y., & Al-ghouti, M. A. (2020). Groundwater for Sustainable Development Approaches to achieve sustainable use and management of groundwater resources in Qatar : A review. *Groundwater for Sustainable Development*, *11*(February), 100367. https://doi.org/10.1016/j.gsd.2020.100367

Aideed, M. S., Ahmed, B. A., & Mukhaysin, A. A. (2015). Existence , growth and reproduction of pearl oyster Pinctada margaritifera in Hadhramout coast / Gulf of Aden. *The Egyptian Journal of Aquatic Research*, *40*(4), 473–481. https://doi.org/10.1016/j.ejar.2014.12.004

Akl, M. A. A., Dawy, M. B., & Serage, A. A. (2014). Analytical & Bioanalytical Techniques Efficient Removal of Phenol from Water Samples Using Sugarcane Bagasse Based Activated Carbon, *5*(2). https://doi.org/10.4172/2155-9872.1000189

Al-Ghouti, M. A., Al Disi, Z. A., Al-Kaabi, N., & Khraisheh, M. (2017). Mechanistic

insights into the remediation of bromide ions from desalinated water using roasted date pits. *Chemical Engineering Journal*, *308*, 463–475. https://doi.org/10.1016/j.cej.2016.09.091

Al-trawneh, S. A., Jiries, A. G., Alshahateet, S. F., & Sagadevan, S. (2021). Phenol removal from aqueous solution using synthetic V-shaped organic adsorbent : Kinetics , isotherm , and thermodynamics studies. *Chemical Physics Letters*, *781*(August), 138959. https://doi.org/10.1016/j.cplett.2021.138959

Alameri, K., Giwa, A., Yousef, L., Alraeesi, A., & Taher, H. (2019). Sorption and removal of crude oil spills from seawater using peat-derived biochar : An optimization study. *Journal of Environmental Management*, *250*(July), 109465. https://doi.org/10.1016/j.jenvman.2019.109465

Albuquerque, F. P. De, Oliveira, J. L. De, Moschini-carlos, V., & Fraceto, L. F. (2020). Science of the Total Environment An overview of the potential impacts of atrazine in aquatic environments : Perspectives for tailored solutions based on nanotechnology, *700*. https://doi.org/10.1016/j.scitotenv.2019.134868

Alhaddad, F. A., Abu-dieyeh, M., Da, D., Helaleh, M., & Al-ghouti, M. A. (2021). Occurrence and removal characteristics of phthalate esters from bottled drinking water using silver modified roasted date pits, 733–751.

Ali, I., & Gupta, V. K. (2006). Advances in water treatment by adsorption technology, (February). https://doi.org/10.1038/nprot.2006.370

Alipour, V., Nasseri, S., Nodehi, R. N., Mahvi, A. H., & Rashidi, A. (2014). ENVIRONMENTAL HEALTH Preparation and application of oyster shell supported zero valent nano scale iron for removal of natural organic matter from aqueous solutions, 1–8. https://doi.org/10.1186/s40201-014-0146-y

Amiard, J., Arnich, N., & Badot, P. (2011). *Shellfish and Residual Chemical*

*Contaminants : Hazards , Monitoring , and Archimer*. https://doi.org/10.1007/978-1-4419-9860-6

Anwar, K., Said, M., Fauzi, A., Abdul, Z., Sohaimi, M., & Hafeez, A. (2021). A review of technologies for the phenolic compounds recovery and phenol removal from wastewater. *Process Safety and Environmental Protection*, *151*, 257–289. https://doi.org/10.1016/j.psep.2021.05.015

Apalangya, V., Rangari, V., Tiimob, B., Jeelani, S., & Samuel, T. (2014). Applied Surface Science Development of antimicrobial water filtration hybrid material from bio source calcium carbonate and silver nanoparticles. *Applied Surface Science*, *295*, 108–114. https://doi.org/10.1016/j.apsusc.2014.01.012

Ayala, A., Muñoz, M. F., & Argüelles, S. (2014). Lipid Peroxidation : Production , Metabolism , and Signaling Mechanisms of Malondialdehyde and 4-Hydroxy-2-Nonenal, *2014*. https://doi.org/10.1155/2014/360438

Azizian, S., Eris, S., & Wilson, L. D. (2018). Re-evaluation of the century-old Langmuir isotherm for modeling adsorption phenomena in solution. *Chemical Physics*, *513*(June), 99–104. https://doi.org/10.1016/j.chemphys.2018.06.022

Babiker, E., Al-ghouti, M. A., Zouari, N., & Mckay, G. (2019). Journal of Environmental Chemical Engineering Removal of boron from water using adsorbents derived from waste tire rubber. *Journal of Environmental Chemical Engineering*, *7*(2), 102948. https://doi.org/10.1016/j.jece.2019.102948

Bal, A., Panda, F., Gourav, S., Das, K., & Kumar, P. (2021). Comparative Biochemistry and Physiology , Part C Modulation of physiological oxidative stress and antioxidant status by abiotic factors especially salinity in aquatic organisms. *Comparative Biochemistry and Physiology, Part C*, *241*(November 2020), 108971. https://doi.org/10.1016/j.cbpc.2020.108971

Baldwin, W., Bain, L., Giulio, R., Kullman, S., Rice, C., Ringwood, A., & Hurk, P. (2020). 20th Pollutant Responses in Marine Organisms (PRIMO 20): Global issues and fundamental mechanisms caused by pollutant stress in marine and freshwater organisms, *227*. https://doi.org/10.1016/j.aquatox.2020.105620

Baveye, P., & Steenhuis, T. S. (2004). THE DESORPTION OF SILVER AND THALLIUM FROM SOILS IN THE PRESENCE OF A CHELATING RESIN WITH THIOL FUNCTIONAL GROUPS, *1*, 41–54.

Bouiahya, K., Es-saidi, I., Bekkali, C. El, Laghzizil, A., Robert, D., Nunzi, J. M., & Saoiabi, A. (2019). Synthesis and properties of alumina-hydroxyapatite composites from natural phosphate for phenol removal from water. *Colloid and Interface Science Communications*, *31*(July), 100188. https://doi.org/10.1016/j.colcom.2019.100188

Bradford, M. M. (1976). A rapid and sensitive method for the quantitation of microgram quantities of protein utilizing the principle of protein-dye binding. In *Analytical Biochemistry* (pp. 248–254). https://doi.org/https://doi.org/10.1016/0003-2697(76)90527-3

Busca, G., Berardinelli, S., Resini, C., & Arrighi, L. (2008). Technologies for the removal of phenol from fluid streams : A short review of recent developments, *160*, 265–288. https://doi.org/10.1016/j.jhazmat.2008.03.045

Bwatanglang, I. B., Magili, S. T., & Kaigamma, I. (2021). Adsorption of phenol over bio-based silica / nanocomposite synthesized from waste eggshells and rice husks. https://doi.org/10.7717/peerj-pchem.17

Campaniello, D., Speranza, B., Altieri, C., Sinigaglia, M., Bevilacqua, A., & Corbo, M. R. (2021). Removal of Phenols in Table Olive Processing Wastewater by Using a Mixed Inoculum of Candida boidinii and Bacillus pumilus : Effects of Inoculation

Dynamics , Temperature , pH , and Effluent Age on the Abatement Efficiency.

Cao, R., Wang, D., Wei, Q., Wang, Q., Yang, D., Liu, H., … Zhao, J. (2018). Integrative Biomarker Assessment of the Influence of Saxitoxin on Marine Bivalves : A Comparative Study of the Two Bivalve Species Oysters , Crassostrea gigas , and Scallops , Chlamys farreri, *9*(August), 1–14. https://doi.org/10.3389/fphys.2018.01173

Cao, Z., Daly, M., Clémence, L., Geever, L. M., Major, I., Higginbotham, C. L., & Devine, D. M. (2016). Applied Surface Science Chemical surface modification of calcium carbonate particles with stearic acid using different treating methods. *Applied Surface Science*, *378*, 320–329. https://doi.org/10.1016/j.apsusc.2016.03.205

Caplat, C., Serpentini, A., Lebel, J. M., Florence, M., & Costil, K. (2016). Achimer Metal bioaccumulation and physiological condition of the Pacific oyster ( Crassostrea gigas ) reared in two shellfish basins and a marina in Normandy ( northwest France ), *106*(1), 202–214.

Chang, H. Y. H., Kuo, Y., & Liu, J. C. (2019). Science of the Total Environment Fluoride at waste oyster shell surfaces – Role of magnesium. *Science of the Total Environment*, *652*, 1331–1338. https://doi.org/10.1016/j.scitotenv.2018.10.238

Chao, W., Jun, X. U. Y., Ying, S. H. I., Chong, W., Lian, D., Wen, G. U., … Wei, Z. H. (2020). Verification on the Developmental Toxicity of Short-term Exposure to Phenol in Rats. *Biomedical and Environmental Sciences*, *33*(6), 403–413. https://doi.org/10.3967/bes2020.055

Checa, A. G., Harper, E. M., & González-segura, A. (2018). Structure and crystallography of foliated and chalk shell microstructures of the oyster Magallana : the same materials grown under different conditions, (April), 1–12.

https://doi.org/10.1038/s41598-018-25923-6

Chen, J., Xiao, S., Deng, Y., Du, X., & Yu, Z. (2011). Fish & Shell fi sh Immunology Cloning of a novel glutathione S-transferase 3 ( GST3 ) gene and expression analysis in pearl oyster , Pinctada martensii. *Fish and Shellfish Immunology*, *31*(6), 823–830. https://doi.org/10.1016/j.fsi.2011.07.023

Chen, L. (2020). Visual system : An understudied target of aquatic toxicology. *Aquatic Toxicology*, *225*(March), 105542. https://doi.org/10.1016/j.aquatox.2020.105542

Chung, Y. T., Ba-Abbad, M. M., Mohammad, A. W., Hairom, N. H. H., & Benamor, A. (2015). Synthesis of minimal-size ZnO nanoparticles through sol–gel method: Taguchi design optimisation. *Materials & Design*, *87*, 780–787. JOUR. https://doi.org/http://dx.doi.org/10.1016/j.matdes.2015.07.040

Claiborne, A. (1985). Catalase activity. In *Greenwald RA (ed) Handbook of Methods for Oxygen Radical Research* (pp. 283–284).

Concetta, A., Burioli, E., Magara, G., Pastorino, P., Caldaroni, B., Menconi, V., … Prearo, M. (2020). Science of the Total Environment Oxidative stress ecology on Paci fi c oyster Crassostrea gigas from lagoon and offshore Italian sites. *Science of the Total Environment*, *739*, 139886. https://doi.org/10.1016/j.scitotenv.2020.139886

Cruz, C., Almeida, L., & Felzenszwalb, I. (2020). Heliyon Nanotechnology activities : environmental protection regulatory issues data, *6*(July). https://doi.org/10.1016/j.heliyon.2020.e05303

Daguer, H., Hoff, R. B., Molognoni, L., Kleemann, C. R., & Felizardo, L. V. (2018). ScienceDirect Outbreaks , toxicology , and analytical methods of marine toxins in seafood. *Current Opinion in Food Science*, *24*, 43–55. https://doi.org/10.1016/j.cofs.2018.10.006

Daraei, H., Mittal, A., Noorisepehr, M., & Daraei, F. (2013). Kinetic and equilibrium studies of adsorptive removal of phenol onto eggshell waste, 4603–4611. https://doi.org/10.1007/s11356-012-1409-8

Dehmani, Y., Alghamdi, Y., Lainé, J., Badawi, M., Amhoud, A., Bonilla-petriciolet, A., … Abouarnadasse, S. (2020). Kinetic , thermodynamic and mechanism study of the adsorption of phenol on Moroccan clay, *312*. https://doi.org/10.1016/j.molliq.2020.113383

Dehmani, Y., Alrashdi, A. A., Lgaz, H., Lamhasni, T., Abouarnadasse, S., & Chung, I. (2020). Removal of phenol from aqueous solution by adsorption onto hematite ( a -Fe 2 O 3 ): Mechanism exploration from both experimental and theoretical studies. *Arabian Journal of Chemistry*, *13*(5), 5474–5486. https://doi.org/10.1016/j.arabjc.2020.03.026

Djebbar, M., Djafri, F., Bouchekara, M., & Djafri, A. (2012). Adsorption of phenol on natural clay, 77–86. https://doi.org/10.1007/s13201-012-0031-8

Dotto, G. L., & Mckay, G. (2020). Current scenario and challenges in adsorption for water treatment. *Journal of Environmental Chemical Engineering*, *8*(4), 103988. https://doi.org/10.1016/j.jece.2020.103988

Duncan, P. F., & Coast, S. (2003). Commercially Important Molluscs, 5222.

Dutta, D., & Das, B. M. (2020). Jo ur na l P re. *Environmental Nanotechnology, Monitoring & Management*, 100418. https://doi.org/10.1016/j.enmm.2020.100418

El-tawil, R. S., El-wakeel, S. T., Abdel-ghany, A. E., Abuzeid, H. A. M., Selim, K. A., & Hashem, A. M. (2019). Heliyon Silver / quartz nanocomposite as an adsorbent for removal of mercury ( II ) ions from aqueous solutions. *Heliyon*, *5*(August), e02415. https://doi.org/10.1016/j.heliyon.2019.e02415

El, R., Ben, M., Daghbouj, N., Castet, S., Besson, P., Michel, S., … Courjault-radé, P. (2018). Seawater quality assessment and identi fi cation of pollution sources along the central coastal area of Gabes Gulf ( SE Tunisia ): Evidence of industrial impact and implications for marine environment protection, *127*(June 2017), 445–452. https://doi.org/10.1016/j.marpolbul.2017.12.012

Eletta, O., Tijani, I., & Ighalo, J. (2020). Adsorption of Pb ( II ) and Phenol from Wastewater Using Silver Nitrate Modified Activated Carbon from Groundnut ( Arachis hypogaea L .) Shells, (August).

EPA. (1980). Ambient Water Quality Criteria for Phenol.

Etim, I. N., Okafor, P. C., & Obadimu, C. O. (2015). Degradation of Phenol in Aqueous System by Solar Photocatalysis , Photolysis and Adsorption Processes Degradation of Phenol in Aqueous System by Solar Photocatalysis , Photolysis and Adsorption Processes, (December 2016).

Fan, L., Zhang, S., Zhang, X., Zhou, H., Lu, Z., & Wang, S. (2015). Removal of arsenic from simulation wastewater using nano-iron / oyster shell composites. *Journal of Environmental Management*, *156*, 109–114. https://doi.org/10.1016/j.jenvman.2015.03.044

Farabegoli, F., Blanco, L., Rodríguez, L. P., Vieites, J. M., & Cabado, A. G. (2018). Phycotoxins in Marine Shellfish : Origin , Occurrence and Effects on Humans. https://doi.org/10.3390/md16060188

Farrington, J. W. (2020). Need to update human health risk assessment protocols for polycyclic aromatic hydrocarbons in seafood after oil spills. *Marine Pollution Bulletin*, *150*(July 2019), 110744. https://doi.org/10.1016/j.marpolbul.2019.110744

Fathy, M., Selim, H., & Shahawy, A. E. L. (2020). RSC Advances adsorbent for

removing phenol from aqueous. *RSC Advances*, *10*(June), 23417–23430. https://doi.org/10.1039/D0RA02960B

Freitas, R., Marques, F., Marchi, L. De, Vale, C., & Jo, M. (2020). Biochemical performance of mussels , cockles and razor shells contaminated by paralytic shellfish toxins, *188*(June). https://doi.org/10.1016/j.envres.2020.109846

Frijhoff, J., Winyard, P. G., Zarkovic, N., Davies, S. S., Stocker, R., Cheng, D., … Poulsen, H. E. (2015). Clinical Relevance of Biomarkers of Oxidative Stress 1, *23*(14). https://doi.org/10.1089/ars.2015.6317

Ganji, D. D., & Kachapi, S. H. H. (2015). *Application of Nonlinear Systems in Nanomechanics and Nanofluids*. *Application of Nonlinear Systems in Nanomechanics and Nanofluids*. Elsevier. https://doi.org/10.1016/B978-0-323-35237-6.00001-7

Ghafari, M., Cui, Y., Alali, A., & Atkinson, J. D. (2019). Phenol adsorption and desorption with physically and chemically tailored porous polymers : Mechanistic variability associated with hyper-cross- linking and amination. *Journal of Hazardous Materials*, *361*(April 2018), 162–168. https://doi.org/10.1016/j.jhazmat.2018.08.068

Gharaati, S. (2019). Extraction Techniques of Phenolic Compounds from Plants. https://doi.org/10.5772/intechopen.84705

Gideon, C., & Faggio, C. (2019). Microplastics in the marine environment : Current trends in environmental pollution and mechanisms of toxicological pro fi le, *68*(December 2018), 61–74. https://doi.org/10.1016/j.etap.2019.03.001

Gong, B., Wu, P., Huang, Z., Li, Y., Dang, Z., & Ruan, B. (2016). Chemosphere Enhanced degradation of phenol by Sphingomonas sp . GY2B with resistance towards suboptimal environment through adsorption on kaolinite. *Chemosphere*,

*148*, 388–394. https://doi.org/10.1016/j.chemosphere.2016.01.003

Gouamid, M., Ouahrani, M. R., & Bensaci, M. B. (2013). Adsorption Equilibrium , kinetics and thermodynamics of methylene blue from aqueous solutions using Date Palm Leaves . *Energy Procedia*, *36*, 898–907. https://doi.org/10.1016/j.egypro.2013.07.103

Guo, X., & Wang, J. (2019). Comparison of linearization methods for modeling the Langmuir adsorption isotherm. *Journal of Molecular Liquids*, *296*, 111850. https://doi.org/10.1016/j.molliq.2019.111850

Häder, D., Banaszak, A. T., Villafañe, V. E., Narvarte, M. A., González, R. A., & Helbling, E. W. (2020). Science of the Total Environment Anthropogenic pollution of aquatic ecosystems : Emerging problems with global implications. *Science of the Total Environment*, *713*, 136586. https://doi.org/10.1016/j.scitotenv.2020.136586

Hadi, M., Mostofi, M., Alimohammadi, M., Alghouti, M., Mubarak, N. M., & Sahu, J. N. (2016). Journal of Industrial and Engineering Chemistry High-performance removal of toxic phenol by single-walled and multi-walled carbon nanotubes : Kinetics , adsorption , mechanism and optimization studies. *Journal of Industrial and Engineering Chemistry*, *35*, 63–74. https://doi.org/10.1016/j.jiec.2015.12.010

Hajji, S., Turki, T., Boubakri, A., Ben, M., & Mzoughi, N. (2017). Study of cadmium adsorption onto calcite using full factorial experiment design Study of cadmium adsorption onto calcite using full factorial experiment design, (July). https://doi.org/10.5004/dwt.2017.21079

Hassan, S. S., Al-ghouti, M. A., Abu-dieyeh, M., & Mckay, G. (2020). Journal of Environmental Chemical Engineering Novel bioadsorbents based on date pits for organophosphorus pesticide remediation from water. *Journal of Environmental*

*Chemical Engineering*, *8*(1), 103593. https://doi.org/10.1016/j.jece.2019.103593

Helm, M. M., & Bourne, N. (2004). *Hatchery culture of bivalves*. Rome.

Heydari, M., & Karimyan, K. (2018). Data in Brief Data for ef fi ciency comparison of raw pumice and manganese-modi fi ed pumice for removal phenol from aqueous environments — Application of response surface methodology. *Data in Brief*, *20*, 1942–1954. https://doi.org/10.1016/j.dib.2018.09.027

Ho, E., Karimi, K., Liu, C., Bhindi, R., & Figtree, G. A. (2013). Redox Biology Biological markers of oxidative stress : Applications to cardiovascular research and practice. *Redox Biology*, *1*(1), 483–491. https://doi.org/10.1016/j.redox.2013.07.006

Hoyos-hernandez, C., Hoffmann, M., Guenne, A., & Mazeas, L. (2014). Chemosphere Elucidation of the thermophilic phenol biodegradation pathway via benzoate during the anaerobic digestion of municipal solid waste. *Chemosphere*, *97*, 115–119. https://doi.org/10.1016/j.chemosphere.2013.10.045

Hu, Q., & Zhang, Z. (2019). Application of Dubinin – Radushkevich isotherm model at the solid / solution interface : A theoretical analysis. *Journal of Molecular Liquids*, *277*, 646–648. https://doi.org/10.1016/j.molliq.2019.01.005

Hurchill, H. U. G. H. C., Eng, H. E. T., & Azen, R. O. M. H. (2004). Correlation of pH-dependent surface interaction forces to amino acid adsorption : Implications for the origin of life, *89*, 1048–1055.

Ighodaro, O. M., & Akinloye, O. A. (2018). First line defence antioxidants-superoxide dismutase ( SOD ), catalase ( CAT ) and glutathione peroxidase ( GPX ): Their fundamental role in the entire antioxidant defence grid. *Alexandria Journal of Medicine*, *54*(4), 287–293. https://doi.org/10.1016/j.ajme.2017.09.001

Inthapanya, X., Wu, S., Han, Z., Zeng, G., Wu, M., & Yang, C. (2019). Adsorptive

removal of anionic dye using calcined oyster shells : isotherms , kinetics , and thermodynamics Adsorptive removal of anionic dye using calcined oyster shells : isotherms , kinetics , and thermodynamics, (February). https://doi.org/10.1007/s11356-018-3980-0

Iurascu, B., Siminiceanu, I., Vione, D., Vicente, M. A., Gil, A., Giuria, V. P., … Analitica, C. (2009). Phenol degradation in water through a heterogeneous photo-Fenton process catalyzed by Fe-treated laponite. *Water Research*, *43*(5), 1313–1322. https://doi.org/10.1016/j.watres.2008.12.032

Jamal, A., Rastkari, N., Dehghaniathar, R., Nabizadeh, R., Nasseri, S., Kashani, H., … Yunesian, M. (2020). Prenatal urinary concentrations of environmental phenols and birth outcomes in the mother-infant pairs of Tehran Environment and Neurodevelopmental Disorders ( TEND ) cohort study. *Environmental Research*, *184*(November 2019), 109331. https://doi.org/10.1016/j.envres.2020.109331

Jasim, S. Y., Saththasivam, J., Loganathan, K., & Ogunbiyi, O. O. (2016). Journal of Water Process Engineering Reuse of Treated Sewage Effluent ( TSE ) in Qatar. *Journal of Water Process Engineering*, *11*, 174–182. https://doi.org/10.1016/j.jwpe.2016.05.003

Jo, P. G., Choi, Y. K., & Choi, C. Y. (2008). Cloning and mRNA expression of antioxidant enzymes in the Pacific oyster , Crassostrea gigas in response to cadmium exposure, *147*, 460–469. https://doi.org/10.1016/j.cbpc.2008.02.001

Jones, S. (2009). Environmental Toxicology: Aquatic. In *Information Resources in Toxicology* (Fourth Edi, pp. 203–216).

Kalesaran, O. J., Lumenta, C., & Mamuaya, G. (2018). Biometric relationships of the black-lip pearl oyster , Pinctada margaritifera from North Sulawesi waters , Indonesia, *11*(5), 1587–1597.

Khraisheh, M., Al-ghouti, M. A., & Almomani, F. (2020). Environmental Technology & Innovation P . putida as biosorbent for the remediation of cobalt and phenol from industrial waste wastewaters. *Environmental Technology & Innovation*, *20*, 101148. https://doi.org/10.1016/j.eti.2020.101148

Kim, W., Sing, R., & Smith, J. A. (2020). Modified Crushed Oyster Shells for Fluoride Removal from Water, 1–13. https://doi.org/10.1038/s41598-020-60743-7

Kottuparambil, S., & Agusti, S. (2020). Chemosphere Cell-by-cell estimation of PAH sorption and subsequent toxicity in marine phytoplankton. *Chemosphere*, *259*, 127487. https://doi.org/10.1016/j.chemosphere.2020.127487

Kulkarni, S. J. (2013). Review on Research for Removal of Phenol from, *3*(4), 1–5.

La, G., Micale, R., Cannizzaro, L., & Paolo, F. (2017). A sustainable phenolic compound extraction system from olive oil mill wastewater. *Journal of Cleaner Production*, *142*, 3782–3788. https://doi.org/10.1016/j.jclepro.2016.10.086

Le, N., Tri, M., Quang, P., Tan, L. Van, Thi, P., Kim, J., … Tahtamouni, T. M. Al. (2020). Journal of Water Process Engineering Removal of phenolic compounds from wastewaters by using synthesized Fe- nano zeolite. *Journal of Water Process Engineering*, *33*(December 2019), 101070. https://doi.org/10.1016/j.jwpe.2019.101070

Lee, S., Jang, Y., Ryu, K., Chae, S., Lee, Y., & Jeon, C. (2011). Mechanical characteristics and morphological effect of complex crossed structure in biomaterials : Fracture mechanics and microstructure of chalky layer in oyster shell. *Micron*, *42*(1), 60–70. https://doi.org/10.1016/j.micron.2010.08.001

Léon, J. J. L., & Matos, T. N. De. (2018). Elucidation of mechanism involved in adsorption of Pb ( II ) onto lobeira fruit ( Solanum lycocarpum ) using Langmuir , Freundlich and Temkin isotherms. *Microchemical Journal*, *137*, 348–354.

https://doi.org/10.1016/j.microc.2017.11.009

Li, H., Meng, F., Duan, W., Lin, Y., & Zheng, Y. (2019). Ecotoxicology and Environmental Safety Biodegradation of phenol in saline or hypersaline environments by bacteria : A review. *Ecotoxicology and Environmental Safety*, *184*(March), 109658. https://doi.org/10.1016/j.ecoenv.2019.109658

Lima, E. C., Gomes, A. A., & Nguyen, H. (2020). Comparison of the nonlinear and linear forms of the van ' t Hoff equation for calculation of adsorption thermodynamic parameters ( Δ S ° and Δ H ° ). *Journal of Molecular Liquids*, *311*, 113315. https://doi.org/10.1016/j.molliq.2020.113315

Lloyd-smith, M. (2018). OCEAN POLLUTANTS GUIDE TOXIC THREATS TO, (October).

Lomartire, S. (2021). Biomarkers based tools to assess environmental and chemical stressors in aquatic systems, *122*. https://doi.org/10.1016/j.ecolind.2020.107207

Lowe, F. (2014). Biomarkers of Oxidative Stress. In *Laher I. (eds) Systems Biology of Free Radicals and Antioxidants*. Springer, Berlin, Heidelberg. https://doi.org/https://doi.org/10.1007/978-3-642-30018-9_4

Luo, L., Zhang, Q., Kong, X., & Huang, H. (2017). Chemosphere Differential effects of bisphenol A toxicity on oyster ( Crassostrea angulata ) gonads as revealed by label-free quantitative proteomics. *Chemosphere*, *176*, 305–314. https://doi.org/10.1016/j.chemosphere.2017.02.146

M.McCord, J., & IrwinFridovich. (1969). Superoxide Dismutase: AN ENZYMIC FUNCTION FOR ERYTHROCUPREIN (HEMOCUPREIN), (22). https://doi.org/10.1016/S0021-9258(18)63504-5

Majid, A., Qayoom, S., & Younis, M. (2019). Heliyon Equilibrium , kinetic and thermodynamic studies of removal of phenol from aqueous solution using surface

engineered chemistry, *5*(July 2018). https://doi.org/10.1016/j.heliyon.2019.e01852

Mamoon, A. Al, & Rahman, A. (2015). Identification of Rainfall Trends in Qatar, (January).

Marshall, D. J. (2006). Reliably estimating the effect of toxicants on fertilization success in marine broadcast spawners, *52*, 734–738. https://doi.org/10.1016/j.marpolbul.2006.05.005

Matranga, Y. Y. Æ. V. (2006). Physical and chemical impacts on marine organisms, 1–5. https://doi.org/10.1007/s00227-005-0204-1

Meena, M. C., Band, R., & Sharma, G. (2015). Phenol and Its Toxicity : A Case Report, *8*(27), 2014–2016.

Messerlian, C., Mustieles, V., Minguez-alarcon, L., & Ford, J. B. (2018). Preconception and prenatal urinary concentrations of phenols and birth size of singleton infants born to mothers and fathers from the Environment and Reproductive Health ( EARTH ) study. *Environment International*, *114*(November 2017), 60–68. https://doi.org/10.1016/j.envint.2018.02.017

Mohammed, S. Z. (2003). Population Parameters of the Pearl Oyster Pinctada radiata ( Leach ) in Qatari Waters , Arabian Gulf ., *27*, 339–343.

Mojoudi, N., Mirgha, N., Soleimani, M., Shariatmadari, H., Belver, C., & Bedia, J. (2019). Phenol adsorption on high microporous activated carbons prepared from oily sludge : equilibrium , kinetic and thermodynamic studies, 1–12. https://doi.org/10.1038/s41598-019-55794-4

Mujtaba, I. M. (2017). process : Model development based on experiment and simulation. *Journal of Water Process Engineering*, *18*(May), 20–28. https://doi.org/10.1016/j.jwpe.2017.05.005

Munari, M., Matozzo, V., Chemello, G., Riedl, V., Pastore, P., Badocco, D., & Gabriella, M. (2019). Seawater acidification and emerging contaminants : A dangerous marriage for haemocytes of marine bivalves. *Environmental Research*, *175*(May), 11–21. https://doi.org/10.1016/j.envres.2019.04.032

Musleh, S. M., Zaitoon, B. A., Yousef, R. I., & Ibrahim, M. (2014). REMOVAL OF PHENOLS FROM AQUEOUS SOLUTIONS USING BI MODIFIED REMOVAL OF PHENOLS FROM AQUEOUS SOLUTIONS USING BI MODIFIED JORDANIAN, (January).

Naguib, D. M., & Badawy, N. M. (2020). Journal of Environmental Chemical Engineering Phenol removal from wastewater using waste products. *Journal of Environmental Chemical Engineering*, *8*(1), 103592. https://doi.org/10.1016/j.jece.2019.103592

Navarro, A. E., Hernandez-vega, A., Masud, E., & Roberson, L. M. (2016). Bioremoval of Phenol from Aqueous Solutions Using Native Caribbean Seaweed. https://doi.org/10.3390/environments4010001

Nicholls, P. (2016). Enzymology and structure of catalases, *8838*(November). https://doi.org/10.1016/S0898-8838(00)51001-0

Noonburg, E. G., Nisbet, R. M., & Klanjscek, T. (2010). Effects of life history variation on vertical transfer of toxicants in marine mammals. *Journal of Theoretical Biology*, *264*(2), 479–489. https://doi.org/10.1016/j.jtbi.2010.02.017

Opiyo, K., Rawson, C., Gagnon, M. M., & Saputra, I. (2021). Biomarkers in Rock Oysters ( Saccostrea mordax ) in Response to Organophosphate Pesticides, *26*(March), 7–16. https://doi.org/10.14710/ik.ijms.26.1.7-16

Ouallal, H., Dehmani, Y., Moussout, H., & Messaoudi, L. (2019). Heliyon Kinetic , isotherm and mechanism investigations of the removal of phenols from water by

raw and calcined clays. *Heliyon*, *5*(April), e01616. https://doi.org/10.1016/j.heliyon.2019.e01616

Patel, H. (2021). Review on solvent desorption study from exhausted adsorbent. *Journal of Saudi Chemical Society*, *25*(8), 101302. https://doi.org/10.1016/j.jscs.2021.101302

Piazza, F., Gough, K., Monthioux, M., Puech, P., Gerber, I. C., Wiens, R., … Gerber, I. C. (2019). Low temperature , pressureless sp2 to sp3 transformation of ultrathin , crystalline carbon films To cite this version : HAL Id : hal-02080627.

Popoola, L. T. (2019). Characterization and adsorptive behaviour of snail calcined particles ( CPs ) towards cationic dye. *Heliyon*, (December 2018), e01153. https://doi.org/10.1016/j.heliyon.2019.e01153

Potters, G. (2013). Marine Pollution, (2002), 0–11.

Qu, C., Liu, S., Tang, Z., Li, J., Liao, Z., & Qi, P. (2019). Fish and Shell fi sh Immunology Response of a novel selenium-dependent glutathione peroxidase from thick shell mussel Mytilus coruscus exposed to lipopolysaccharide , copper and benzo [ α ] pyrene. *Fish and Shellfish Immunology*, *89*(April), 595–602. https://doi.org/10.1016/j.fsi.2019.04.028

Ragadhita, R., Bayu, A., & Nandiyanto, D. (2021). Indonesian Journal of Science & Technology How to Calculate Adsorption Isotherms of Particles Using Two-Parameter Monolayer Adsorption Models and Equations, *6*(1), 205–234.

Rahimi, M., Moghadas, S., Motamedi, E., Nasiri, J., Reza, M., & Sabokdast, M. (2020). Heliyon Pro fi cient dye removal from water using biogenic silver nanoparticles prepared through solid-state synthetic route. *Heliyon*, *6*(March), e04730. https://doi.org/10.1016/j.heliyon.2020.e04730

Rand, G. M., & Petrocelli, S. R. (1985). *Fundamentals of aquatic toxicology: methods*

*and applications*. Washington: Hemisphere Pub. Corp..

Rathi, B. S., Kumar, P. S., & Show, P. (2020). A review on effective removal of emerging contaminants from aquatic systems : Current trends and scope for further research. *Journal of Hazardous Materials*, (September), 124413. https://doi.org/10.1016/j.jhazmat.2020.124413

Raza, A., Su, W., Gao, A., Mehmood, S. S., Hussain, M. A., Nie, W., … Zhang, X. (2021). Catalase ( CAT ) Gene Family in Rapeseed ( Brassica napus L .): Genome-Wide Analysis , Identification , and Expression Pattern in Response to Multiple Hormones and Abiotic Stress Conditions, 1–20.

Raza, W., Lee, J., Raza, N., Luo, Y., & Kim, K. (2019). Journal of Industrial and Engineering Chemistry Removal of phenolic compounds from industrial waste water based on membrane-based technologies. *Journal of Industrial and Engineering Chemistry*, *71*, 1–18. https://doi.org/10.1016/j.jiec.2018.11.024

Repetto, M., Semprine, J., & Boveris, A. (2012). Lipid Peroxidation: Chemical Mechanism, Biological Implications and Analytical Determination. https://doi.org/DOI: 10.5772/45943

Robledo, J. A. F., Yadavalli, R., Allam, B., Pales, E., Gerdol, M., Greco, S., … Metzger, M. J. (2019). From the raw bar to the bench : Bivalves as models for human health. *Developmental and Comparative Immunology*, *92*(November 2018), 260–282. https://doi.org/10.1016/j.dci.2018.11.020

Rodriguez-blanco, J. D., Rodriguez-blanco, J. D., Shaw, S., & Benning, L. G. (2010). Nanoscale, (June 2014). https://doi.org/10.1039/c0nr00589d

Rolland, M., Lyon-caen, S., Sakhi, A. K., Pin, I., & Sabaredzovic, A. (2020). Exposure to phenols during pregnancy and the first year of life in a new type of couple-child cohort relying on repeated urine biospecimens. *Environment International*,

*139*(February), 105678. https://doi.org/10.1016/j.envint.2020.105678

Sahu, O., Govardhana, D., Gabbiye, N., & Engidayehu, A. (2017). Sorption of phenol from synthetic aqueous solution by activated saw dust : Optimizing parameters with response surface methodology. *Biochemistry and Biophysics Reports*, *12*(July), 46–53. https://doi.org/10.1016/j.bbrep.2017.08.007

Sandamalika, W. M. G., Priyathilaka, T. T., Lee, S., Yang, H., & Lee, J. (2019). Fish and Shell fi sh Immunology Immune and xenobiotic responses of glutathione S-Transferase theta ( GST- θ ) from marine invertebrate disk abalone ( Haliotis discus discus ) : With molecular characterization and functional analysis. *Fish and Shellfish Immunology*, *91*(May), 159–171. https://doi.org/10.1016/j.fsi.2019.04.004

Sauvé, S., & Desrosiers, M. (2014). A review of what is an emerging contaminant, 1–7.

Shaban, Y. A., Sayed, M. A. El, Maradny, A. A. El, Kh, R., Farawati, A., & Zobidi, M. I. Al. (2013). Chemosphere Photocatalytic degradation of phenol in natural seawater using visible light active carbon modified ( CM ) -n-TiO 2 nanoparticles under UV light and natural sunlight illuminations. *Chemosphere*, *91*(3), 307–313. https://doi.org/10.1016/j.chemosphere.2012.11.035

Shan, D., Zhu, M., Han, E., Xue, H., & Cosnier, S. (2007). Calcium carbonate nanoparticles : A host matrix for the construction of highly sensitive amperometric phenol biosensor, *23*, 648–654. https://doi.org/10.1016/j.bios.2007.07.012

Sharan, R., Singh, G., & Gupta, S. K. (2009). Adsorption of Phenol from Aqueous Solution onto Fly Ash from a Thermal, (Iarc 1987), 267–279.

Singh, H., Bhardwaj, N., Kumar, S., & Khatri, M. (2020). Environmental Nanotechnology , Monitoring & Management Environmental impacts of oil spills

and their remediation by magnetic nanomaterials. *Environmental Nanotechnology, Monitoring & Management*, *14*(November 2019), 100305. https://doi.org/10.1016/j.enmm.2020.100305

Singh, N. B., Nagpal, G., & Agrawal, S. (2018). Environmental Technology & Innovation Water purification by using Adsorbents : A Review. *Environmental Technology & Innovation*, *11*, 187–240. https://doi.org/10.1016/j.eti.2018.05.006

Singh, N., & Singh, J. (2007). AN ENZYMATIC METHOD FOR REMOVAL OF, *6068*. https://doi.org/10.1081/PB-120004125

Sobiesiak, M. (2017). Chemical Structure of Phenols and Its Consequence for Sorption Processes. In *Phenolic Compounds*. https://doi.org/10.5772/67213

Stewart, A. J., Ridge, O., Universities, A., & Ridge, O. (2008). Relevant Websites, (2), 2682–2689.

Subhan, A., Chandra, P., Alam, M. M., & Asiri, A. M. (2018). Journal of Environmental Chemical Engineering Development of Bis-Phenol A sensor based on Fe 2 MoO 4 · Fe 3 O 4 · ZnO nanoparticles for sustainable environment. *Journal of Environmental Chemical Engineering*, *6*(1), 1396–1403. https://doi.org/10.1016/j.jece.2018.01.057

Subramani, K., Elhissi, A., Subbiah, U., & Ahmed, W. (2019). Chapter1:Introduction to nanotechnology. In *Nanobiomaterials in Clinical Dentistry (Second Edition)* (pp. 3–18). Elsevier. Retrieved from https://doi.org/10.1016/B978-0-12-815886-9.00001-2

Tang, G., Jia, C., Wang, G., Yu, P., & Jiang, X. (2020). Adsorption mechanism of bacteria onto a Na-montmorillonite surface with organic and inorganic calcium.

Tang, W., Huang, H., Gao, Y., Liu, X., Yang, X., Ni, H., & Zhang, J. (2015). Preparation of a novel porous adsorption material from coal slag and its adsorption

properties of phenol from aqueous solution. *JMADE*, *88*, 1191–1200. https://doi.org/10.1016/j.matdes.2015.09.079

TOXICOLOGICAL PROFILE FOR PHENOL. (2008). *U.S. DEPARTMENT OF HEALTH AND HUMAN SERVICES*.

Tsai, H. C., Lo, S. L., & Kuo, J. (2011). Using pretreated waste oyster and clam shells and microwave hydrothermal treatment to recover boron from concentrated wastewater. *Bioresource Technology*, *102*(17), 7802–7806. https://doi.org/10.1016/j.biortech.2011.06.036

Tsai, H., Lo, S., & Kuo, J. (2011). Bioresource Technology Using pretreated waste oyster and clam shells and microwave hydrothermal treatment to recover boron from concentrated wastewater. *Bioresource Technology*, *102*(17), 7802–7806. https://doi.org/10.1016/j.biortech.2011.06.036

Tsuchida, S. (1997). Glutathione Transferases, *2*, 297–307.

Tubaro, A., Sosa, S., & Hungerford, J. (2012). Toxicology and diversity of marine toxins. In R. Gupta (Ed.), *Veterinary Toxicology* (second edi, pp. 896–934). academic press.

Ugraskan, V., Isik, B., Yazici, O., & Cakar, F. (2022). Removal of Safranine T by a highly efficient adsorbent ( Cotinus Coggygria leaves ): Isotherms , kinetics , thermodynamics , and surface properties. *Surfaces and Interfaces*, *28*(October 2021), 101615. https://doi.org/10.1016/j.surfin.2021.101615

Valavanidis, A., Vlahogianni, T., Dassenakis, M., & Scoullos, M. (2006). Molecular biomarkers of oxidative stress in aquatic organisms in relation to toxic environmental pollutants, *64*, 178–189. https://doi.org/10.1016/j.ecoenv.2005.03.013

Vilhena, M. P. S. P., Costa, M. L., Berrêdo, J. F., Paiva, R. S., & Moreira, M. Z. (2021).

Trace elements and δ 13 C and δ 15 N isotopes in sediments , phytoplankton and oysters as indicators of anthropogenic activities in estuaries in the Brazilian Amazon. *Regional Studies in Marine Science*, *41*, 101618. https://doi.org/10.1016/j.rsma.2021.101618

Villegas, L. G. C., Mashhadi, N., Chen, M., Mukherjee, D., Taylor, K. E., & Biswas, N. (2016). A Short Review of Techniques for Phenol Removal from Wastewater. *Current Pollution Reports*, 157–167. https://doi.org/10.1007/s40726-016-0035-3

Wang, L., Song, X., & Song, L. (2018). The oyster immunity. *Developmental and Comparative Immunology*, *80*, 99–118. https://doi.org/10.1016/j.dci.2017.05.025

Wang, W. (2018). carbonate – silica frameworks thermally activated from porous fossil bryophyte : adsorption studies for heavy metal uptake, 25754–25766. https://doi.org/10.1039/c8ra04825h

Wang, Y., Song, J., Zhao, W., He, X., Chen, J., & Xiao, M. (2011). In situ degradation of phenol and promotion of plant growth in contaminated environments by a single Pseudomonas aeruginosa strain. *Journal of Hazardous Materials*, *192*(1), 354–360. https://doi.org/10.1016/j.jhazmat.2011.05.031

Water, N., & Management, Q. (2000). Australian and New Zealand Guidelines for Fresh and Marine Water Quality, *1*(4).

Wells, P. G. (2020). *Aquatic Toxicology : Concepts , Practice , New Directions*. https://doi.org/10.1002/9780470744307.gat092

WHO. (2011). *Guidelines for Drinking-water Quality* (4th ed.). World Health Organization.

Wu, Q., Chen, J., Clark, M., & Yu, Y. (2014). Applied Surface Science Adsorption of copper to different biogenic oyster shell structures. *Applied Surface Science*, *311*, 264–272. https://doi.org/10.1016/j.apsusc.2014.05.054

Wu, Y., Guan, C., Griswold, N., Hou, L., Fang, X., Hu, A., … Yu, C. (2020). Zero-valent iron-based technologies for removal of heavy metal ( loid ) s and organic pollutants from the aquatic environment : Recent advances and perspectives. *Journal of Cleaner Production*, *277*, 123478. https://doi.org/10.1016/j.jclepro.2020.123478

Zanette, J., Alves, E., Almeida, D., Zaccaron, A., Guzenski, J., Fernando, J., … Bainy, D. (2011). Science of the Total Environment Salinity in fl uences glutathione S - transferase activity and lipid peroxidation responses in the Crassostrea gigas oyster exposed to diesel oil. *Science of the Total Environment, The*, *409*(10), 1976–1983. https://doi.org/10.1016/j.scitotenv.2011.01.048

Zhang, R., Pearce, G. L., Penn, M. S., Topol, E. J., Sprecher, D. L., & Hazen, S. L. (2001). Association Between Myeloperoxidase Levels and Risk of Coronary Artery Disease, *286*(17).

Zhao, L., Zhang, H., Zhao, B., & Lyu, H. (2022). Activation of peroxydisulfate by ball-milled α -FeOOH / biochar composite for phenol removal : Component contribution and internal mechanisms ☆, *293*(August 2021).

APPENDIX

Anova: Two-Factor With Replication Gills Total protein

| SUMMARY | 0 h | 24 h | 48 h | 72 h | 96 h | Total |
|---|---|---|---|---|---|---|
| *0 ppm* | | | | | | |
| Count | 6 | 6 | 6 | 6 | 6 | 30 |
| Sum | 125.9 | 123.5 | 118.9 | 104.8 | 91.1 | 564.2 |
| Average | 20.98333 | 20.58333 | 19.81667 | 17.46667 | 15.18333 | 18.80667 |
| Variance | 0.213667 | 0.233667 | 0.373667 | 0.118667 | 0.389667 | 5.161333 |
| *1 ppm* | | | | | | |
| Count | 6 | 6 | 6 | 6 | 6 | 30 |
| Sum | 127.8 | 124.3 | 118.6 | 103.7 | 90 | 564.4 |
| Average | 21.3 | 20.71667 | 19.76667 | 17.28333 | 15 | 18.81333 |
| Variance | 0.332 | 0.181667 | 0.566667 | 0.153667 | 0.396 | 5.990851 |
| *2 ppm* | | | | | | |
| Count | 6 | 6 | 6 | 6 | 6 | 30 |
| Sum | 130.1 | 125.3 | 121.5 | 101.6 | 89.9 | 568.4 |
| Average | 21.68333 | 20.88333 | 20.25 | 16.93333 | 14.98333 | 18.94667 |
| Variance | 1.285667 | 0.393667 | 0.271 | 0.102667 | 0.165667 | 7.148092 |
| *5 ppm* | | | | | | |
| Count | 6 | 6 | 6 | 6 | 6 | 30 |
| Sum | 125.1 | 124.4 | 120.6 | 101.1 | 88 | 559.2 |
| Average | 20.85 | 20.73333 | 20.1 | 16.85 | 14.66667 | 18.64 |
| Variance | 0.423 | 0.398667 | 0.436 | 0.311 | 0.526667 | 6.64869 |
| *10 ppm* | | | | | | |
| Count | 6 | 6 | 6 | 6 | 6 | 30 |
| Sum | 127.9 | 127.8 | 120.4 | 103 | 88.6 | 567.7 |
| Average | 21.31667 | 21.3 | 20.06667 | 17.16667 | 14.76667 | 18.92333 |
| Variance | 0.349667 | 1.244 | 0.446667 | 0.170667 | 0.650667 | 7.330816 |
| *Total* | | | | | | |
| Count | 30 | 30 | 30 | 30 | 30 | |
| Sum | 636.8 | 625.3 | 600 | 514.2 | 447.6 | |
| Average | 21.22667 | 20.84333 | 20 | 17.14 | 14.92 | |
| Variance | 0.536506 | 0.485989 | 0.395172 | 0.200414 | 0.401655 | |

ANOVA

| *Source of Variation* | *SS* | *df* | *MS* | *F* | *P-value* | *F crit* |
|---|---|---|---|---|---|---|

| | | | | | | |
|---|---|---|---|---|---|---|
| Treatment | 1.774933 | 4 | 0.443733 | 1.094557 | 0.362254 | 2.444174 |
| Time | 879.3163 | 4 | 219.8291 | 542.2523 | 6.29E-78 | 2.444174 |
| Treatment × Time | 6.1224 | 16 | 0.38265 | 0.943883 | 0.521786 | 1.725034 |
| Within | 50.675 | 125 | 0.4054 | | | |
| | | | | | | |
| Total | 937.8886 | 149 | | | | |

Anova: Two-Factor With Replication Digestive glands Total protein

| SUMMARY | 0 h | 24 h | 48 h | 72 h | 96 h | Total |
|---|---|---|---|---|---|---|
| *0 ppm* | | | | | | |
| Count | 6 | 6 | 6 | 6 | 6 | 30 |
| Sum | 287.8 | 289.6 | 283.1 | 259.7 | 249.1 | 1369.3 |
| Average | 47.96667 | 48.26667 | 47.18333 | 43.28333 | 41.51667 | 45.64333 |
| Variance | 1.954667 | 2.854667 | 2.341667 | 1.301667 | 0.753667 | 9.294264 |
| | | | | | | |
| *1 ppm* | | | | | | |
| Count | 6 | 6 | 6 | 6 | 6 | 30 |
| Sum | 293 | 282 | 277.3 | 261.6 | 249 | 1362.9 |
| Average | 48.83333 | 47 | 46.21667 | 43.6 | 41.5 | 45.43 |
| Variance | 4.962667 | 2.24 | 1.661667 | 0.32 | 0.356 | 8.56769 |
| | | | | | | |
| *2 ppm* | | | | | | |
| Count | 6 | 6 | 6 | 6 | 6 | 30 |
| Sum | 284.1 | 289.9 | 281.8 | 264 | 251.9 | 1371.7 |
| Average | 47.35 | 48.31667 | 46.96667 | 44 | 41.98333 | 45.72333 |
| Variance | 0.279 | 5.613667 | 6.674667 | 2.324 | 2.037667 | 8.685989 |
| | | | | | | |
| *5 ppm* | | | | | | |
| Count | 6 | 6 | 6 | 6 | 6 | 30 |
| Sum | 292.5 | 286.2 | 276.2 | 262.2 | 246.3 | 1363.4 |
| Average | 48.75 | 47.7 | 46.03333 | 43.7 | 41.05 | 45.44667 |
| Variance | 1.671 | 6.66 | 6.834667 | 1.384 | 2.059 | 11.21844 |
| | | | | | | |
| *10 ppm* | | | | | | |
| Count | 6 | 6 | 6 | 6 | 6 | 30 |
| Sum | 276.6 | 286.8 | 276.6 | 256.3 | 244 | 1340.3 |
| Average | 46.1 | 47.8 | 46.1 | 42.71667 | 40.66667 | 44.67667 |
| Variance | 0.404 | 3.04 | 4.32 | 1.997667 | 2.138667 | 9.030126 |
| | | | | | | |
| *Total* | | | | | | |
| Count | 30 | 30 | 30 | 30 | 30 | |
| Sum | 1434 | 1434.5 | 1395 | 1303.8 | 1240.3 | |
| Average | 47.8 | 47.81667 | 46.5 | 43.46 | 41.34333 | |

| | | | | | | |
|---|---|---|---|---|---|---|
| Variance | 2.651724 | 3.753161 | 4.00069 | 1.460414 | 1.474954 | |

ANOVA

| *Source of Variation* | *SS* | *df* | *MS* | *F* | *P-value* | *F crit* |
|---|---|---|---|---|---|---|
| Treatment | 20.66293 | 4 | 5.165733 | 1.951258 | 0.106067 | 2.444174 |
| Time | 990.8743 | 4 | 247.7186 | 93.57098 | 1.23E-36 | 2.444174 |
| Treatment × Time | 35.30107 | 16 | 2.206317 | 0.833394 | 0.645877 | 1.725034 |
| Within | 330.9233 | 125 | 2.647387 | | | |
| | | | | | | |
| Total | 1377.762 | 149 | | | | |

Anova: Two-Factor With Replication Gills CAT

| SUMMARY | 0 h | 24 h | 48 h | 72 h | 96 h | Total |
|---|---|---|---|---|---|---|
| *0 ppm* | | | | | | |
| Count | 6 | 6 | 6 | 6 | 6 | 30 |
| Sum | 346 | 343.7 | 345.7 | 344 | 348 | 1727.4 |
| Average | 57.66667 | 57.28333 | 57.61667 | 57.33333 | 58 | 57.58 |
| Variance | 2.394667 | 1.397667 | 1.193667 | 0.802667 | 0.572 | 1.165793 |
| | | | | | | |
| *1 ppm* | | | | | | |
| Count | 6 | 6 | 6 | 6 | 6 | 30 |
| Sum | 346.4 | 346.5 | 360.5 | 393.5 | 420.5 | 1867.4 |
| Average | 57.73333 | 57.75 | 60.08333 | 65.58333 | 70.08333 | 62.24667 |
| Variance | 3.942667 | 5.523 | 1.385667 | 3.849667 | 1.997667 | 27.25499 |
| | | | | | | |
| *2 ppm* | | | | | | |
| Count | 6 | 6 | 6 | 6 | 6 | 30 |
| Sum | 356.8 | 362.2 | 376.7 | 410 | 440.4 | 1946.1 |
| Average | 59.46667 | 60.36667 | 62.78333 | 68.33333 | 73.4 | 64.87 |
| Variance | 0.390667 | 1.050667 | 3.905667 | 1.342667 | 1.396 | 30.067 |
| | | | | | | |
| *5 ppm* | | | | | | |
| Count | 6 | 6 | 6 | 6 | 6 | 30 |
| Sum | 350 | 362.7 | 387.6 | 426.9 | 456.5 | 1983.7 |
| Average | 58.33333 | 60.45 | 64.6 | 71.15 | 76.08333 | 66.12333 |
| Variance | 2.918667 | 0.863 | 1.524 | 6.631 | 8.349667 | 48.94461 |
| | | | | | | |
| *10 ppm* | | | | | | |
| Count | 6 | 6 | 6 | 6 | 6 | 30 |
| Sum | 344.8 | 357.5 | 381.8 | 430.2 | 458.6 | 1972.9 |
| Average | 57.46667 | 59.58333 | 63.63333 | 71.7 | 76.43333 | 65.76333 |

| | | | | | | |
|---|---|---|---|---|---|---|
| Variance | 2.394667 | 2.973667 | 1.442667 | 1.596 | 1.242667 | 55.59275 |

| *Total* | | | | | |
|---|---|---|---|---|---|
| Count | 30 | 30 | 30 | 30 | 30 |
| Sum | 1744 | 1772.6 | 1852.3 | 2004.6 | 2124 |
| Average | 58.13333 | 59.08667 | 61.74333 | 66.82 | 70.8 |
| Variance | 2.622299 | 3.85292 | 8.374264 | 30.66855 | 50.08138 |

ANOVA

| *Source of Variation* | *SS* | *df* | *MS* | *F* | *P-value* | *F crit* |
|---|---|---|---|---|---|---|
| Treatment | 1509.919 | 4 | 377.4798 | 154.4997 | 2.21E-47 | 2.444174 |
| Time | 3465.265 | 4 | 866.3163 | 354.5768 | 3.51E-67 | 2.444174 |
| Treatment × Time | 957.0587 | 16 | 59.81617 | 24.48231 | 5.11E-31 | 1.725034 |
| Within | 305.405 | 125 | 2.44324 | | | |
| Total | 6237.648 | 149 | | | | |

Anova: Two-Factor With Replication Digestive gland CAT

| SUMMARY | 0 h | 24 h | 48 h | 72 h | 96 h | Total |
|---|---|---|---|---|---|---|
| *0 ppm* | | | | | | |
| Count | 6 | 6 | 6 | 6 | 6 | 30 |
| Sum | 306 | 309.7 | 312.8 | 313.1 | 316.3 | 1557.9 |
| Average | 51 | 51.61667 | 52.13333 | 52.18333 | 52.71667 | 51.93 |
| Variance | 0.536 | 0.217667 | 0.302667 | 0.373667 | 0.477667 | 0.678034 |
| *1 ppm* | | | | | | |
| Count | 6 | 6 | 6 | 6 | 6 | 30 |
| Sum | 302.8 | 311.4 | 319.5 | 316 | 327.6 | 1577.3 |
| Average | 50.46667 | 51.9 | 53.25 | 52.66667 | 54.6 | 52.57667 |
| Variance | 0.326667 | 0.552 | 0.431 | 0.390667 | 1.116 | 2.44392 |
| *2 ppm* | | | | | | |
| Count | 6 | 6 | 6 | 6 | 6 | 30 |
| Sum | 301.2 | 311.9 | 329.1 | 323 | 345.6 | 1610.8 |
| Average | 50.2 | 51.98333 | 54.85 | 53.83333 | 57.6 | 53.69333 |
| Variance | 0.208 | 0.977667 | 0.879 | 0.970667 | 3.168 | 7.637885 |
| *5 ppm* | | | | | | |
| Count | 6 | 6 | 6 | 6 | 6 | 30 |
| Sum | 302 | 312.8 | 333.9 | 336.4 | 360.4 | 1645.5 |
| Average | 50.33333 | 52.13333 | 55.65 | 56.06667 | 60.06667 | 54.85 |

| | | | | | | |
|---|---|---|---|---|---|---|
| Variance | 0.578667 | 1.234667 | 1.575 | 0.734667 | 1.118667 | 12.72052 |
| *10 ppm* | | | | | | |
| Count | 6 | 6 | 6 | 6 | 6 | 30 |
| Sum | 307 | 320.3 | 344.8 | 352.8 | 379.9 | 1704.8 |
| Average | 51.16667 | 53.38333 | 57.46667 | 58.8 | 63.31667 | 56.82667 |
| Variance | 1.362667 | 1.157667 | 0.474667 | 0.932 | 2.089667 | 19.7234 |
| *Total* | | | | | | |
| Count | 30 | 30 | 30 | 30 | 30 | |
| Sum | 1519 | 1566.1 | 1640.1 | 1641.3 | 1729.8 | |
| Average | 50.63333 | 52.20333 | 54.67 | 54.71 | 57.66 | |
| Variance | 0.669195 | 1.103092 | 4.203552 | 6.771966 | 16.18662 | |

ANOVA

| *Source of Variation* | *SS* | *df* | *MS* | *F* | *P-value* | *F crit* |
|---|---|---|---|---|---|---|
| Treatment | 453.4297 | 4 | 113.3574 | 127.7372 | 3.57E-43 | 2.444174 |
| Time | 867.2404 | 4 | 216.8101 | 244.3133 | 4.63E-58 | 2.444174 |
| Treatment × Time | 274.7403 | 16 | 17.17127 | 19.3495 | 1.66E-26 | 1.725034 |
| Within | 110.9283 | 125 | 0.887427 | | | |
| Total | 1706.339 | 149 | | | | |

## Anova: Two-Factor With Replication Gills SOD

| SUMMARY | 0 h | 24 h | 48 h | 72 h | 96 h | Total |
|---|---|---|---|---|---|---|
| *0 ppm* | | | | | | |
| Count | 6 | 6 | 6 | 6 | 6 | 30 |
| Sum | 174 | 174.2 | 178.1 | 182.7 | 185 | 894 |
| Average | 29 | 29.03333 | 29.68333 | 30.45 | 30.83333 | 29.8 |
| Variance | 0.872 | 0.462667 | 0.509667 | 0.995 | 0.982667 | 1.224138 |
| *1 ppm* | | | | | | |
| Count | 6 | 6 | 6 | 6 | 6 | 30 |
| Sum | 181.8 | 184.8 | 209.9 | 215.1 | 226.1 | 1017.7 |
| Average | 30.3 | 30.8 | 34.98333 | 35.85 | 37.68333 | 33.92333 |
| Variance | 1.688 | 1.204 | 3.593667 | 0.271 | 0.473667 | 9.906678 |
| *2 ppm* | | | | | | |
| Count | 6 | 6 | 6 | 6 | 6 | 30 |
| Sum | 184.1 | 194.3 | 231.9 | 239.9 | 256.1 | 1106.3 |
| Average | 30.68333 | 32.38333 | 38.65 | 39.98333 | 42.68333 | 36.87667 |

| | | | | | | |
|---|---|---|---|---|---|---|
| Variance | 4.821667 | 0.881667 | 0.527 | 4.089667 | 3.969667 | 24.20047 |

| *5 ppm* | | | | | | |
|---|---|---|---|---|---|---|
| Count | 6 | 6 | 6 | 6 | 6 | 30 |
| Sum | 187.3 | 199.1 | 240.1 | 261.2 | 284.3 | 1172 |
| Average | 31.21667 | 33.18333 | 40.01667 | 43.53333 | 47.38333 | 39.06667 |
| Variance | 0.877667 | 3.901667 | 2.401667 | 0.474667 | 0.329667 | 39.91264 |

| *10 ppm* | | | | | | |
|---|---|---|---|---|---|---|
| Count | 6 | 6 | 6 | 6 | 6 | 30 |
| Sum | 186.6 | 190.2 | 257.9 | 288.4 | 312.7 | 1235.8 |
| Average | 31.1 | 31.7 | 42.98333 | 48.06667 | 52.11667 | 41.19333 |
| Variance | 0.788 | 0.936 | 3.985667 | 1.118667 | 2.113667 | 76.38961 |

| *Total* | | | | | | |
|---|---|---|---|---|---|---|
| Count | 30 | 30 | 30 | 30 | 30 | |
| Sum | 913.8 | 942.6 | 1117.9 | 1187.3 | 1264.2 | |
| Average | 30.46 | 31.42 | 37.26333 | 39.57667 | 42.14 | |
| Variance | 2.219724 | 3.383034 | 23.59826 | 39.49151 | 58.25834 | |

ANOVA

| *Source of Variation* | *SS* | *df* | *MS* | *F* | *P-value* | *F crit* |
|---|---|---|---|---|---|---|
| Treatment | 2392.45 | 4 | 598.1124 | 353.7508 | 4.01E-67 | 2.444174 |
| Time | 3108.247 | 4 | 777.0618 | 459.5896 | 1.04E-73 | 2.444174 |
| Treatment × Time | 1077.779 | 16 | 67.36118 | 39.84046 | 2.75E-41 | 1.725034 |
| Within | 211.3467 | 125 | 1.690773 | | | |
| | | | | | | |
| Total | 6789.822 | 149 | | | | |

Anova: Two-Factor With ReplicationDigestive gland SOD

| SUMMARY | 0 h | 24 h | 48 h | 72 h | 96 h | Total |
|---|---|---|---|---|---|---|
| *0 ppm* | | | | | | |
| Count | 6 | 6 | 6 | 6 | 6 | 30 |
| Sum | 114.2 | 117.5 | 120.2 | 124.9 | 127.2 | 604 |
| Average | 19.03333 | 19.58333 | 20.03333 | 20.81667 | 21.2 | 20.13333 |
| Variance | 0.194667 | 0.377667 | 0.274667 | 0.205667 | 0.196 | 0.862299 |

| *1 ppm* | | | | | | |
|---|---|---|---|---|---|---|
| Count | 6 | 6 | 6 | 6 | 6 | 30 |
| Sum | 123.3 | 130.3 | 142.2 | 158.4 | 163 | 717.2 |
| Average | 20.55 | 21.71667 | 23.7 | 26.4 | 27.16667 | 23.90667 |

| | | | | | | |
|---|---|---|---|---|---|---|
| Variance | 0.451 | 1.333667 | 0.896 | 0.292 | 0.274667 | 7.377195 |
| | | | | | | |
| *2 ppm* | | | | | | |
| Count | 6 | 6 | 6 | 6 | 6 | 30 |
| Sum | 120 | 142.6 | 161.4 | 176.5 | 190 | 790.5 |
| Average | 20 | 23.76667 | 26.9 | 29.41667 | 31.66667 | 26.35 |
| Variance | 0.636 | 0.610667 | 0.68 | 0.653667 | 1.126667 | 18.21914 |
| | | | | | | |
| *5 ppm* | | | | | | |
| Count | 6 | 6 | 6 | 6 | 6 | 30 |
| Sum | 124.3 | 132.5 | 178.8 | 193.6 | 209.3 | 838.5 |
| Average | 20.71667 | 22.08333 | 29.8 | 32.26667 | 34.88333 | 27.95 |
| Variance | 0.505667 | 1.837667 | 1.792 | 2.166667 | 3.029667 | 34.06397 |
| | | | | | | |
| *10 ppm* | | | | | | |
| Count | 6 | 6 | 6 | 6 | 6 | 30 |
| Sum | 123.7 | 133.3 | 192.5 | 215.7 | 241.9 | 907.1 |
| Average | 20.61667 | 22.21667 | 32.08333 | 35.95 | 40.31667 | 30.23667 |
| Variance | 0.581667 | 1.017667 | 1.197667 | 0.611 | 0.977667 | 61.69206 |
| | | | | | | |
| *Total* | | | | | | |
| Count | 30 | 30 | 30 | 30 | 30 | |
| Sum | 605.5 | 656.2 | 795.1 | 869.1 | 931.4 | |
| Average | 20.18333 | 21.87333 | 26.50333 | 28.97 | 31.04667 | |
| Variance | 0.81454 | 2.757885 | 19.84447 | 28.16769 | 45.04533 | |

ANOVA

| *Source of Variation* | *SS* | *df* | *MS* | *F* | *P-value* | *F crit* |
|---|---|---|---|---|---|---|
| Treatment | 1808.07 | 4 | 452.0174 | 515.523 | 1.24E-76 | 2.444174 |
| Time | 2550.027 | 4 | 637.5068 | 727.0724 | 1.67E-85 | 2.444174 |
| Treatment × Time | 884.5963 | 16 | 55.28727 | 63.05477 | 7.13E-52 | 1.725034 |
| Within | 109.6017 | 125 | 0.876813 | | | |
| | | | | | | |
| Total | 5352.295 | 149 | | | | |

Anova: Two-Factor Without Replication (OSNP , pH6)

| *Treatment* | *Count* | *Sum* | *Average* | *Variance* |
|---|---|---|---|---|
| 0 ppm | 3 | 72.19 | 24.06333 | 143.6997 |
| 10 ppm | 3 | 80.76 | 26.92 | 107.4871 |
| 15 ppm | 3 | 74.75 | 24.91667 | 112.0282 |
| 20 ppm | 3 | 62.87 | 20.95667 | 18.87613 |

| | | | | |
|---|---|---|---|---|
| 30 ppm | 3 | 59.57 | 19.85667 | 9.792133 |
| 40 ppm | 3 | 53.92 | 17.97333 | 7.687433 |
| 50 ppm | 3 | 53.55 | 17.85 | 19.4943 |
| 60 ppm | 3 | 52.66 | 17.55333 | 8.776933 |
| 80 ppm | 3 | 49.96 | 16.65333 | 6.969733 |
| 100 ppm | 3 | 50.56 | 16.85333 | 13.71803 |
| Temperature | | | | |
| 25° C | 10 | 254.76 | 25.476 | 42.29749 |
| 35° C | 10 | 154.46 | 15.446 | 4.844671 |
| 45° C | 10 | 201.57 | 20.157 | 37.9168 |

ANOVA

| *Source of Variation* | *SS* | *df* | *MS* | *F* | *P-value* | *F crit* |
|---|---|---|---|---|---|---|
| Treatment | 372.0918 | 9 | 41.34353 | 1.891484 | 0.119411 | 2.456281149 |
| Temperature | 503.6206 | 2 | 251.8103 | 11.52043 | 0.0006 | 3.554557146 |
| Error | 393.4389 | 18 | 21.85772 | | | |
| | | | | | | |
| Total | 1269.151 | 29 | | | | |

Anova: Two-Factor Without Replication (OSNP-S, pH 6)

| *Treatment* | *Count* | *Sum* | *Average* | *Variance* |
|---|---|---|---|---|
| 0 ppm | 3 | 37.27 | 12.42333 | 368.7296 |
| 10 ppm | 3 | 56.22 | 18.74 | 31.2663 |
| 15 ppm | 3 | 47.93 | 15.97667 | 13.58653 |
| 20 ppm | 3 | 44.68 | 14.89333 | 30.44123 |
| 30 ppm | 3 | 42.61 | 14.20333 | 19.33663 |
| 40 ppm | 3 | 44.67 | 14.89 | 13.6087 |
| 50 ppm | 3 | 50.35 | 16.78333 | 1.135633 |
| 60 ppm | 3 | 49.11 | 16.37 | 0.13 |
| 80 ppm | 3 | 48.89 | 16.29667 | 0.768133 |
| 100 ppm | 3 | 50.65 | 16.88333 | 4.179233 |
| Temperature | | | | |
| 25° C | 10 | 111.81 | 11.181 | 59.84285 |
| 35° C | 10 | 183.21 | 18.321 | 1.296166 |
| 45° C | 10 | 177.36 | 17.736 | 20.29898 |

ANOVA

| *Source of Variation* | *SS* | *df* | *MS* | *F* | *P-value* | *F crit* |
|---|---|---|---|---|---|---|
| Treatment | 80.87745 | 9 | 8.986384 | 0.248066 | 0.981091 | 2.456281 |
| Temperature | 314.2995 | 2 | 157.1498 | 4.33806 | 0.028997 | 3.554557 |
| Error | 652.0646 | 18 | 36.22581 | | | |

| | | |
|---|---|---|
| Total | 1047.242 | 29 |

Anova: Two-Factor Without Replication (OSNP, pH10)

| *Treatment* | *Count* | *Sum* | *Average* | *Variance* |
|---|---|---|---|---|
| 5 ppm | 3 | 44.97 | 14.99 | 1.8723 |
| 10 ppm | 3 | 60.95 | 20.31667 | 0.812233 |
| 15 ppm | 3 | 50.88 | 16.96 | 1.9123 |
| 20 ppm | 3 | 57.4 | 19.13333 | 1.019633 |
| 30 ppm | 3 | 50.59 | 16.86333 | 0.592133 |
| 40 ppm | 3 | 46.37 | 15.45667 | 1.071233 |
| 50 ppm | 3 | 47.1 | 15.7 | 1.5777 |
| 60 ppm | 3 | 47.83 | 15.94333 | 9.140133 |
| 80 ppm | 3 | 50.03 | 16.67667 | 0.132133 |
| 100 ppm | 3 | 56.24 | 18.74667 | 7.704133 |
| Temperature | | | | |
| 25° C | 10 | 175.51 | 17.551 | 4.167077 |
| 35° C | 10 | 171.52 | 17.152 | 7.245329 |
| 45° C | 10 | 165.33 | 16.533 | 3.041668 |

ANOVA

| *Source of Variation* | *SS* | *df* | *MS* | *F* | *P-value* | *F crit* |
|---|---|---|---|---|---|---|
| Treatment | 83.68108 | 9 | 9.297898 | 3.606509 | 0.009877 | 2.456281 |
| Temperature | 5.262287 | 2 | 2.631143 | 1.020579 | 0.380318 | 3.554557 |
| Error | 46.40558 | 18 | 2.578088 | | | |
| | | | | | | |
| Total | 135.3489 | 29 | | | | |

Anova: Two-Factor Without Replication (OSNP-S, pH 10)

| *Treatment* | *Count* | *Sum* | *Average* | *Variance* |
|---|---|---|---|---|
| 5 ppm | 3 | 39.65 | 13.21667 | 42.46063 |
| 10 ppm | 3 | 47.34 | 15.78 | 48.31 |
| 15 ppm | 3 | 56.8 | 18.93333 | 36.23093 |
| 20 ppm | 3 | 70.12 | 23.37333 | 5.971233 |
| 30 ppm | 3 | 60.46 | 20.15333 | 4.929233 |
| 40 ppm | 3 | 53.4 | 17.8 | 1.7764 |

| | | | | |
|---|---|---|---|---|
| 50 ppm | 3 | 55.27 | 18.42333 | 5.523733 |
| 60 ppm | 3 | 50.55 | 16.85 | 18.2476 |
| 80 ppm | 3 | 55.44 | 18.48 | 4.7164 |
| 100 ppm | 3 | 59.37 | 19.79 | 2.2519 |
| Temperature | | | | |
| 25° C | 10 | 217.49 | 21.749 | 6.473388 |
| 35° C | 10 | 177.14 | 17.714 | 16.87043 |
| 45° C | 10 | 153.77 | 15.377 | 13.56325 |

ANOVA

| *Source of Variation* | *SS* | *df* | *MS* | *F* | *P-value* | *F crit* |
|---|---|---|---|---|---|---|
| Treatment | 199.1447 | 9 | 22.12719 | 2.994232 | 0.022789 | 2.456281 |
| Temperature | 207.8173 | 2 | 103.9086 | 14.06083 | 0.00021 | 3.554557 |
| Error | 133.0189 | 18 | 7.389937 | | | |
| | | | | | | |
| Total | 539.9808 | 29 | | | | |